CONCORDIA UNIVERSITY

Technical Note No. TN-EMC-81-03
Final Report
May 13, 1981

"Prediction by Numerical Computation of the Reradiation from and the Detuning of Power Transmission Lines"

C.W. Trueman and S.J. Kubina
Electromagnetics Laboratory
Concordia University/Loyola Campus
7141 Sherbrooke St. W.
Montreal, Quebec H4B 1R6

FACULTY OF ENGINEERING

1455 de Maisonneuve Blvd., West
MONTREAL, H3G 1M8, Canada

Technical Note No. TN-EMC-81-03
Final Report
May 13, 1981

"Prediction by Numerical Computation of the Reradiation from and the Detuning of Power Transmission Lines"

C.W. Trueman and S.J. Kubina
Electromagnetics Laboratory
Concordia University/Loyola Campus
7141 Sherbrooke St. W.
Montreal, Quebec H4B 1R6

APPROVED FOR PUBLIC RELEASE, DISTRIBUTION UNLIMITED

SCIENTIFIC AUTHORITY
G.M. ROYER

Prepared for:

Communications Research Centre
Ottawa, Ontario K1A 0S5
Contract No. 0SU80-00121

CONCORDIA UNIVERSITY

21 May 1981

Dr. J.S. Belrose
Communications Research Centre
Radio Communications Laboratory
P.O. Box 11490, Station "H"
Shirley Bay
Ottawa, Ontario
K2H 8S2

Dear Dr. Belrose:

Enclosed please find an unbound copy of our Final Report. Hope it reaches you in time for the meeting.

Yours truly,

S.J. Kubina

Dr. S.J. Kubina, Eng.
Principal Investigator
CRC Contract

cc: Mr. M. Royer ✓
CRC

Ms. J. St. Pierre
DSS

Miss A.J. Williams
Concordia University
University Research

enclosures (2)

SJK/PJF

P.S. We have just received bound copies — one is enclosed.
S.

LOYOLA CAMPUS
7141 SHERBROOKE STREET WEST
MONTREAL, QUEBEC H4B 1R6

TABLE OF CONTENTS

Page

Prediction by Numerical Computation of the Reradiation from and the Detuning of Power Transmission Lines

by C.W. Trueman

and S.J. Kubina

1. Introduction

This report documents the results obtained in the second year of the AM Reradiation Project at Concordia University. The objective of this project is to construct computer models for the calculation of the RF behaviour of high-voltage power transmission lines at MF-AM frequencies, using modern numerical techniques based on Pocklington's Integral Equation(1) and the Numerical Electromagnetics Code(NEC,2) computer program. The work reported here is a continuation of that done in the first year of the project as documented in reference (3).

In the first year of this project, it was established that computational methods are able to predict the reradiated field from an evenly spaced power line illuminated by an isotropic broadcast antenna, over a perfectly conducting ground. A computer model called the "single wire tower" model was developed to represent power line towers of the "VLS" type, and it was shown that this model matches the azimuth patterns measured at NRC for the straight, evenly-spaced power line, and also that the frequency dependence of the measured patterns is duplicated in the computed patterns over the "two wavelength loop resonance" frequency range. The "single wire tower" model was then applied to compute the azimuth pattern of the site at Hornby, Ontario where an array of 27 towers on two power lines is illuminated by an omnidirectional broadcast antenna. The

elementary "detuning" measure of loading the skywire at its center with a high resistance was investigated.

This report extends the application of the "single wire tower" model in several directions. The frequency dependence is studied from 200 to 1100 kHz and two bands of resonance are identified, with RF current modes having distinct patterns of nulls on the skywire. The currents flowing on the towers and skywires of the Hornby model are examined, and a model with more towers on the dogleg is constructed. The problem of null-filling is addressed by reproducing NRC's measured patterns for a two element array near a five tower power line. The problem of "detuning" by isolating towers from the skywire is studied. "Detuning" by the use of stub traps is investigated for the case of three towers, by reproducing the NRC measured patterns. The design of detuning stubs for the one wavelength and the two wavelength resonance modes is addressed, and the best length and connection point is found by computation. A more practical stub is considered, which is confined to the tower and does not connect to the skywire, and it is found that this design merits further study. A preliminary study of the modelling of the finite conductivity of the ground is presented as an introduction to the more exhaustive study proposed for the third year of the project.

2. Current Distribution on the Hornby Power Lines

This section examines the RF current distribution that flows on the towers and skywires of the Hornby power lines. These currents give rise to the azimuth patterns reported in reference (3). A new format for the plotting of RF current distributions is introduced, and the interpretation of the figures for the straight evenly-spaced power line is discussed, and then the currents flowing on the power lines of the Hornby site model are described.

2.1 Interpretation of Current Distribution Graphs

The RF current distribution on the straight evenly spaced power line is examined in this section to explain how current distribution graphs such as Fig. 2.1 are interpreted, and to develop the postulate that the phase behaviour of the current on the skywires of the power line indicates whether the power line is at or near resonance at the particular frequency of the plot.

Figs. 2.1 and 2.2 show the currents flowing on the straight, evenly-spaced power line at 760 and 860 kHz. The geometry is given below in Fig.5.1. Here, a nine tower power line was used, with each tower being 50.9 m (167 ft) tall. The wire radii were 2 m for the broadcast tower, 3.51 m for the power line towers, and 0.71 m for the skywire. All other dimensions are as given in the figure. The format of the display lends itself to plotting the currents on complex structures such as the Hornby site model, or models using detuning stubs. Fig. 2.1(a) depicts the magnitude and phase of the tower currents at 760 kHz. The plot shows the magnitude and phase of the current at two points on each of the nine towers of the power line. The left hand point for each tower is near the base, at 12.6 m above the ground on the 50.6 m tall tower. Thus for tower # 1 the current at this point is about 300 microamps with a phase of about 90 degrees, and the current on the center tower, tower # 5, is about 500 microamps with phase of about 135 degrees, both relative to a one volt, zero phase generator at the base of the broadcast tower. The right hand point for each tower is the current at a height of 38 meters from the ground. From the graph it is seen that the current tapers in magnitude going from tower to tower away from the center of the power line, and that the phase differs by 180 degrees on adjacent towers. Part (b) of Fig. 2.1 shows the magnitude and phase of the skywire currents. The graph shows that the phase can be decomposed into a constant term plus a linear-with-distance term, where for a pure travelling wave the absolute value of the slope is equal to the wave number. Constant phase with distance indicates a standing wave on the skywire, whereas linear phase

with distance is characteristic of a travelling wave. Thus on the skywire connecting towers 5 and 6 in Fig. 2.1(b), the phase indicates that an almost pure travelling wave is present. However, on the skywires elsewhere, there is a constant phase component with a weaker travelling wave component superimposed, and so the current is mainly a standing wave.

In contrast to the behaviour in Fig. 2.1 at 760 kHz, Fig. 2.2(a) and (b) show the RF currents on the towers and skywires of the evenly-spaced power line at 860 kHz. Fig. 3.16 of the Final Report(3) shows that for this case, 760 kHz is on the skirts of the resonance curve, whereas 860 kHz is near the peak. Thus Fig. 2.1 shows typical "below-resonance" behaviour for the RF current, and Fig. 2.2 shows "at-resonance" behaviour. Note that "at-resonance" the currents are very much larger than "below-resonance". Thus the vertical scale in Fig. 2.1 is 220 microamps, but is 550 microamps in Fig. 2.2. The phase behaviour of the skywire currents provides a clear indication of resonance. Thus "at-resonance" in Fig. 2.2(b) the skywire current is an almost pure standing wave, and has constant phase with position, with a negligible travelling wave term. As the frequency is changed away from resonance, the skywire current acquires an ever-increasing travelling wave term. Thus at 760 kHz in Fig. 2.1 the skywire current has an easily seen linear progression of phase with distance, superimposed on its standing wave component.

This behaviour of the skywire current's phase can be used to interpret the currents flowing on the Hornby site model, as discussed in the next section.

2.2 Hornby Site Current Distribution

An analysis of the plan of the site at Hornby shows that the tower spacings vary from about 215 to about 290 m. These loop sizes lie just below two wavelength loop resonance at 740 kHz, while at 860 kHz the larger tower spacings are expected to be in strong resonance. This is borne out by the azimuth patterns presented in reference (3) Fig. 3.38 and 3.39, which show weak scalloping at 740 kHz but a much stronger effect at 860 kHz.

Fig. 2.3 shows the numbering scheme for the towers on the Hornby site, and is an aid in the interpretation of the RF current distributions of Fig. 2.4 at 740 kHz and Fig. 2.5 at 860 kHz. The precise dimensions of the site shown in Fig. 2.3 are given in reference (3), Fig. 3.32. The broadcast tower was 195 m (640 ft) tall with a 2 m radius. The nine power line towers were 50.9 m tall, with a 3.51 m wire radius, and the skywire radius was 0.71 m. Fig. 2.4 shows that at 740 kHz, the phase of the RF current on most skywires is strongly a

travelling wave, and so the loops are below resonance. The current on the towers on both the front and rear line is strongest near the broadcast antenna. Also, the front line does not "shield" the rear line at this frequency, because the currents on both lines have about the same magnitude. The current on the dogleg, towers # 12, 10 and 8 of the rear line, is strong and is not seen to decrease with distance from the broadcast antenna. Note that the behaviour of the current on the skywires directly opposite the antenna is different from elsewhere. The current has a zero value at a point on this skywire, between tower numbers 2 and 1 on the front line and tower numbers 2 and 1 on the rear line.

Fig. 2.5 shows the current at 860 kHz. Note the change of vertical scale, indicating that the currents are about four times as strong as at 740 kHz. At this frequency, the larger tower spacings are expected to be in strong "two-wavelength" resonance. Indeed, the phase on the skywires between tower numbers 4 and 2, 1 and 3, 3 and 5, and 5 and 7 on the front line has a strong constant component. Similarly, a strong standing wave component is evident between towers 4 and 2, 1 and 3, and 5 and 7 on the rear line. There is overall a greater degree of "constant phase" behaviour than at 740 kHz, although the picture is nowhere near as clear as it was for the evenly-spaced power line case.

The current magnitudes at 860 kHz behave quite differently than at 740 kHz. Thus in Fig. 2.5, on the front line the current is strongest on towers 3, 5 and 7 near the antenna, and the current noticeably tapers going from tower 1 through 2, 4, 6, and 8 to 10. The towers of the rear line show even more interesting behaviour. The currents are for the most part weaker than on the front line, suggesting that a significant degree of shielding is operative at frequencies near resonance. Also, note that going along the rear line onto the dogleg, from tower 2 through 4, 6, 8 and 10 to 12, the current increases greatly. This suggests that the towers of the dogleg which have been omitted from the model must carry strong currents, and so the azimuth pattern for the actual site is expected to be somewhat different from the computations and measurements in reference (3), and is presented in the next section.

2.3 Hornby Model with More Towers on the Dogleg

Fig. 2.6 shows the azimuth pattern at 860 kHz with four additional towers included on the dogleg, namely towers 14, 16, 18 and 20 in the plan of Fig. 2.3. In comparison with reference (3) Fig. 3.38, it is seen that the azimuth pattern does not change greatly. Fig. 2.7 shows the RF current distribution on the model. The tower and skywire currents on the front line are almost the same as in Fig. 2.5, except that the maximum current

is reduced by about 100 microamps. The currents on the towers and skywires of the rear line are now somewhat stronger than before. Also, the current on the additional towers of the dogleg clearly decreases with distance along the dogleg, suggesting that enough towers are now included on the dogleg. Reference (3) Fig. 3.32 gives the tower to tower spacings on this part of the dogleg, which averages about 850 ft. and is clearly below two wavelength resonance. This is confirmed in Fig. 2.7 by the travelling wave current seen on the skywires connecting these towers.

2.4 Summary

The RF current distribution graphs of Fig 2.4 and 2.5 are useful in assessing whether the frequency of the broadcast antenna is near a resonance of the power line, without having to resort to expensive frequency-sweep computations. The strength of the RF current on the towers and skywires near the ends of the power line relative to the strength of the current near the antenna indicates whether enough towers have been included in the model. Also, the detailed distribution and strength of the RF current may be a good guide to the placement of detuning stubs on the skywires.

3. Prediction of Null-Filling by Computation

Many MF radio stations must employ a directional broadcast antenna in order to meet a licencing stipulation that the radiated signal must be below a specified level over a specified arc in order to avoid interference with another station which operates on the same frequency. When a power line is constructed near such a broadcast array, even small amounts of RF energy reradiated by the power line into the "restricted arc" can violate the station's licencing provision.

In this project, attention has thus far been directed to the prediction of the "scalloping" of the circular azimuth pattern of an omnidirectional broadcast antenna by reradiation. In the case of "scalloping", the broadcast engineer's chief concern is that the level of the RF signal be sufficiently strong in all directions. Thus deep minima in the "omnidirectional" pattern must be avoided. It has been found in this project that it is useful to view the towers of the power line as an "array antenna" which has a radiation pattern that in general consists of some strong "main lobes" plus a great many "sidelobes". The large minima in the omnidirectional antenna's pattern are caused by the main lobe of the pattern of the array of power line towers, and so the prediction of "scalloping" is essentially the prediction of the magnitude and phase of the power line tower array's main lobe.

The case of "null-filling" is different. Here, the "main lobe" of the power line tower array will generally not fall in the direction of the broadcast array pattern's minimum, unless the geometry happens to be most unfavourable. Otherwise, it will be the sidelobes of the power line tower array's pattern which coincide with the direction of the broadcast antenna pattern's minimum and which are responsible for reradiation in that direction. Thus the prediction of "null-filling" is the problem of predicting the sidelobes or "fine details" of the tower array's radiation pattern.

The measurement portion of this project has provided some results by which the success of the computation of null filling can be assessed. Interim Report # 1(4) uses the two-element antenna of Fig. 3.1 to generate a figure of eight pattern with the maxima oriented "broadside" at 0 and 180 degrees. The measured minima are 38 dB down from the main lobes. A power line of five towers is then introduced into the array's main lobe at 180 degrees, and the pattern is measured with and without the skywire connecting the towers.

3.1 Results of Null-Filling Computations

Fig. 3.2 compares the computed and the measured azimuth patterns for the two element array with no power line, and demonstrates that an accurate pattern is computed for the array. The position of the five tower power line relative to the array is shown in Fig. 3.3. The dimensions are those used in the computation. At 1000 kHz, the "loop size" is (2x300)+(4x50.6) = 803.3 m, which is 2.67 wavelengths. This is well above the frequency at which "two wavelength" resonance would be expected. Thus the power line is essentially non-resonant.

Figs. 3.4 and 3.5 compare the results of the computation with the measured pattern for the cases of "towers only" and "towers plus skywires" respectively. The towers were modelled as in reference (3) by using the "single wire tower model" with the tower radius of 3.51 m and the skywire radius of 0.71 m. The towers were taken to be 50.6 m tall. With no skywire, the 5 element "tower array" reradiates strongly into the minima of the directional array. The computed pattern is not identical to the measured one, but it is seen that the structure of the minima is the same for both the measured and the computed patterns. Thus three lobes are seen in both patterns in the minimum at 270 degrees. Also, the level of the computation accurately "predicts" the level of the measured pattern in the minimum.

For the case of towers interconnected by skywires, Fig. 3.5 shows that the reradiation effect is not as strong. The measured pattern is quite assymetric. The agreement in Fig. 3.5 must thus be considered acceptable.

3.2 Conclusions

Further investigation of the problem of the prediction of null-filling by computation must await the availability of more measured patterns. It would be of particular interest to have a knowledge of the frequency dependence of the reradiated field at frequencies near the operating frequency of the directional array.

4. Detuning by Isolating Towers

By breaking the electrical connection between the top of the tower and the skywire, the tower is "isolated" and two adjacent resonant two-wavelength loops are broken. Interim Report # 4(5) showed for the straight, evenly-spaced power line that isolating 9 of the 13 towers resulted in a large reduction in the degree of scalloping of the omnidirectional pattern. Interim Report # 5(6) showed that a similar reduction can be achieved for the pattern of the full Hornby site model. This section investigates the utility of the computer model in predicting the patterns with some towers isolated.

4.1 Simple Model

The simplest possible model of the isolated tower is that of Fig. 4.1 and is obtained from the "single wire tower model" of the power line in reference (3) Fig. 4.3, by disconnecting the tower wire from the skywire and separating the top of the tower wire from the skywire center by a "gap" which is at least as large as the skywire radius. The tower can never be fully "open-circuited" from the skywire, in the sense that there is capacitive coupling between the tower and skywire which cannot be suppressed. In this model, the amount of capacitive coupling can be controlled by adjusting the size of the gap between the tower top and the skywire.

The straight, evenly spaced power line shown in Fig. 5.1 was used to study the effect of isolating towers. A model with 13 towers was used, with the tower wire radius chosen as 3.51 m, and the skywire radius as 0.71 m. This power line is strongly resonant at 860 kHz and so is suitable for studying "detuning" measures. The required gap size in Fig. 4.1 was chosen empirically by computing the azimuth pattern for three different gap sizes, namely equal to the skywire radius, twice that radius and four times that radius. The computation was done to match Fig. 12 in reference (5) which uses a 13 tower power line with towers # 1, 5, 9 and 13 connected to the skywire and all others isolated. The "best" single wire tower model of reference (3) was used, with 50.6 m tall towers of radius 3.51 m, and a skywire of radius 0.71 m. Fig. 4.2 compares the measured pattern to that computed with a gap size of four times the skywire radius. The two patterns are similar and differ mainly near zero and 180 degrees.

Figs. 4.3(a) and (b) show the RF currents on the towers and skywires of the power line. The current on the top segment of each isolated tower is only half the value of the current on the bottom segment. Note that this is not so for towers 1,5,9 and 13 which are connected to the skywire. The three "center"

towers are isolated but carry the largest currents, and in fact carry twice as much current as the adjacent connected towers. In the phase behaviour, it is seen that the towers can be grouped into five "center" towers with phase of about 100 degrees, and two groups of "outer" towers with phase averaging about 40 degrees. The grouping is also evident from the skywire phase behaviour. It is seen that the "outer" skywires connecting towers 1 to 5, and towers 9 to 13 carry primarily travelling wave currents. However the "center" skywires connecting towers 5 to 9 carry strong standing waves.

4.2 Frequency Dependence

An initial investigation of the frequency dependence of the detuning achieved by "isolating" towers was carried out by isolating only towers # 3 and 7 on a nine tower, straight, evenly-spaced power line. The azimuth pattern was then computed and the max-to-min ratio determined over a range of frequencies, and the results are shown in Fig. 4.4 . It is seen that at some frequencies, such as 810 kHz, the power line has been detuned effectively but at others, such as 750 and 910 kHz, the max-to-min ratio is worse.

4.3 Conclusion

The agreement between the measured and computed patterns in Fig. 4.2 needs to be improved for the computer model of the isolated tower to be considered satisfactory. An improved model could then be used to investigate the problem of which towers to isolate to detune a given power line configuration. In view of Fig. 4.4, isolating some towers without a systematic understanding of the effect on resonant frequency can make the scalloping of the pattern worse than it was with all towers connected to the skywire.

5. Frequency Dependence From 200 To 1100 kHz

This chapter examines the resonant behaviour of the evenly-spaced power line over a wide frequency range using the "single wire" tower model. A power line of the dimensions shown in Fig. 5.1 is used, and is excited by an omnidirectional antenna of height 195 m (640 ft). The broadcast tower radius was 2 m, the power line tower radius was 3.51 m and the skywire radius was 0.71 m. The stability of the numerical solution of the Pocklington Integral Equation(1) by the NEC computer code is examined and the solution is found to degrade in the one wavelength resonance region, and this difficulty is discussed before the frequency dependence of the reradiation effect on the azimuth pattern is presented. A useful parameter called the "integrated current" is defined as an alternative to the max-to-min ratio for the study of the resonances of the power line. Polar plots of the azimuth pattern in both the one and two wavelength resonance regions are presented, and the distribution of RF current corresponding to each resonant mode is discussed.

5.1 Convergence of the Solution

The RF currents flowing over the wires of the power line are determined by an approximate solution of Pocklington's Integral Equation(1), which expresses the boundary condition that the total axial field along each of the wires must be zero. This integral equation is reduced to a matrix equation by dividing each wire into "segments", and the RF current amplitude and phase on each segment becomes one unknown in the matrix equation that is obtained. The number of segments to be used on a given wire is determined by "rules of thumb" which state that :

i) segments should be shorter than one tenth of a wavelength, and a length of one-twentieth is usually short enough ;

ii) segments should not be so short that the ratio of the length of the segment to its diameter is less than ten ; and

iii) segments on two wires that form a junction should be comparable in length.

A good "confidence check" of the solution can be made by obtaining a solution with a number of segments chosen according to these rules, then doubling the number of segments, and obtaining a second solution. This tests the mathematical property of "convergence", being that the solution should tend to become constant and independent of the number of segments as the number of segments is increased. Thus if doubling the number of segments results in little change in the solution, then greater confidence can be placed in the result. However, if a large change results, then the solution must be treated with healthy skepticism, although not rejected entirely.

A simple assessment of the "convergence" of the numerical solution can be made by graphing a convenient parameter of the solution against the number of segments. Thus Fig. 5.2 shows the max-to-min ratio of the azimuth pattern as a function of the number of segments at five frequencies, for a power line having five towers. The ideal result would be a horizontal line at high numbers of segments, and is obtained nearly enough at 350 and 1260 kHz. At 450 and 840 kHz, the solution changes by about five percent for each increase of 100 segments, and these cases are typical of the behaviour that must be considered acceptable. However at the one wavelength resonant frequency of 420 kHz the max-to-min ratio changes rapidly with the number of segments. A further increase beyond 300 segments violates rule (ii) given above. The reason for the difficulty with convergence is associated with a mathematical limitation of Pocklington's Equation. For the present purposes, the convergence study in Fig. 5.2 points out that the precise values of RF current, azimuth radiated field and max-to-min ratio must be treated with caution near the one wavelength resonant frequency of 420 kHz, but the solution is satisfactory at nearby frequencies such as 360 and 450 kHz.

Fig. 5.3 shows the changes in the azimuth pattern that are encountered as the number of segments increases at the troublesome frequency of 420 kHz. The change seen with an increase from 50 to 100 total segments is quite substantial, but the changes that come about by increasing the number of segments from 100 to 200 to 300 are not large and mainly consist of the deepening of the minimum at 180 degrees azimuth. The qualitative nature of the patterns remains the same.

Thus the assessment of convergence provides a "confidence check" in the solution. The poor convergence at 420 kHz is indicative of a limitation in the method in the region of 420 kHz, but does not mean that the solution is useless. Instead, the precise numerical results must be interpreted cautiously but the qualitative effect of the presence of a resonance is indisputable and so a considerably perturbed radiation pattern is expected .

5.2 Verification Against Measured Results

Fig. 5.4 compares the computed azimuth patterns with the measurements of Lavrench and Dunn(7) at 515 and 860 kHz. The power line has thirteen towers for both the measurements and the computations. An antenna height of 195 m (640 ft) has been used for the calculations at both frequencies.

At 515 kHz as shown in Fig. 5.4(a), the main difference between the measured and the computed azimuth pattern is the depth of the minima, which are much deeper in the measurement. The frequency of the measurement for Fig. 5.4 was chosen to give

the largest max-to-min ratio, and so the measurement model is at resonance. As shown below the computer model with nine towers has a resonance peak at about 520 kHz, and is somewhat above resonance at 530 kHz. It would be of interest to compare the frequency dependence of the measured patterns with the computed results in the one wavelength resonance region. Fig. 5.4(b) shows the comparison of the measured and computed patterns at the two wavelength resonant frequency of 860 kHz. The agreement is satisfactory.

5.3 Frequency Dependence For a Five Tower Power Line

5.3.1 Max-to-Min Ratio

Fig. 5.5 shows the max-to-min ratio of the azimuth pattern from 200 to 1100 kHz. There are two distinct resonance regions, extending from 390 to 510 kHz for "one wavelength resonance" and 790 to 990 kHz for "two wavelength resonance" where these limits have been chosen for a max-to-min ratio of 3 dB. These resonance regions are separated by extensive frequency bands in which the power line is non-resonant and the azimuth pattern is nearly circular.

The one-wavelength resonance band is characterized by two closely spaced peaks at about 420 kHz and an isolated peak at 480 kHz. The resonance mode of the pair of peaks will be termed "one wavelength loop resonance". The RF current distributions are discussed in Sect. 5.5 below. It was indicated above that the numerical solution converges poorly in this frequency range, and so the max-to-min ratio computed with a total of 300 segments is also shown. It is qualitatively the same, and shows sharper peaks at slightly lower frequencies. The isolated peak at 480 kHz has an RF current distribution which will be termed "two wavelength double-loop" resonance, and is discussed further in Sect. 5.5.

The two wavelength resonance region is characterized by a broad peak at 840 kHz for the five tower power line, and a gradual "roll-off" of the max-to-min ratio above this frequency. The RF current mode of the peak at 840 kHz is "two wavelength loop resonance", and a second resonance mode at 940 kHz exists, which has an RF current mode called "four wavelength double-loop resonance" and is discussed further below.

Above 1000 kHz the pattern is nearly circular. At frequencies above 1200 kHz, the monopole antenna illuminating the power line becomes taller than three-quarters of a wavelength and radiates poorly in the azimuth plane, and so the azimuth pattern becomes dominated by the weak reradiated fields and the max-to-min ratio of this low level pattern is large. It is of little interest to study the azimuth pattern resulting from such a tall broadcast antenna.

The use of a parameter directly related to RF current to reveal the resonances is dealt with next.

5.3.2 The Integrated Current

A parameter directly based on RF current which is suitable for assessing the effect of reradiation on the azimuth pattern can be defined by noting that the strength of the azimuth field radiated by a vertical wire of length "L" carrying complex current I(z) is proportional to the integral

$$I_{av} = \int I(z) \, dz$$

which will be termed the "integrated current" for the wire. By comparing the integrated current due to a tower to that due to the broadcast antenna, the possible effect of the tower current on the azimuth pattern can be assessed. Thus if the tower's integrated current is 0.2 of that flowing on the broadcast antenna, then at an azimuth angle where both fields arrive in phase, the net field would be 1.2 times that of the broadcast antenna alone, and if the fields arrive in phase opposition, the net field would be 0.8 of the antenna's. Thus the worst case max-to-min ratio for the pattern of the antenna plus the one tower would be 20 log(1.2/0.8) = 3.5 dB. Evidently the ratio of the integrated current on a tower to the integrated current on the antenna, or "integrated current ratio", is a useful parameter for assessing the possible effect of reradiation.

Fig. 5.6 compares the base current on the broadcast monopole to the integrated current. With the one volt excitation used, the base current is equal to the admittance of the broadcast antenna in the presence of the five tower power line. As expected the broadcast monopole has a resonance at about 350 kHz where it is about one-quarter wavelength high, and at 1100 kHz where it is about three quarters of a wavelength in height. The integrated current has similar peaks but the maximum at 1100 kHz is much smaller because much of the power is radiated into the elevation plane at this frequency. The integrated current reflects only the fields radiated into the azimuth plane.

Fig. 5.7 shows the resonances of the five tower power line in terms of the integrated current ratio. The ratio is of the integrated current on the center tower to that on the broadcast antenna. The two resonance regions seen in the max-to-min ratio graph of Fig. 5.5 are also present in the integrated current ratio, although their structure is somewhat different. In the one-wavelength region the convergence of the numerical solution is worrisome for the integrated currents as it was for the max-to-min ratio, which is, of course, derived from the same

currents. Thus the figure compares the solutions with 100 and 300 segments on the power line. Only one peak is seen in Fig. 5.7 at 420 kHz for "one wavelength loop resonance". The peak at 480 kHz corresponding to "two wavelength double-loop resonance" is present. The two wavelength resonance region is characterized by two equal peaks corresponding to "two wavelength loop resonance" at 850 kHz, and "four wavelength double-loop resonance" at 950 kHz.

The next two sections report on the azimuth pattern and the RF current distribution throughout this frequency range.

5.4 Azimuth Pattern as a Function of Frequency

Below the start of the one wavelength resonance region at 380 kHz, the azimuth pattern is almost circular. Fig. 5.8 shows the changes in the azimuth pattern throughout the one wavelength resonance region. At 400 kHz, there is a minimum at zero degrees azimuth, and a maximum at 180 degrees. These quickly change to a peak at zero degrees and a minimum at 180 degrees, at 420 kHz. Above 420 kHz, the lobe at zero degrees azimuth grows relative to the remainder of the pattern, becoming quite pronounced at 480 kHz. At 500 kHz the pattern is returning to circular, and becomes highly so at higher frequencies until the two-wavelength resonance region is encountered.

Fig. 5.9 shows the pattern throughout the two wavelength resonance region. The pattern is characterized by maxima at about 50 and 150 degrees and minima at about 30 and 130 degrees. These features increase in intensity up to 840 kHz then gradually smooth out with increasing frequency. At 1000 kHz the pattern is a circle with ripples of small amplitude due to reradiation. The patterns become increasingly circular up to 1100 kHz.

5.5 RF Current Distribution and Resonance Modes

This section displays the RF current distribution on the towers and skywires in the format of Fig. 5.10 at 200 kHz. At the left the magnitude and phase of the current at two points on each of the five towers is given. Thus for each tower the left point is located at a distance of one-quarter the tower height or 12.6 m above the tower base, and the right hand point at 37.9 m above the base. In Fig. 5.10, the center tower carries the strongest current, which is about twice as strong as the current on the end towers. Note the current scale of 40 microamps. The three center tower currents are at a phase of minus ninety degrees relative to the one volt, zero phase excitation of the broadcast antenna. The end towers are at a phase of about minus forty-five degrees. The right hand portion of the figure shows the current on the four skywires

interconnecting the towers. The current has a strong travelling wave component, exhibited by the phase behaviour, which varies roughly linearly with distance along the skywires. This "travelling wave" behaviour is characteristic of non-resonant skywire currents.

Fig. 5.11 shows the RF current distribution that exists on the towers and skywires at "one wavelength loop resonance" at 420 kHz. The tower currents are all in phase, and the three center towers carry currents twice as strong as the end towers. The skywire currents are pure standing waves, have constant-phase-with-distance, and exhibit zero current at the skywire centers with corresponding sharp 180 degree phase reversals. The RF current distribution for "one wavelength loop resonance" can be visualized as in Fig. 5.12.

Fig. 5.13 shows the RF current distribution at 460 kHz, in the trough between one wavelength loop resonance and the two wavelength double-loop resonance mode discussed below. The center loops are not resonant but the two end loops carry typically resonant current distributions.

Fig. 5.14 shows the current distribution at 480 kHz and illustrates "two wavelength double-loop resonance". Here the resonant path consists of a tower, the skywire to the second tower, that tower and a return path in ground. This path spans two loops and is of length (2x50.9 + 2x274) x2 = 1300 m and is two wavelengths long at 462 kHz, which is reasonably near the 480 kHz value evident in the computed results. The current distribution is similar to the familiar RF current for two wavelength loop resonance, except spread across two skywires of the power line, and is sketched in Fig. 5.15. In this double-loop mode a minimum in the current is expected at about 40 percent of the tower spacing from one tower, then again at about 60 percent of the spacing on the next skywire, and is clearly seen in Fig. 5.14. The important difference between the modes of Fig. 5.11 and 5.14 is that in the former the current has a minimum at the skywire center, while in the latter the minima are shifted from the center.

Fig. 5.16 shows the RF current distribution at the non-resonance frequency of 700 kHz. The magnitude of the current is much smaller than in Fig. 5.14, because the scale is changed from 5000 microamps to 200 microamps. Note the linear-phase-with-distance behaviour.

Fig. 5.17 shows the RF current distribution of "two-wavelength loop resonance" at 840 kHz. Here the path of a tower, the skywire to the next tower, that tower, and the return path in ground is two wavelengths long. Adjacent tower currents differ in phase by 180 degrees, and the skywire current exhibits constant phase with distance behaviour, and abrupt phase reversals at minima in the current. The skywire current has a

maximum at the skywire center, and sharp minima near each tower. The RF current distribution for this mode can be visualized as in Fig. 5.18.

Fig. 5.19 shows the computed RF current distribution for "four wavelength double-loop resonance". Here a two-loop path is about four wavelengths long and the current distribution can be idealized as in Fig. 5.20. Thus three peaks and four minima are expected across two skywires. Also, the minima are unsymmetric with respect to the center of a skywire, but are symmetric about the center tower of the double loop. This behaviour is evident in Fig. 5.19.

Fig. 5.21 shows the RF current at the top end of the frequency band under study, at 1100 kHz. The current is typically non-resonant.

5.6 Resonance Chart

The frequencies at which "loop resonance" and "double loop resonance" are expected to be present can be estimated by setting the total path length equal to multiples of the wavelength. Thus if "h" is the tower height and "s" is the tower spacing, then "n-wavelength loop resonance" is expected for the path length around one complete loop, namely $2 \times (2h + s)$, equal to n times the wavelength. Similarly, for "n wavelength double loop resonance", the loop length of a path spanning two skywires, namely $2 \times (2h + 2s)$, must equal n wavelengths. For $h = 50.6$ m, these estimates of resonant frequency are plotted in Fig. 5.22 as a function of the tower spacing "s". For the 274 m tower spacing, the chart gives estimates of the resonant frequencies which are in reasonable agreement with the frequency sweep computations of Figs. 5.5 and 5.7.

5.7 Frequency Dependence for a Nine Tower Power line

Increasing the number of towers from five to nine creates paths for additional resonance modes. Fig. 5.23 shows the max-to-min ratio as a function of frequency with nine towers. In comparison to Fig. 5.5, it is seen that an additional peak at about 520 kHz and another at 1020 kHz are present. Note that the frequency step of 20 kHz in Fig. 5.23 is not fine enough to resolve two closely spaced peaks such as those of Fig. 5.5.

5.8 Summary

This chapter has investigated the resonant modes of the evenly spaced power line with five towers, and identified a one-wavelength and a two-wavelength resonance region. Each

region exhibits two important resonant modes, one of which is a simple loop resonance and the other a resonance mode across two loops. The azimuth patterns in each resonance region have been presented and the RF current distribution has been exhibited for each mode. With more towers, additional resonance modes are possible and the spectrum exhibits additional maxima.

It should be emphasized that this study has involved one very specific excitation, and that the results would differ if another excitation were used. It is expected that the frequencies of resonance of the power line are independent of the excitation, and that the resonant modes described could be excited with other broadcast antenna configurations. However, there may be other resonance modes at other frequencies which are weakly excited in the present study, but which could be much more strongly excited by other broadcast antenna configurations.

6. Detuning Power Line Resonances with Stubs

It has been demonstrated by direct measurement in reference (8) using the 200 scale factor model of the evenly spaced power line that by adding the "stub detuner" shown in Fig. 6.1 to each skywire the azimuth pattern becomes nearly circular and so the resonance of the power line is effectively suppressed. Such a detuner was described by Sawada and Nakamura in reference (9). This chapter establishes the validity of a computer model of the stub detuner by comparison with measurements, and then investigates the design of stub detuners for both the one and the two wavelength loop resonance modes. The frequency dependence of the line with each detuner in place is examined over a wide band to show that the detuners shift the resonant frequencies. In conclusion, the elevation patterns are examined to demonstrate that the detuners do not radiate at high angles.

6.1 Validity of the Detuner Model

6.1.1 Behaviour with no Detuning Stubs

The validity of the "single wire" tower computer model for the representation of the 200-scale factor towers without detuners is demonstrated in this section. Fig. 6.1 shows the geometry of the three tower model, which was used without the detuning stubs for the results of this section. The dimensions were (full scale) : tower height 50.6 m(166 ft) ; tower separation 274.3 m(900 ft) ; distance to antenna 448.1 m(1470 ft) ; tower "equivalent radius" 3.51 m ; and skywire "equivalent radius" 0.71 m . At 860 kHz, the computed azimuth pattern is that shown in Fig. 6.2 as crosses. The measured pattern, which is shown as a solid line, is taken from reference (8) Fig. 13 and was measured at a scaled frequency of 172 MHz. The patterns are in good agreement although the slight shift in the depth of the minima and the angles of the maxima and minima suggests that a small discrepancy exists either between the frequency of the computation and the measurement, or in the model dimensions between the two cases.

In reference (10), Lavrench reported the azimuth pattern measured in the frequency range of two wavelength loop resonance and the max-to-min ratio of these patterns is plotted in Fig. 6.3. It is seen that the power line is resonant at about 860 kHz. The max-to-min ratio was computed at the same frequencies, and is also plotted in Fig. 6.3. The agreement is considered satisfactory. The width of the two resonance curves is comparable, which is notable because previous computed resonance curves have been too narrow. Also, note that with only three towers the azimuth pattern is "scalloped" much less

than with thirteen towers, and indeed the "scalloping" of less than 1 dB at CBL's frequency of 740 kHz hardly requires "detuning" at all.

For later reference, the RF currents flowing on the three towers without detuning stubs at 860 kHz are plotted in Fig. 6.4. The currents on the three tower model behave as expected from previous work. The current is strongest on the center tower. The phase changes by 180 degrees from tower to tower. The current on the skywires is a standing wave because it has constant phase with position, indicating the frequency is near the power line's resonant frequency. The current has a maximum at about the center of the skywire, and has nulls with corresponding abrupt 180 degree phase reversals at about 60 m from each tower.

6.1.2 Pattern with One Detuning Stub

A measured azimuth pattern at 860 kHz using one detuning stub of the type shown in Fig.6.1 on each skywire is reported in reference (6) Fig. 17. The geometry of the experimental model differs somewhat from that of Fig. 6.1 in that the stubs were located near tower # 2 on the skywire connecting tower # 1 to # 2, and near tower # 3 on the other skywire. Also, the stub was "hung" below the skywire in the measurement but located at the same height and behind the skywire in the calculation. The measurement was repeated for stub spacings "d" varying from 0.32m(12.5 inches) to 1.27 m(50 inches) full scale and little change was noted in the pattern. For convenience, the computer model was set up as shown in Fig. 6.1, with the stub behind and at the same level as the skywire. The skywire's 'equivalent radius' of 0.71 m was used for the stub as well, and so to avoid overlapping of the stub and the skywire, "d" had to be chosen greater than 1.42 m. A spacing of one-twentieth of a wavelength or 17.4 m at 860 kHz was chosen. The length of the stub was one quarter wavelength at 860 kHz, or 87.2 m. Thus the stub in the computation had an electrical path length (d+l) which is significantly longer than that used in the measurement. In spite of these differences, the computer model reproduces the measured pattern very closely as shown in Fig. 6.5. Unfortunately, no measured data is available for the frequency dependence.

Fig. 6.6 shows the currents on the towers and skywires in part (a) and on the connecting links and stubs in part (b), respectively. In comparison with Fig. 6.4, the tower and skywire currents have been reduced by a factor of six. The skywire currents are completely altered in character. The skywire can now be divided into two portions, each carrying a travelling wave. The two portions are separated by the null in the current that occurs at about forty percent of the length of the skywire from the tower nearest the stub. Fig. 6.7 is a sketch of the pattern of the current flow on the model. The

currents are primarily travelling waves and flow essentially up tower # 1 and along the skywire, decreasing to zero in magnitude. Then, starting again from zero, the travelling wave flows along the skywire, and is joined by an incoming wave from the adjacent skywire, and flows down the center tower. The structure behaves as three top loaded monopole antennas.

6.1.3 Mechanism Which Makes Detuning with Stubs Effective

Put simply, the stub is a low impedance element which is connected across a high impedance point on the skywire-image-skywire transmission line, and so upsets the resonance present on that line. The stub is effective by virtue of its being placed near a location on the skywire where the current on the "un-detuned" line has a minimum. At such a point, the current magnitude is small so the circumferential H-field is small, but the current is changing rapidly so the linear charge density is high and the radial E-field is high. A useful definition of "impedance" is the ratio of radial E to circumferential H, and a current minimum is therefore a point of high E, low H and so high impedance. To disturb the resonant structure considerably, a low-impedance element should be connected at such a high impedance point. One such point is the current minimum on the skywire near each of the towers. A stub of length approximately a quarter wave presents a suitable low impedance element to connect at this point. At the open end of the stub, H is approximately zero because the current is zero, and so the impedance is high. However, approximately one quarter wave away from the open end, H is a maximum, and the radial E field is small because the current magnitude has a maximum and its derivative, proportional to the linear charge density, is zero. Radial E is proportional to the linear charge density as well, and so radial E has a minimum. Thus at about a quarter wave from the open end, the stub presents a low impedance - small E over large H. This low impedance element is connected to a high-impedance point on the original structure, namely at the current minimum, and so alters the current distribution and destroys the resonance. Note that the location of the connection point for the stub in Fig. 6.6 corresponds closely with the location of the current minimum on the skywire in Fig. 6.4, which is a high impedance point on the transmission line.

It is demonstrated in Sections 6.2.1 and 6.3.1 that the stub performs best when it is connected at the location of the current minimum on the resonant structure, and that the stub becomes much less effective as it is moved away from this optimum position. Before this study is presented, a further comparison with the NRC measurements is given.

6.1.4 Frequency Dependence with one Detuning Stub

Fig. 6.8 compares the max-to-min ratio for the three tower

power line using one detuning stub as described above, with that of Fig. 6.3 using no stub. It is seen that the power line is effectively detuned over the range shown in the figure, particularly near the stub's "design frequency" of 860 kHz. Above this frequency the max-to-min ratio rises sharply. An investigation of the frequency dependence over a wider range is presented below.

6.1.5 Frequency Dependence with Two Detuning Stubs

In reference (10), Lavrench reports the measured azimuth pattern as a function of frequency with two detuning stubs connected to each skywire of the three tower, 200 scale factor model, as shown in Fig. 6.9. The lengths were chosen to be one-quarter wavelength at the full scale frequencies of 740 and 860 kHz, and were 87.38 m and 101.09 m full scale, respectively. The gap between the open ends of the stubs corresponds to 0.32 m full scale, and that value was used in the calculations. The separation "d" of the stub from the skywire was maintained at 17.4 m in the calculation. Fig. 6.10 shows the measured and computed max-to-min ratio of the pattern as a function of frequency. With the two stubs in place, the frequency dependence is quite flat and no resonance is evident. The computed curve is about three-quarters of a dB less than the measured curve. This discrepancy may be due either to the fact that the stubs in the computer model are somewhat longer than in the measurement because "d" was used as 17.4 m, or to the close spacing of the ends of the two stubs used to compute Fig. 6.9. The wires used for the stubs had radii equal to the skywire radius, and two such large wires spaced so closely couple capacitively. A larger spacing of the open ends of the stubs, or a closer spacing of the stub and the skywire may give results which agree more closely with the measured max-to-min ratio.

This section has demonstrated that the computational technique can successfully predict the azimuth pattern and frequency dependence of the three tower, 200 scale factor power line, when it is "detuned" with stub traps. The following sections investigate the stub's effectiveness for the one and for the two wavelength loop resonance modes, as a function of the stub's length and location on the skywire.

6.2 Stub Detuning for the One Wavelength Loop Resonance Mode

6.2.1 Stub Design

Fig. 6.11 shows the detuner configuration used for detuning the one wavelength loop resonance mode at 430 kHz. The tower spacing is somewhat less than one half wavelength, and so the detuner of length equal to roughly one-quarter wavelength extends from near the center of the skywire to a point beyond the adjacent tower. The spacing of the stub, "d", was chosen as

5 m, being a "safe" value to use with the NEC code in conjunction with the stub and skywire radii of 0.71 m. The design of the stub then consists of choosing the total length, s = d + b and the stub position, "p", to obtain the best performance.

It is expected th of the stub at the overall length will be near one-quarter wavelength. A "design" frequency of 430 kHz was chosen for this detuner, and the study was carried out using a five tower power line. The initial position of the detuner was chosen as p = 137 m, or halfway between the towers. Fig. 6.12 shows the max-to-min ratio as a function of the stub length, s . It is seen that the stub is effective for a wide range of lengths from about 120 to about 190 m, but is most effective when about 175 m long, which is one quarter of the free space wavelength in total path length d + b at the design frequency of 430 kHz.

Fig. 6.13 shows how the max-to-min ratio changes as the stub is moved along the skywire from p = 95 to p = 172 m. The stub is quite effective for all positions tried, and the max-to-min ratio is always less than one dB, indicating that the pattern is almost circular. The best location is at about 120 m. Thus neither the position nor the stub length for the one wavelength resonance region is critical.

6.2.2 Out of Band Response

Fig. 6.14 shows the max-to-min ratio of the azimuth pattern of the five tower power line, with a detuner connected to each skywire, with length s = 174 m at position p = 102 m. Although p = 102 m is not quite the optimum position, Fig. 6.13 shows that there is only a difference of 0.2 dB in the resulting max-to-min ratio. The stub effectively suppresses the reradiation in a band roughly 100 kHz wide centered around its design frequency of 430 kHz. In comparison with Fig. 5.5, it is seen that the stub does away with the resonances at 430 and 480 kHz but new resonances are introduced at 230 kHz, and at 510 and 560 kHz. These modes involve current paths along the stubs. In contrast, the two wavelength resonance region is not affected at all by the presence of the detuners. This is probably because the detuner is connected at a low impedance point in the RF current distribution for two wavelength resonance. The graph shows that if a power line is detuned with stubs designed for a certain frequency, then a station on a nearby frequency can be strongly affected by the "detuned" power line, even though it was not affected prior to "detuning".

6.3 Stub Detuning For the Two Wavelength Loop Resonance Mode

In this section a stub detuner is designed for the two wavelength resonance mode, at 860 kHz, for a nine tower power

line. In addition, the "straight" and the "bent" stubs of Fig. 6.15 are compared. The "straight" stub is used here to demonstrate that the detuner acts as a low impedance element connected at a high impedance point on the skywire and image transmission line, and not as a high impedance element in series at the center of the skywire, as suggested in reference (9). In fact it is shown that the behaviour of the "straight" and the "bent" stubs is very similar. The former provides a simplified heuristic model for understanding stub design, whereas the latter may be developed into a practical detuner for real power lines.

6.3.1 Stub Design

The separation of the stub and end effects at the open wire end contribute additional length to the stub so that the optimum choice is not simply one-quarter of the free space wavelength at the design frequency. Also, as will be shown, the effectiveness of the stub is strongly dependent on where it connects to the skywire. In the following, a comparison is made between the "straight" stub oriented perpendicular to the skywire, as shown in Fig. 6.15, and the "bent stub" which is parallel to the skywire for most of its length. Each stub must be "designed" by choosing its length s = d + b and its position p.

Fig. 6.16 shows the max-to-min ratio at 860 kHz as a function of the position "p" of the stub, being the point where the stub is connected to the skywire. Evidently both straight and bent stubs perform best when connected about 50 m from the tower, and the max-to-min ratio rises sharply as the stub is moved away from this position. The current distribution on the nine tower power line is similar to that on the three tower line of Fig. 6.4, and shows that the best connection point is also the location of the sharp minimum in the current on the skywire. Such a "current zero" is a high impedance point on the transmission line. Fig. 6.16 does not imply that bent stubs are better than straight stubs, however, because here the straight stub is not of optimal length.

Fig. 6.17 examines the effect of stub length when the stub is placed in the best position from Fig. 6.16. The max-to-min ratio has minimum at an "optimum" length, and the max-to-min ratio rises rapidly as the stub length is changed. Thus the straight stub works best when it is of length about 110 m, and the bent stub is best of length about 105 m. The two behave in a very similar manner. The choice of the length of the bent stub is somewhat more critical than that of the straight stub because the curves of Fig. 6.17 rise more rapidly for the bent stub.

6.3.2 Out of Band Response

Fig. 6.18 shows the response of the nine tower power line

including a bent stub on each skywire, designed for 860 kHz. It is seen in comparison with Fig. 5.23 that the resonance between 800 and 900 kHz is suppressed, but that the line is still resonant around 1000 kHz. But the resonant behaviour in the one wavelength resonance region is altered completely by the detuner intended for two wavelength loop resonance. A strong resonance is introduced at 370 kHz, being excessive in the computation because no resistive loss in the wires has been accounted for in the present computer model. The large max-to-min ratio represents a deep null in the radiation pattern. Also, a new resonance at 640 kHz is introduced by the detuner. Thus the addition of detuners for two wavelength loop resonance can affect other stations at quite different frequencies by changing dramatically the behaviour of the power line.

6.4 Elevation Patterns with Detuning Stubs

The detuning stubs would be of little value if they were to radiate in the elevation planes, and in this section it is established that the detuners suppress radiation in elevation as well as in azimuth.

The five tower power line shown in Fig. 5.1 carries the strong RF currents of the "two wavelength loop resonance" mode at 860 kHz, and the scalloped azimuth pattern is shown in Fig. 5.9(c). Fig. 6.19 shows the elevation patterns for azimuth angles of 0, 45, 90, 135, and 180 degrees. The elevation pattern for zero degrees azimuth is the same as that for the broadcast antenna with no power line. The elevation pattern for 135 degrees azimuth shows that the power line radiates strongly at 30 degrees elevation. Note that each pattern of this set is individually normalized to unity and field strengths cannot be compared with Fig. 5.9. Fig. 6.19 shows the E-theta polarization as a solid line, and also shows the E-phi polarization as small circles. Thus in Fig. 6.19 (b) the phi polarization has a lobe at 30 degrees elevation, or 30 degrees up from the horizon, which is 60 degrees from the vertical. The level of this lobe is about 0.27 of the maximum of the theta-polarized field. Similarly in the pattern for 135 degrees azimuth, there is a strong lobe in the phi polarizatin as shown in Fig. 6.19 (d).

When a "straight" detuning stub of length 115 m and spacing 50 m from the tower is included on each of the four skywires of the five tower power line of Fig. 5.1, the reradiation in the elevation plane is fully suppressed, as shown in Fig. 6.20. Also, when a "bent" detuning stub of length 105 m and spacing 50 m from the tower is included on each skywire, the reradiation in elevation is also effectively suppressed, as shown in Fig. 6.21. The "bent" stub design also radiates less in the cross-polarized component than does the "straight" stub. Also, the figure shows that the power line's radiation in the

phi-polarization is effectively suppressed by the use of the detuning stubs. Thus in Fig. 6.20 the largest radiation in the phi component occurs in the elevation pattern for 90 degrees azimuth, where the phi- polarized field has a small lobe at about 50 degrees elevation, at a level of about 0.15 of the main lobe of the theta-polarized field. The "bent" stub suppresses radiation in the phi polarization even better than does the "straight" stub, as demonstrated by the elevation patterns of Fig. 6.21.

Thus it has been demonstrated in this section that the detuning stubs do not themselves radiate in elevation, and in addition are effective in suppressing the reradiation from the power line into the elevation planes.

6.5 Capacitive-Loaded Short Stub

A more practical design than the "bent stub" may be the capacitive-loaded (C-loaded) short stub shown in Fig. 6.22. This stub behaves as a short length of transmission line which is loaded at its end by an ideal capacitance, of value chosen so as to make the input impedance small, as seen at the terminals where the stub is connected to the power line. The dimensions chosen for this study were : power line tower height "h" 50.6 m ; stub length "b" 42.2 m ; and stub separation "d" 15 m. Thus the total length of the stub is s = d + b = 57.2 m or 0.16 wavelength at 860 kHz. This C-loaded short stub is effective in detuning the two wavelength resonance mode, provided that the appropriate capacitance value is chosen. Thus Fig. 6.23 shows the max-to-min ratio of the azimuth pattern as a function of the capacitance in picofarads. The pattern with no stubs has a max-to-min ratio of about 6 dB and so a poor choice of capacitance does improve the pattern somewhat. The best choice of about 250 picofarads smooths the azimuth pattern to within one dB. Note that the unstable behaviour between 200 and 240 picofarads appears to be due to an inadequacy of the NEC computer program for this specific problem. This short investigation was of an exploratory nature and no special attempt was made to duplicate the experimental geometry tried in the measurements at NRC reported in reference (11).

Thus the results corroborate that the C-loaded short stub is a useful alternative to the bent stub on the skywire, and its design should be investigated further.

6.6 Summary

This chapter has investigated the detuning of power lines with stubs. It was found that the "bent detuning stub" hung parallel to the skywire is effective for both the one and the two wavelength resonance modes, that it should be made about a

quarter of a wavelength long, and that it must be connected to the skywire at a minimum in the RF current on the resonant structure. An alternative stub design was also considered, consisting of a short stub on the tower, loaded at its open end by a capacitance. This stub design was found to be effective and merits further computational study.

7. Preliminary Study with Finite Ground Conductivity

In this initial study a 195 m (640 ft) monopole antenna over an eight radial ground screen was used to illuminate a three tower power line, using the 50.9 m (167 ft) tower height and 274.3 m (900 ft) tower spacing derived from the Hornby site. In the following, the RF currents on this structure and the azimuth and elevation patterns are compared for three cases, namely : (i) perfect ground using the method of images ; (ii) finite conductivity ground using the Sommerfeld-Norton model with "typical" permittivity and conductivity values provided by the CBC ; and (iii) the Fresnel reflection coefficient model for lossy ground. The Sommerfeld-Norton ground ("SN ground") uses the Sommerfeld integrals for ground fields when the interaction distance is small and Norton's asymptotic approximations for larger distances(12,13). It is a rigourously correct mathematical model for structures entirely above the ground. For wires that connect to the ground, the NEC computer code assumes that the derivative of the current with respect to distance along the wire is zero at the connection point to ground, in order to obtain a boundary condition necessary for the solution to proceed. This assumption is rigourously correct only for a perfect ground, but is considered quite reasonable for modelling the bases of those hydro towers which are well grounded.

The Fresnel ground uses plane wave reflection coefficients to compute the interaction of segments above a lossy ground, and is not rigourously valid for segments close to or connected to ground.

7.1 The Monopole and Ground Screen

A 195 m (640 ft) monopole over a ground screen of eight radial wires was used as a source antenna, as shown in Fig. 7.1. The radials were uniformly spaced and chosen to be 0.4 wavelengths long at the operating frequency of 860 kHz. The antenna was modelled with eight segments and each radial wire with four segments. The computer code does not allow any part of any wire to lie below the ground surface at z=0, nor can wires lie in the z=0 plane. For this reason the radials of the ground screen were arbitrarily raised to five meters or 5/348 of the wavelength above the ground(13). Recent work has shown that this can be reduced to an insignificant height above the ground plane without loss of accuracy in the results.

Fig. 7.2 shows the elevation pattern of the monopole and eight radials, computed at a distance of 10,000 meters which is 28 wavelengths at 860 kHz. The figure compares the elevation patterns with a perfectly conducting ground to that with the Sommerfeld-Norton ground model and the Fresnel ground model, using as ground parameters a relative permittivity of 15 and a

conductivity of 0.02 mhos meter. The three cases give rise to quite similar elevation patterns, the main difference being that with finite ground conductivity the field goes to zero as the surface of the ground is approached(as theta approaches ninety degrees). This happens because only the "space wave" and not the "ground wave" has been included in the computation(11,12). The elevation pattern has a small lobe near 30 degrees from the vertical because the 195 m monopole is somewhat taller than a quarter wavelength at 860 kHz. It is of interest to note that the Fresnel ground model generates a result which is close to that of the Sommerfeld-Norton ground model.

When the ground wave is included in the calculation of the far field, then the field becomes constant as theta approaches ninety degrees, as shown in Fig. 7.3. The ground wave is not readily included in the computation of elevation patterns, due to a limitation of the NEC computer code(12,13).

7.2 Antenna Plus Power Line

A three tower, two loop "power line" was introduced near the antenna as shown in Fig. 7.4, using radii of 3.51 m for the towers and 0.71 m for the skywires, respectively. The elevation pattern is very similar to that with no power line, and will not be shown. Fig. 7.5 compares the azimuth patterns for the perfect ground, Sommerfled-Norton ground model, and the Fresnel ground. The field with the perfect ground is somewhat stronger than that using either of the finite conductivity models. The patterns with the Sommerfeld-Norton ground model and the Fresnel ground model are quite similar. The perfect ground model gives rise to larger variations with azimuth direction, having a max-to-min ratio of 3.6 dB compared to 3.4 dB with the Sommerfeld-Norton ground model. The Fresnel ground model gives an azimuth pattern quite similar to the Sommerfeld-Norton model, but with a somewhat smaller max-to-min ratio.

To compare the methods in terms of running time, note that the SN ground model requires an investment of 220 CPU seconds to generate a table of values from which the Sommerfeld integrals are calculated by interpolation, and then a further 308 seconds to compute the RF currents and radiation patterns in the presence of the ground. The table of values can be reused for other configurations at the same frequency with the same ground. The Fresnel ground requires 255 CPU seconds but the perfect ground only 66 seconds. Clearly the perfect ground approximation is quite economical compared to the other models. Also, the rigourous SN ground model requires only 25 percent more running time than the Fresnel model, given the table of values for the evaluation of the Sommerfeld integrals.

7.3 Comparison of the RF Current Distributions

Figs. 7.6 and 7.7 show the RF current distributions with the perfect ground model and with the Sommerfeld-Norton ground model, respectively. Thus Fig. 7.6(a) and 7.7(a) show at the left the current on one radial of the eight wire ground screen, and at the right the current on the monopole, and demonstrate that the inclusion of the finite conductivity of the ground in the model has little effect on these currents. Comparing the RF current distribution on the towers and skywires of the power line in Figs. 7.6 (b) and 7.7 (b) shows that the current distribution with the perfect ground model is almost identical to that with the Sommerfeld-Norton ground model. The two are identical in phase, and differ in magnitude by a simple scale factor. Thus above perfect ground the current near the base of the center tower is 1100 microamps, whereas above a ground of finite conductivity, this current is reduced to 900 microamps, both relative to a one volt source at the base of the broadcasting tower.

7.4 Summary

This preliminary investigation of the effect of the finite conductivity of the ground on the reradiated fields indicates that the radiation patterns in the presence of the imperfect ground will not be greatly different from those computed over a perfectly conducting ground. The investigation must now be extended to include an assessment of the changes that take place in the resonant frequencies of the power line when the finite conductivity of the ground is included in the computations.

8. Summary and Recommendations

This chapter summarizes the state of development of the numerical modelling of the reradiation of RF energy at MF frequencies from high-voltage power lines, and makes recommendations for further work.

8.1 Electrically Equivalent Tower Models

The "single wire tower model" with the equivalent tower radius of 3.51 m and skywire radius of 0.71 m was developed in reference (3) to represent power line towers of the "V1S" design, of height 50.6 m. The equivalent radii were chosen based on Jaggard's isoperimetric inequalities(14), which specify a range of possible radii. The best value within that range was chosen by carrying out a parametric study of the resonant frequency of the power line as a function of the radii of both the tower and the skywire, and "matching" the frequency of two wavelength loop resonance of the 600 scale factor measurement model. It is recommended that a catalog of such simple models be developed in a similar way, each electrically equivalent to a specific tower design. A step in this direction is the development of a model of the type "Z7S" tower, for which some measured patterns are already available(7).

8.2 Prediction of Null Filling

Chapter 3 demonstrated that the "single wire tower model" provides a good indication of the level of radiation into the nulls of a directional pattern to be expected from a power line, but the measured data available were not sufficiently extensive to establish whether the precise structure of the reradiated field in the null is obtained. Further measurements are required, particularly at frequencies where the power line is resonant, and for configurations where the power line is not oriented such that the axis of the power line aligns with the nulls in the directional pattern. Swept frequency measurements would be valuable.

The computation of scalloping and of null filling are similar problems, but the latter is considered more difficult because it requires the prediction of the sidelobes of the radiation pattern of the array of power line towers, whereas scalloping requires the prediction of the magnitude and of phase of the main lobe of the array's pattern. Much of the results being obtained for scalloping, such as resonant behaviour and detuning, are directly applicable to the problem of null-filling.

8.3 Resonances of the Evenly-Spaced Power Line

The evenly spaced power line has been studied as a simplified case in which all the tower-skywire-tower-plus-images loops resonate at the same frequency and so the resonant behaviour is quite pronounced. The "single wire tower" model of the type V1S tower was used in Chapter 5 to predict the resonant behaviour from 200 to 1100 kHz, and two resonance bands were identified, each with RF current modes displaying nulls on the skywire in distinct, characteristic locations. Only a small portion of the computed max-to-min ratio curve of Fig. 5.5 has been confirmed by scale model measurements, namely in the region of two-wavelength loop resonance. Additional frequency sweep measurements have become available(7), and should be used to further study the resonance behaviour.

It is recommended that the study of the resonances of the evenly spaced power line be extended to cover the full AM broadcast band, and this study can be expected to uncover three, four, and five wavelength resonance bands near 1200, 1600 and 2000 kHz, respectively.

8.4 Detuning by Isolating Towers

It was shown in Chapter 4 that a simple model of an isolated tower predicts an azimuth pattern in reasonable agreement with the scale model measurements. A model which is more precisely electrically equivalent is considered desirable. It was shown that isolating towers has an effect on the resonant behaviour of the line which cannot be understood in a simple way, for the "isolated" towers can carry strong RF currents. That no simple theory exists to dictate which towers should be isolated makes it necessary to treat a site by trial and error, involving alterations to a "live" high-voltage power line, and extensive measurements in the field. It has not been established at this time whether or not the computer model of a complex site could be used to predict which towers need to be isolated. "Stub detuners" appear to provide a more predictable detuning technique.

8.5 Stub Detuner Design

The design of a stub detuner to suppress a specific resonance mode was investigated in Chater 6. It was found that the detuner should be about a quarter of the free space wavelength in electrical path length, and that the stub should be connected to the skywire at a point where the RF current has a null. It was found that the resonant behaviour of the power line over the full frequency range can be altered by the addition of stubs designed for a single specific frequency, and so the "detuning" of the line for one station may be the undoing

of another.

At this stage, a detuner design which is practical for implementation on actual power lines is required. The C-loaded, short stub appears to be promising. It is recommended that the performance of this device be investigated for a range of lengths, and locations on the resonant structure. As a first step the specific geometry used in previous NRC measurements(11) should be established and modelled. Balmain's ferrite rings(15) may also be useful for detuning by adding series inductance at suitably chosen high-current locations on the resonant structure.

8.6 Modelling of Finite Ground Conductivity

The results of Chapter 7 indicate in a tentative way that the power line over a ground of finite conductivity of typical value for Southern Ontario does not behave in a greatly different way from the power line over perfect ground. The differences in behaviour are of interest, and it is recommended that further studies be undertaken as follows. Firstly, the effect of the ground must be investigated as a function of the ground's permittivity and conductivity. It is of interest to determine the lowest conductivity for which the azimuth pattern is similar to the perfect ground case. Such studies must be confined to a single frequency or perhaps to the specific set of frequencies corresponding to the loop resonance modes. A second study would investigate the effect of a ground of typical conductivity on the resonant frequency of the power line, in the one and two wavelength resonance bands. Shifts in resonant frequency with changes in conductivity are of particular interest.

The verification of such computations by measurement is a particularly difficult problem. No suitable test range exists for scale model measurements, nor is there agreement as to what such a range would consist of. Full scale measurements by the Ontario Hydro Research Division(16) on a three tower "power line" at Milton, Ontario provide a possible corroboration of the computed RF current distribution, and it is recommended that the Milton test site be modelled computationally. In addition, Ontario Hydro's measurements of the RF current distribution on the towers of the power lines at Hornby, Ontario may provide a useful check of the computations.

8.7 Modelling Complex Sites

Given a suitably optimized computer model which is "electrically equivalent" to the specific type of power line tower used on a particular site, the results of reference (3) and Chapter 2 show that the computer model predicts an azimuth

pattern such as Fig. 2.6 which is similar to and preserves the main features of the patterns measured on the 600 scale factor model over a perfectly conducting ground. The RF current distributions on the computer model show where the skywire current has nulls and hence pinpoint suitable locations for the connection of detuning stubs. Further development of the methodology for modelling complex sites requires that the finite conductivity of the ground be included in the computation, although it is not clear that such an enormous computation is economically possible. It may be useful to include the actual heights of the towers of the power line in the computation. In addition, given the large size of a site such as Hornby, Ontario, the land on which the power lines is built is not a particularly good approximation to a flat plane, and this has an unknown effect on the current distributions on the power lines. This is not readily included in the model at present, and would require the development of a considerably more sophisticated version of the NEC computer code.

A model of a complex site could potentially be used to investigate the effect of adding detuners to particular skywires or towers, to determine the minimum number of detuners required to "treat" a given site. It may or may not be necessary to include the effect of finite ground conductivity in such an investigation.

The ultimate goal of this work is the ability to analyse a complex site illuminated by a directional array, and to determine whether reradiation is present at significant levels. The model could then be used to design the optimum detuner configuration for the site by choosing current distribution, and then adding detuners until an adequate reduction in the reradiated field is achieved. The carrying out of the work recommended above would be a significant step in the achievement of this goal.

REFERENCES

1. R. Mittra, ed., "Computer Techniques in Electromagnetics", Pergammon Press, 1973.

2. G.J. Burke, A.J. Poggio, J.C. Logan and J.W. Rockway, "NEC - Numerical Electromagnetics Code for Antennas and Scattering", 1979 International Symposium Digest, Antennas and Propagation, Vol. I, pp. 147-150, IEEE Publication No, 79CH1456-3AP, University of Washington, Seattle, Washington, June, 1979.

3. C.W. Trueman and S.J. Kubina, "AM Reradiation Project", Final Technical Report, TN-EMC-80-03, March, 1980.

4. J.S. Belrose, reported in "The Effects of Re-Radiation from Highrise Buildings, Transmission Lines, Towers and Other Structures Upon AM Broadcasting Directional Arrays", Interim Report No. 1, DOC Project No. 4-284-15010, October 26, 1977.

5. J.S. Belrose, reported in "The Effects of Re-Radiation from Highrise Buildings, Transmission Lines, Towers and Other Structures Upon AM Broadcasting Directional Arrays", Interim Report No. 4, DOC Project No. 4-284-15010, November 1, 1978.

6. J.S. Belrose, reported in "The Effects of Re-Radiation from Highrise Buildings, Transmission Lines, Towers and Other Structures Upon AM Broadcasting Directional Arrays", Interim Report No. 5, DOC Project No. 4-284-15010, February 14, 1979.

7. J.S. Belrose, reported in "The Effects of Re-Radiation from Highrise Buildings, Transmission Lines, Towers and Other Structures Upon AM Broadcasting Directional Arrays", Interim Report No. 10, DOC Project No. 4-284-15010, October 9, 1980.

8. J.S. Belrose, reported in "The Effects of Re-Radiation from Highrise Buildings, Transmission Lines, Towers and Other Structures Upon AM Broadcasting Directional Arrays", Interim Report No. 7, DOC Project No. 4-284-15010, October 10, 1979.

9. Y. Sawada and H. Nakamura, "Development of a New Wave Trap by Parallel Sub-Conductors", ETJ of Japan, Vol. 8, No. 1/2, pp. 70-77, 1963.

10. W. Lavrench, private communication, September 28, 1979.

11. J.S. Belrose, reported in "The Effects of Re-Radiation from Highrise Buildings, Transmission Lines, Towers and Other Structures Upon AM Broadcasting Directional Arrays", Interim Report No. 8, DOC Project No. 4-284-15010, January 30, 1980.

12. G.J. Burke and A.J. Poggio, "Numerical Electromagnetic Code(NEC) - Method of Moments", Technical Document No. 116, prepared for the Naval Electronic Systems Command (ELEX 3041), January 2, 1980.

13. G.J. Burke, E.K. Miller, J.N. Brittingham, D.L. Lager, R.J. Lytle, and J.T. Okada, "Computer Modelling of Antennas Near Ground", Lawrence Livermore Laboratory Technical Report No. UCID-18626, May 13, 1980.

14. D.L. Jaggard, "An Application of Isoperimetric Inequalities to the Calculation of Equivalent Radii", Proc. of the National Radio Science Meeting, Boulder, Colorado, Nov. 1979.

15. K.G. Balmain, "Reradiation of AM Broadcast Signals from Power Lines and Buildings", Progress Report No. 4, University of Toronto, Feb. 6, 1981.

16. D.E. Jones, "Interim Report to Meeting No. 15 of the Working Group on Reradiation Problems in AM Broadcasting", Ontario Hydro, Research Division, Feb. 6, 1981.

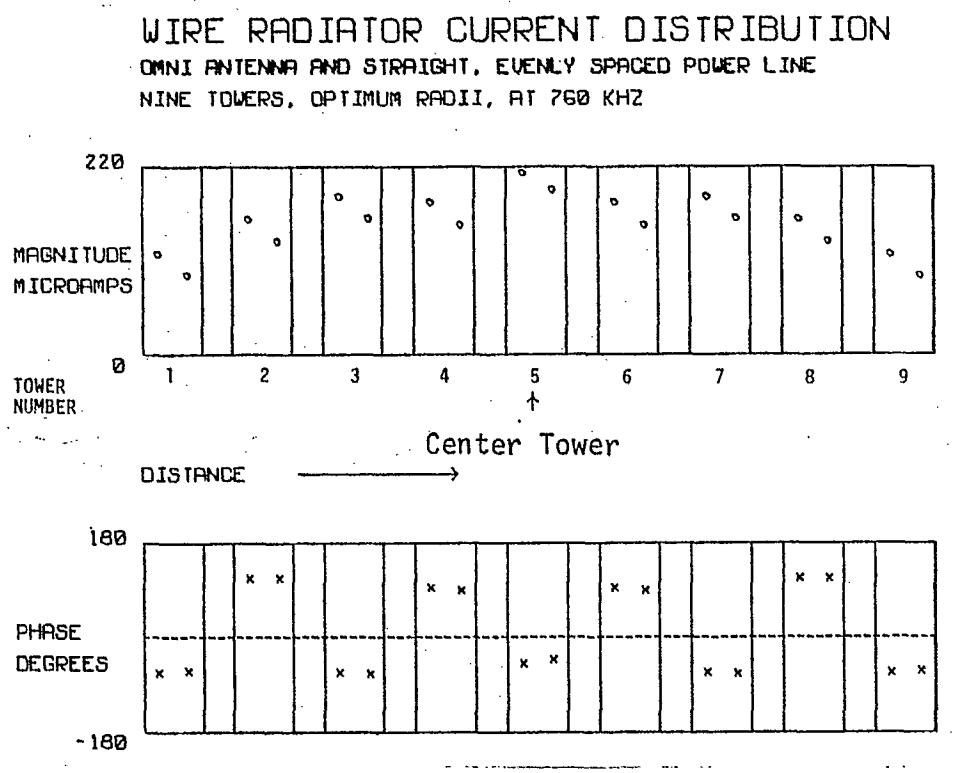

Figure 2.1 (a)

RF currents on the towers, at 760 kHz.

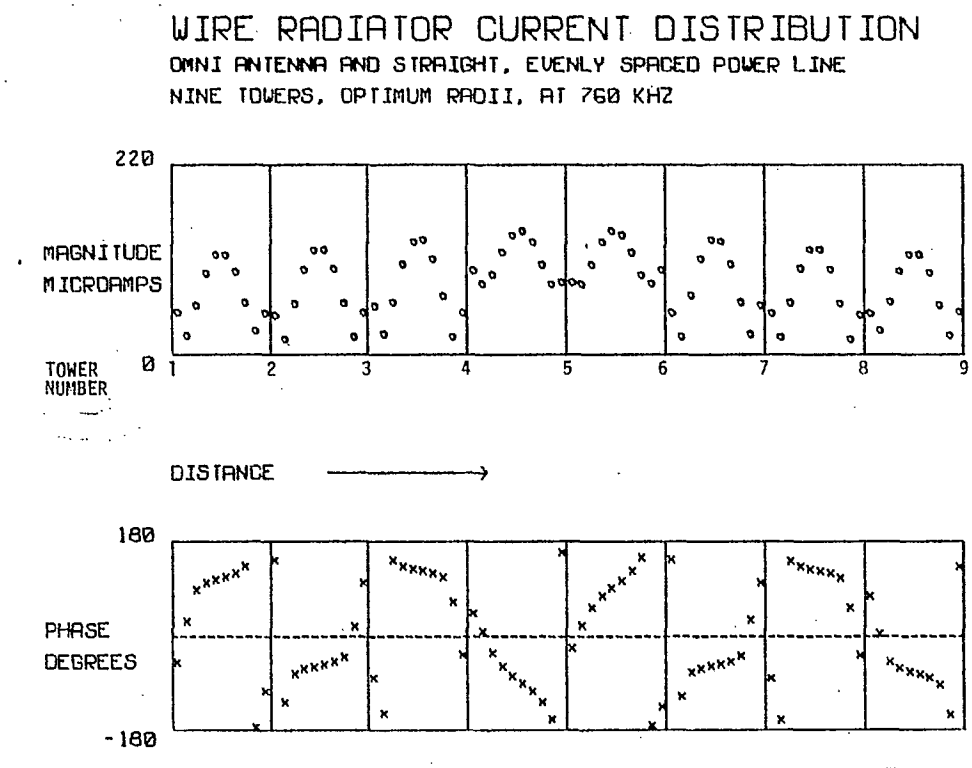

Figure 2.1 (b)

RF currents on the skywires, at 760 kHz.

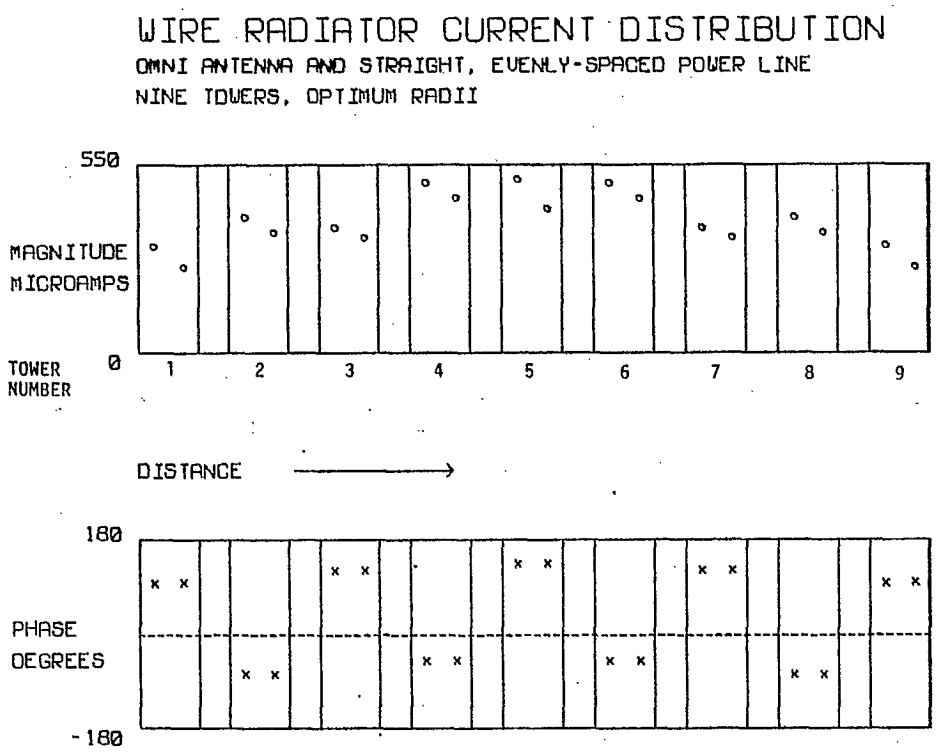

Figure 2.2 (a)

RF currents on the towers at 860 kHz.

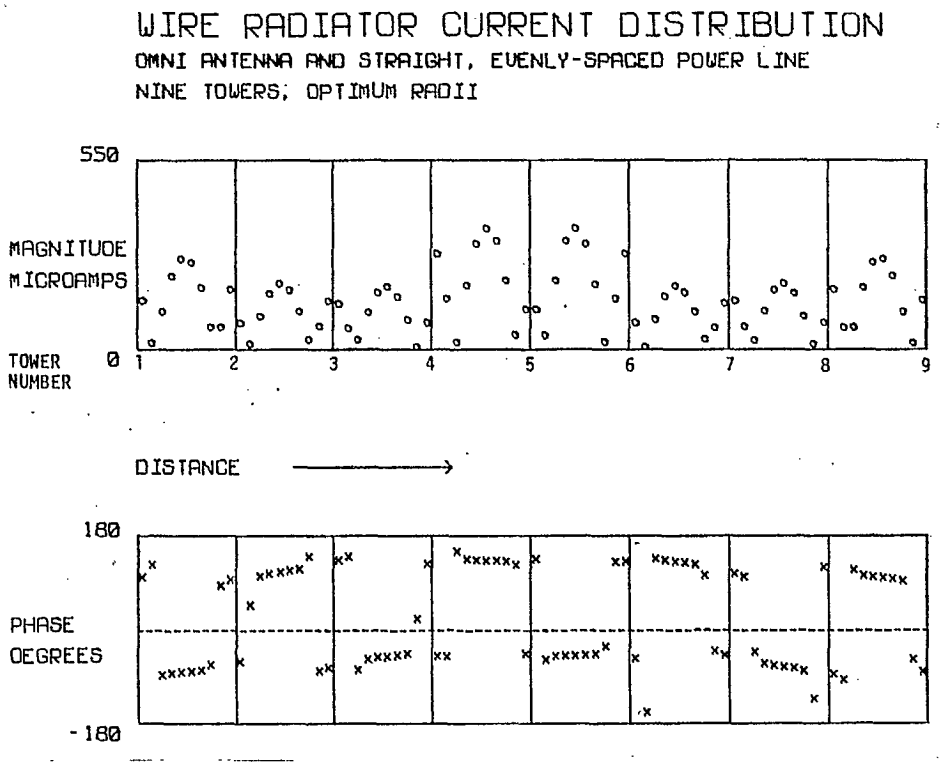

Figure 2.2 (b)

RF currents on the skywires at 860 kHz.

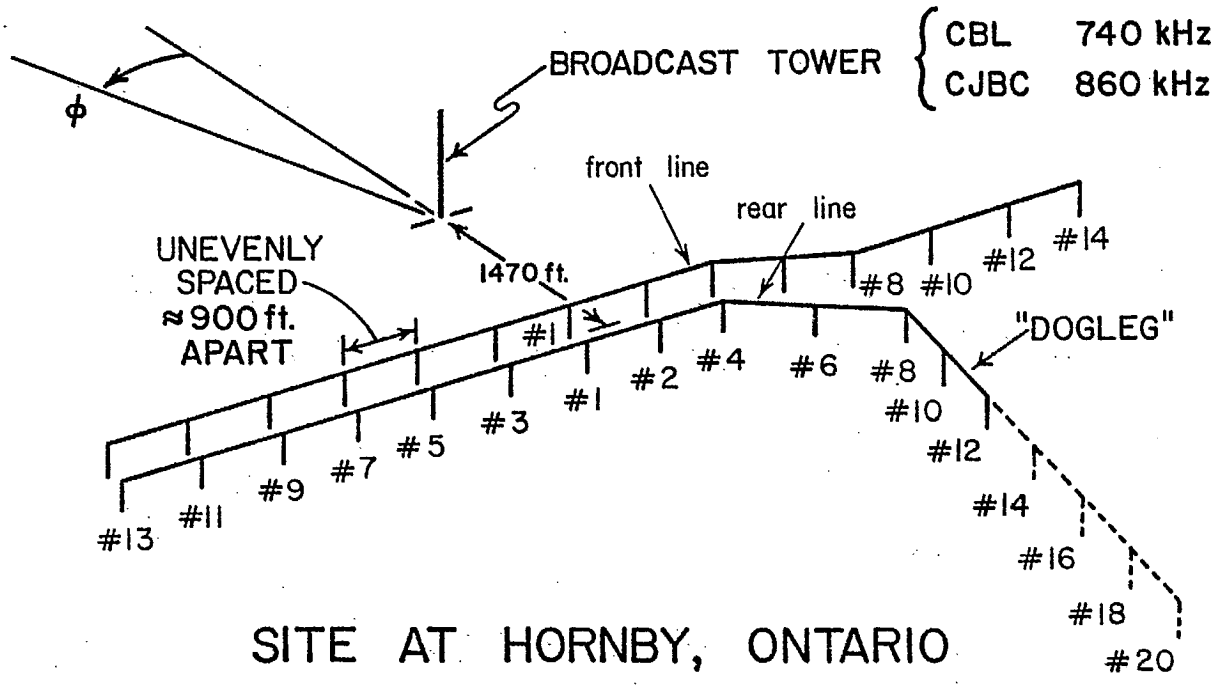

Figure 2.3
Tower numbering for the Hornby site model.

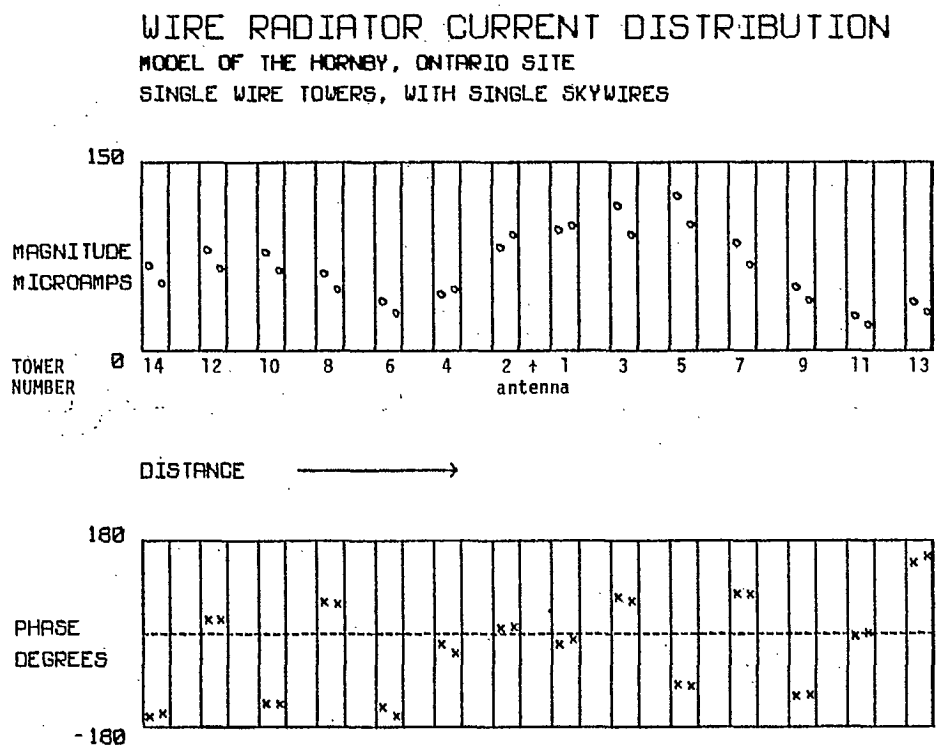

Figure 2.4 (a)

RF currents on the towers of the front line at 740 kHz.

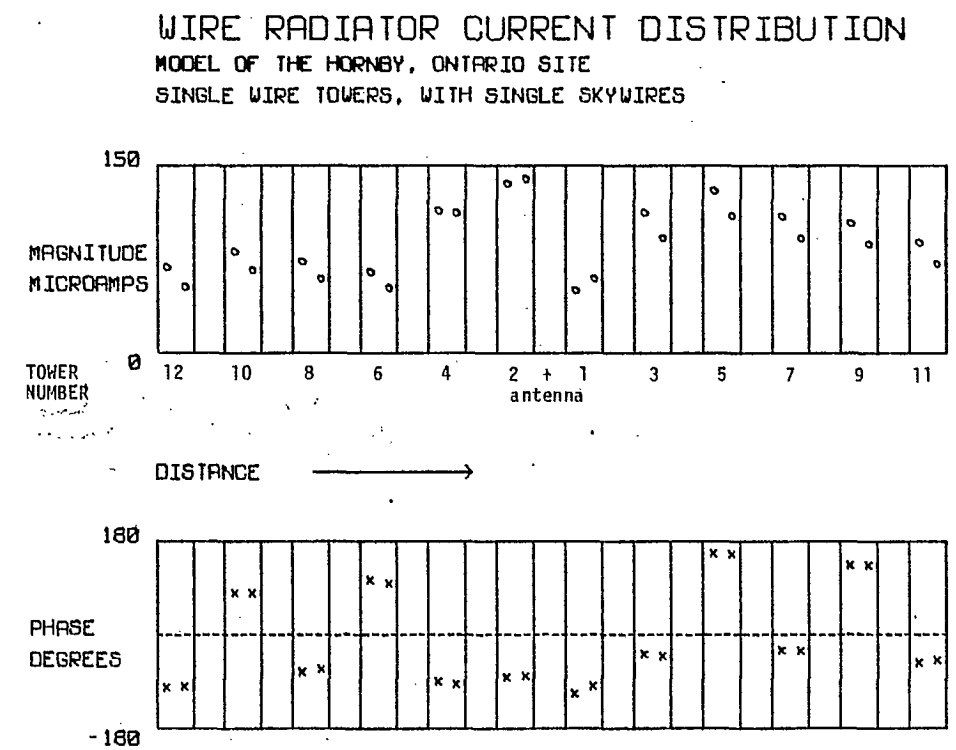

Figure 2.4 (b)

RF currents on the towers of the rear line at 740 kHz.

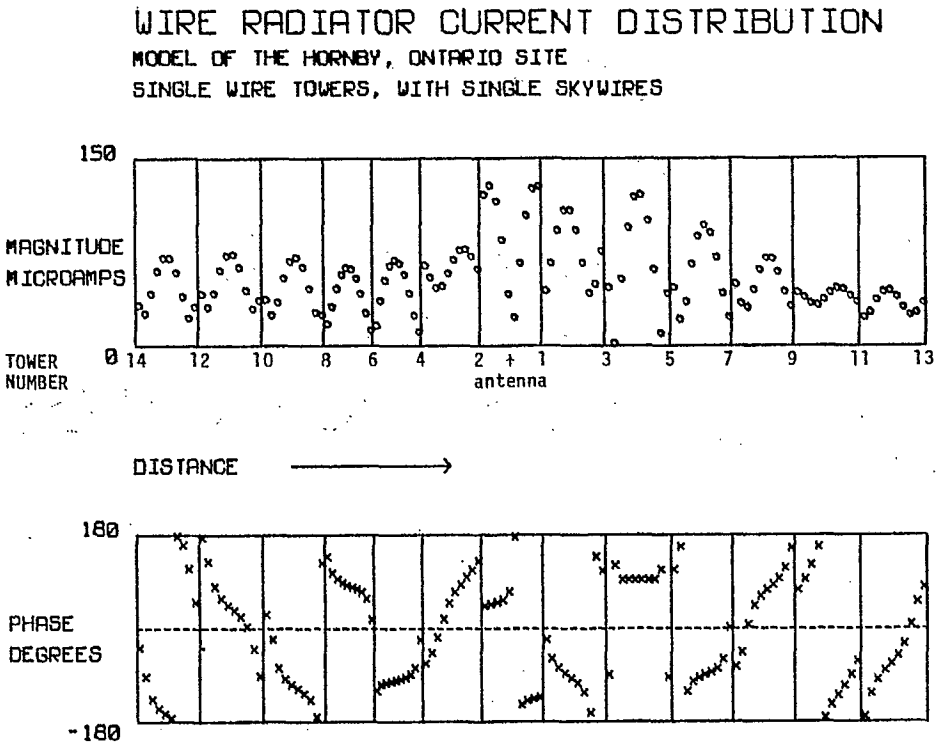

Figure 2.4 (c)

RF currents on the skywires of the front line at 740 kHz.

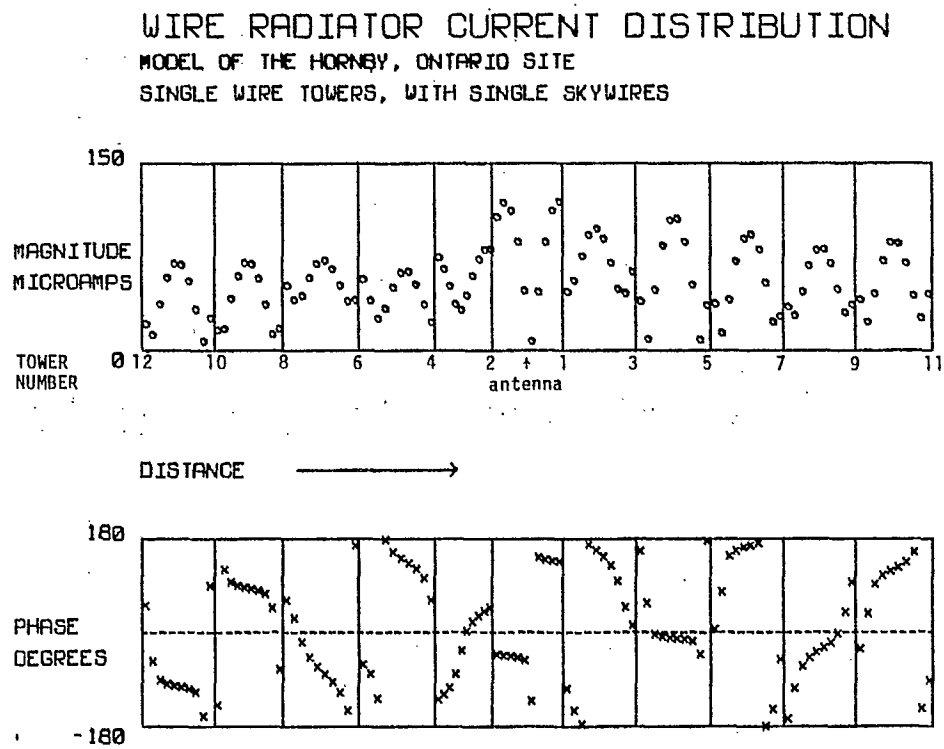

Figure 2.4 (d)

RF currents on the skywires of the rear line at 740 kHz.

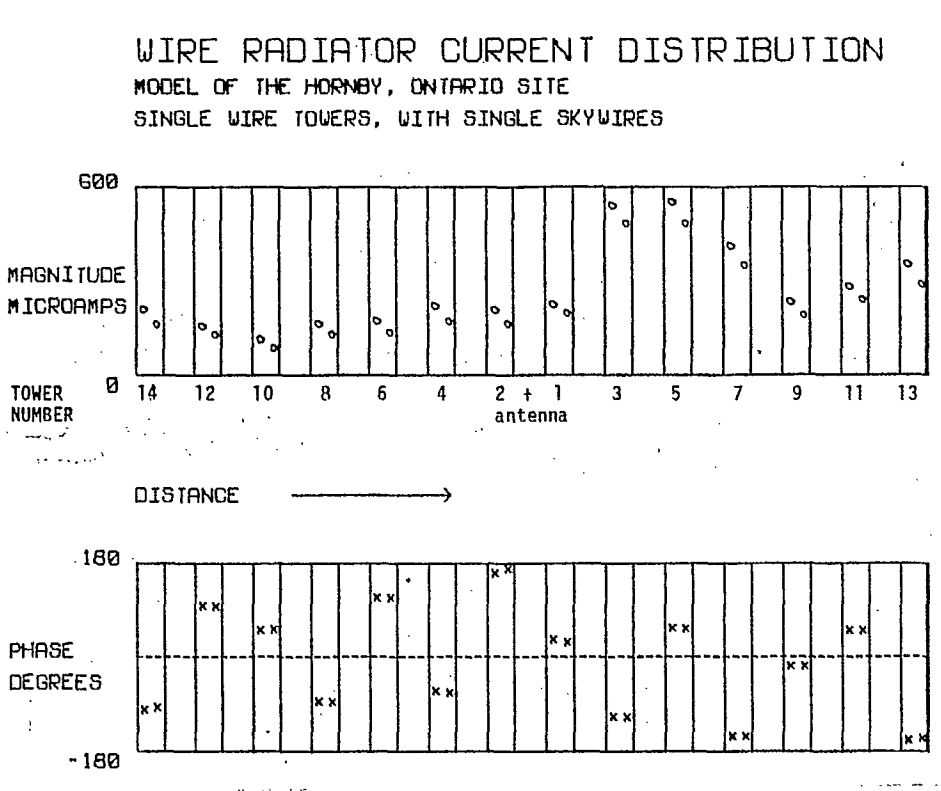

Figure 2.5 (a)

RF currents on the towers of the front line at 860 kHz.

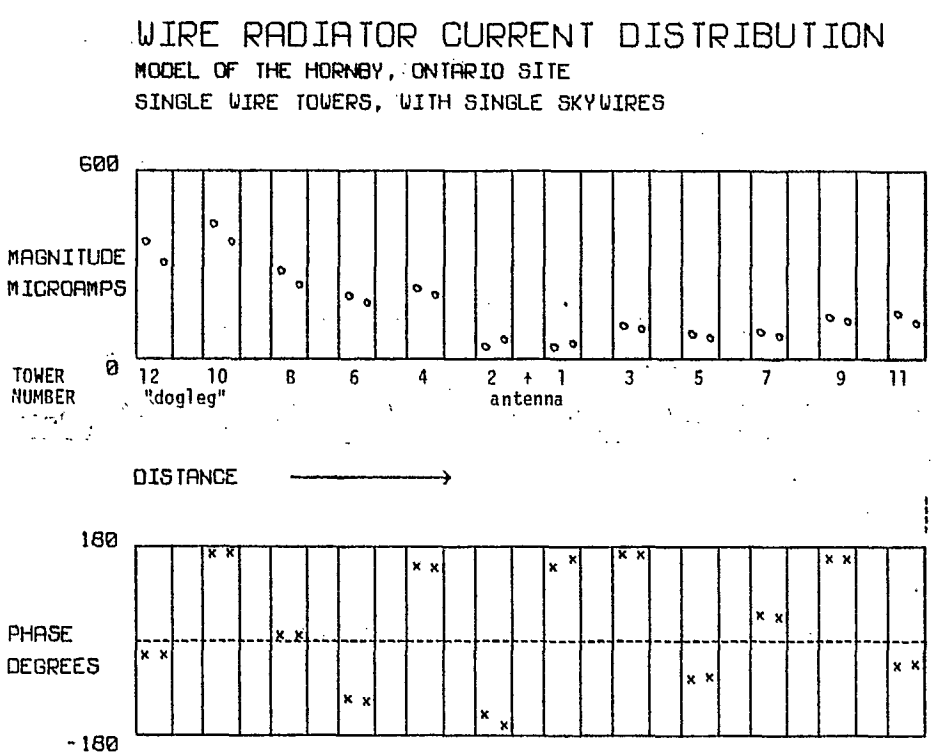

Figure 2.5 (b)

RF currents on the towers of the rear line at 860 kHz.

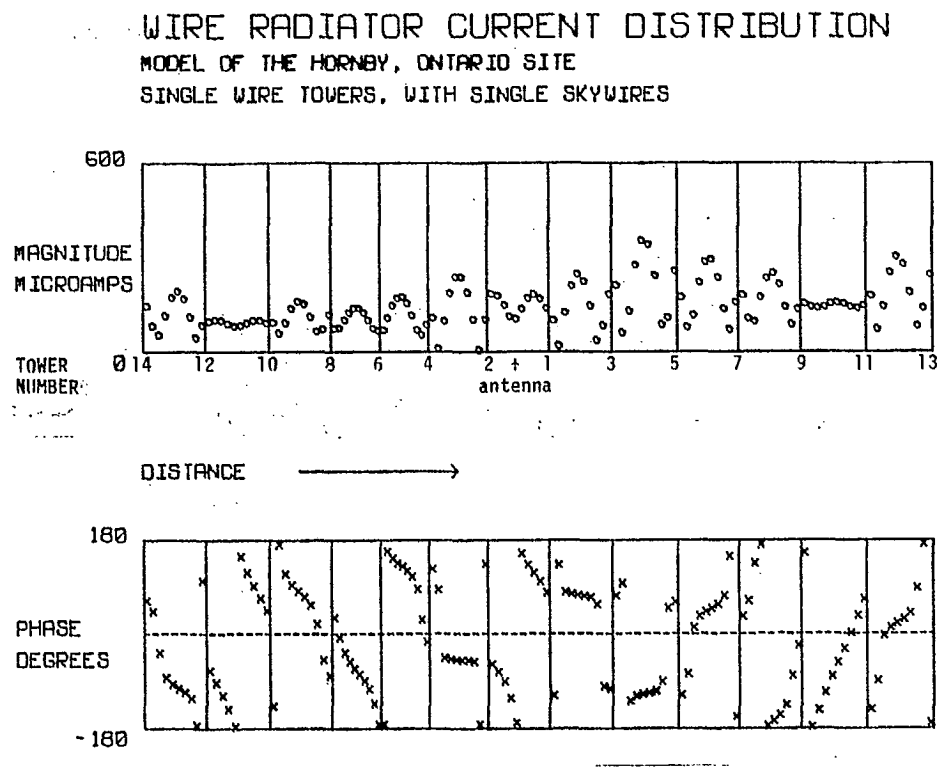

Figure 2.5 (c)

RF currents on the skywires of the front line at 860 kHz.

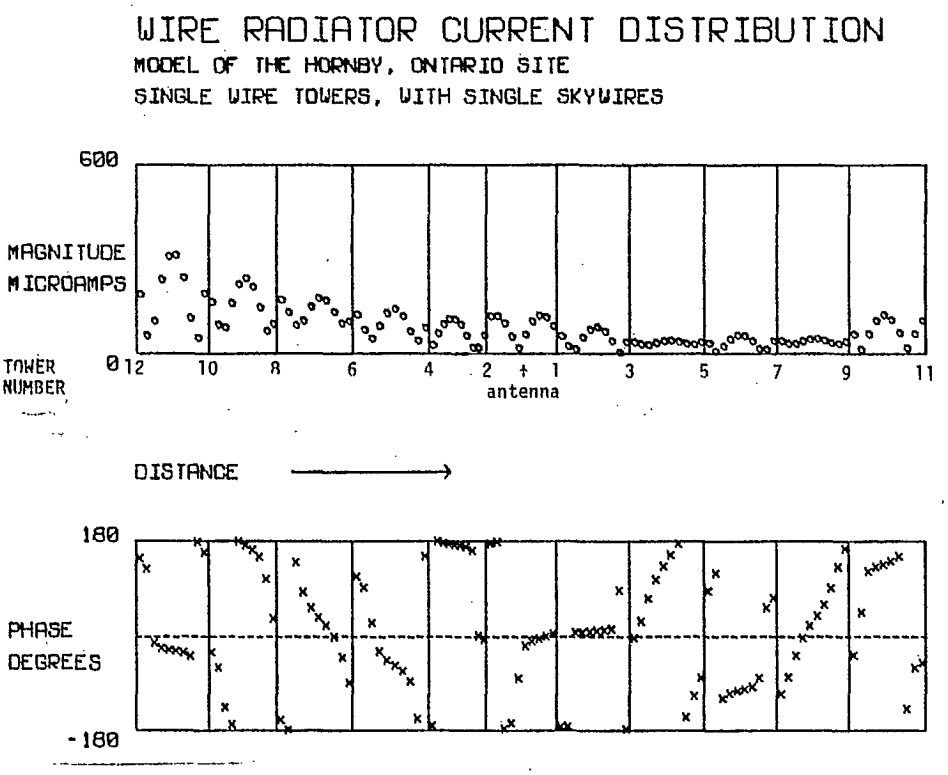

Figure 2.5 (d)

RF currents on the skywires of the rear line at 860 kHz.

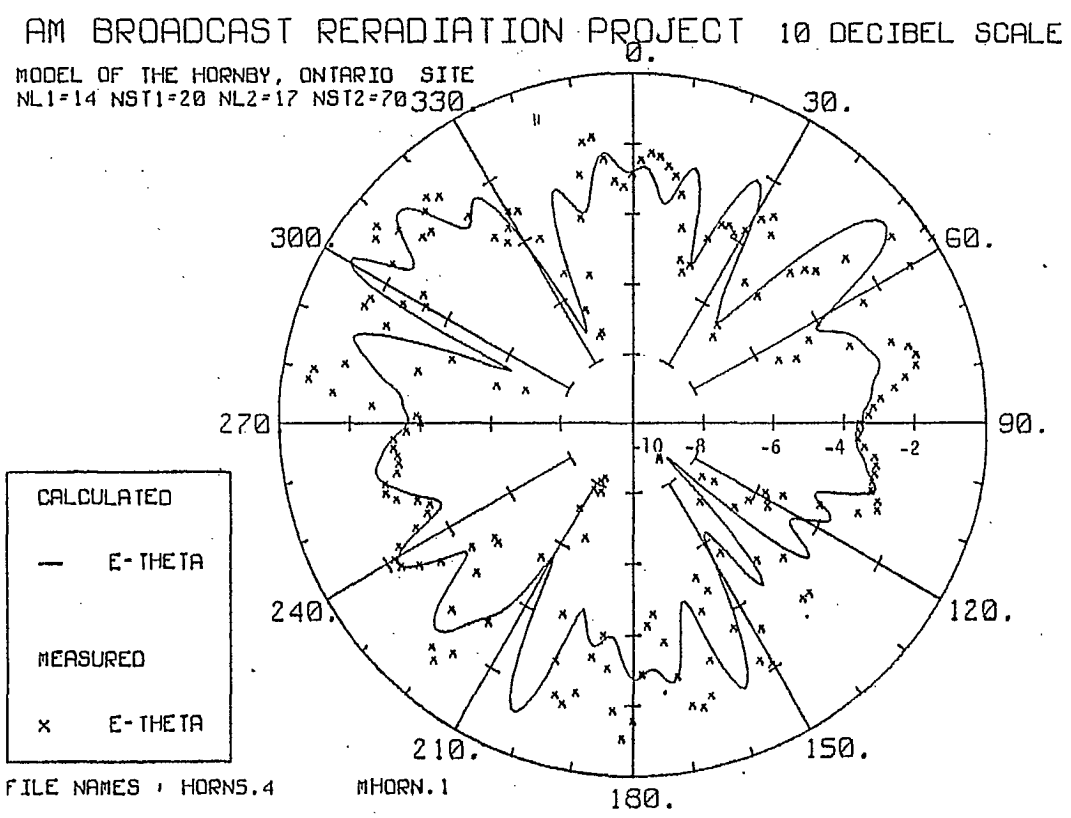

Figure 2.6

Azimuth pattern for the Hornby site at 860 kHz including seven towers in the dogleg, being numbers 8, 10, 12, 14, 16, 18, and 20 in Figure 2.3.

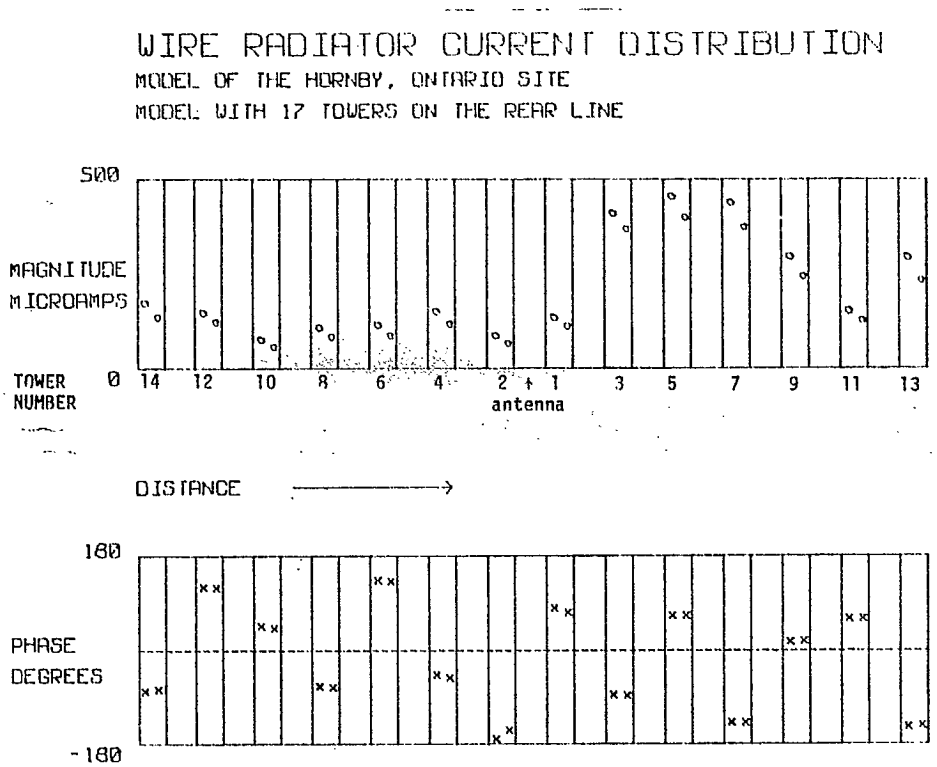

Figure 2.7 (a)

RF currents on the towers of the front line at 860 kHz.

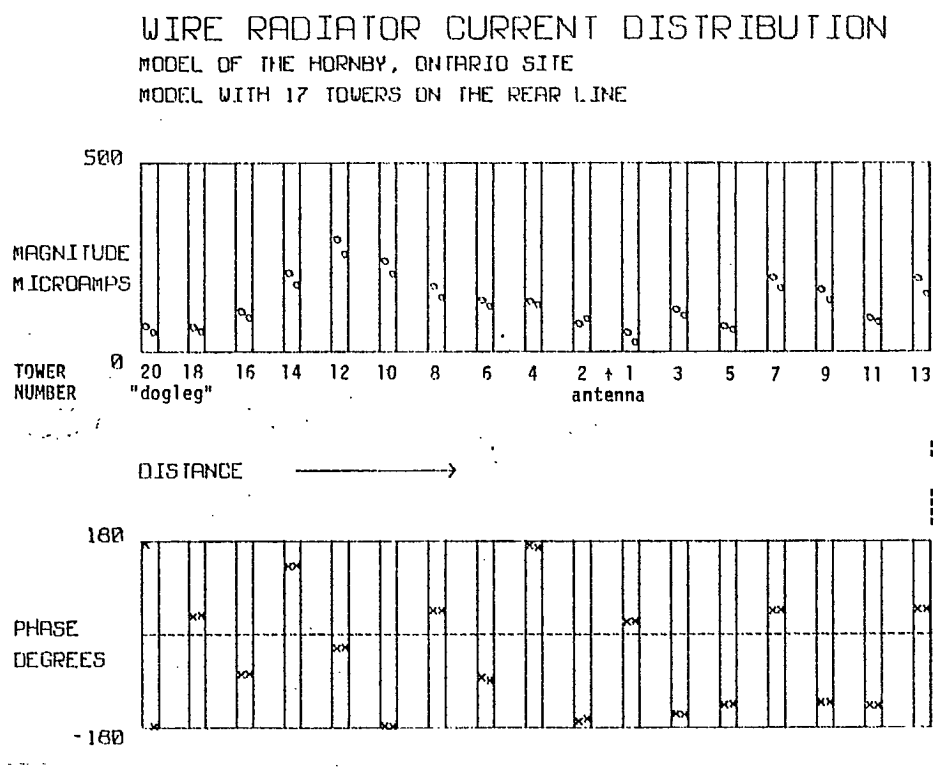

Figure 2.7 (b)

RF currents on the towers of the rear line at 860 kHz.

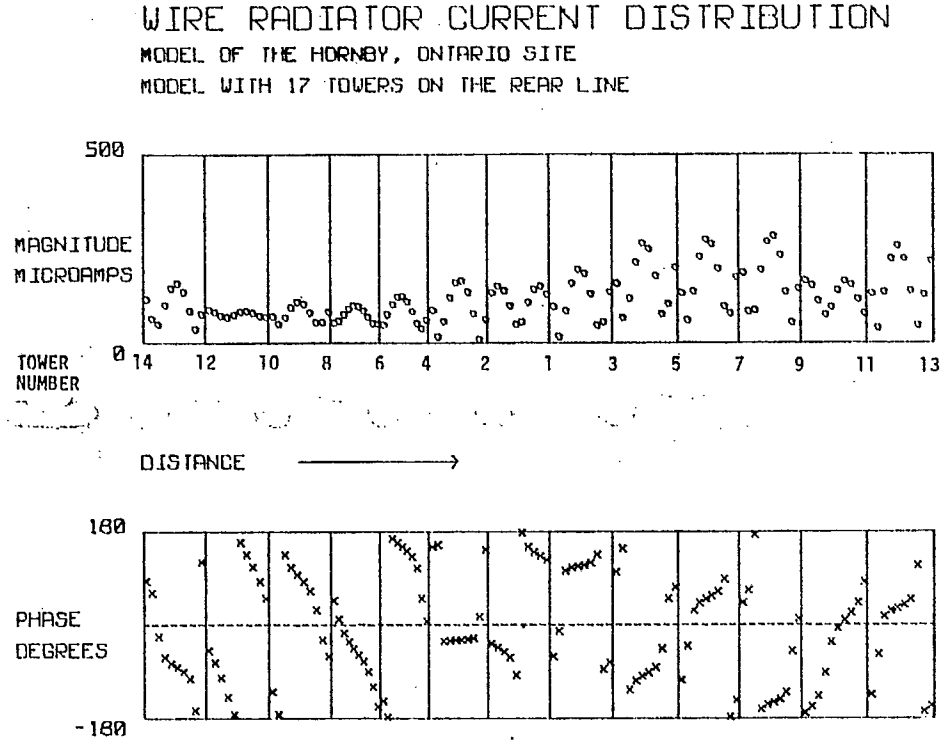

Figure 2.7 (c)

RF currents on the skywires of the front line at 860 kHz.

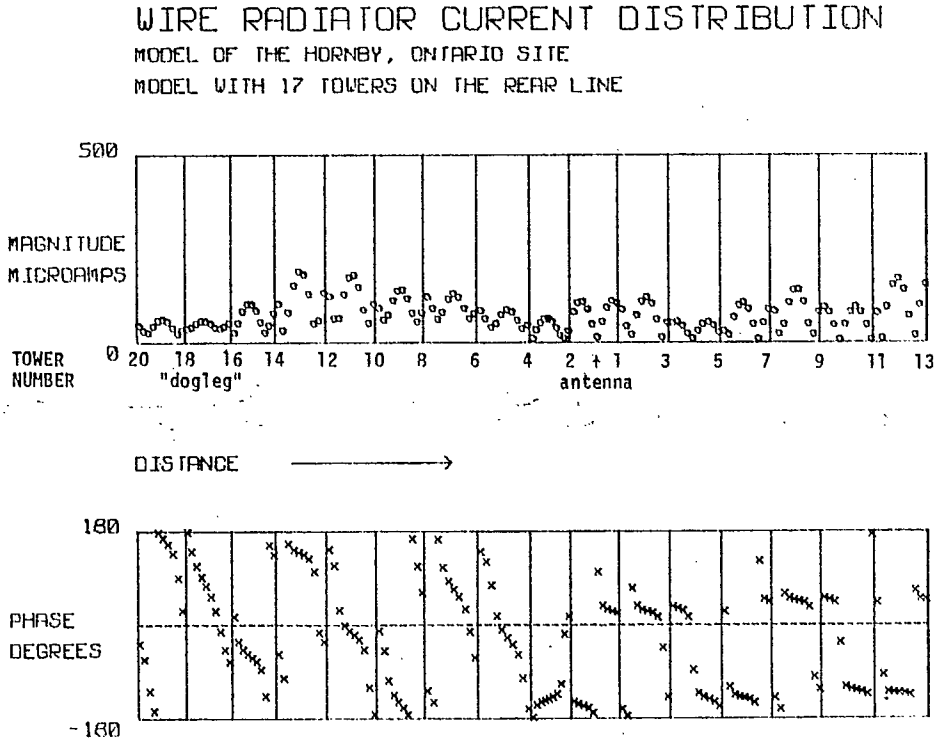

Figure 2.7 (d)

RF currents on the skywires of the rear line at 860 kHz.

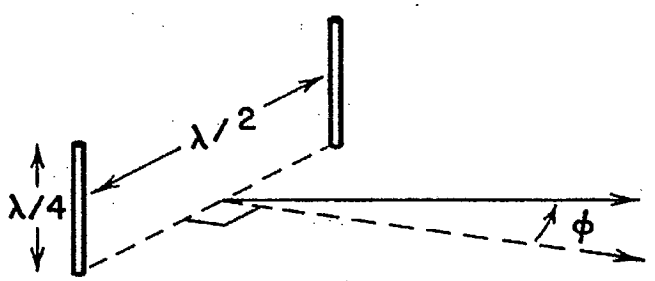

Figure 3.1

The towers are fed in phase, are 75 m tall, of radius 2 m, are located 150 m apart, and are operated at 1,000 kHz m in the computer model.

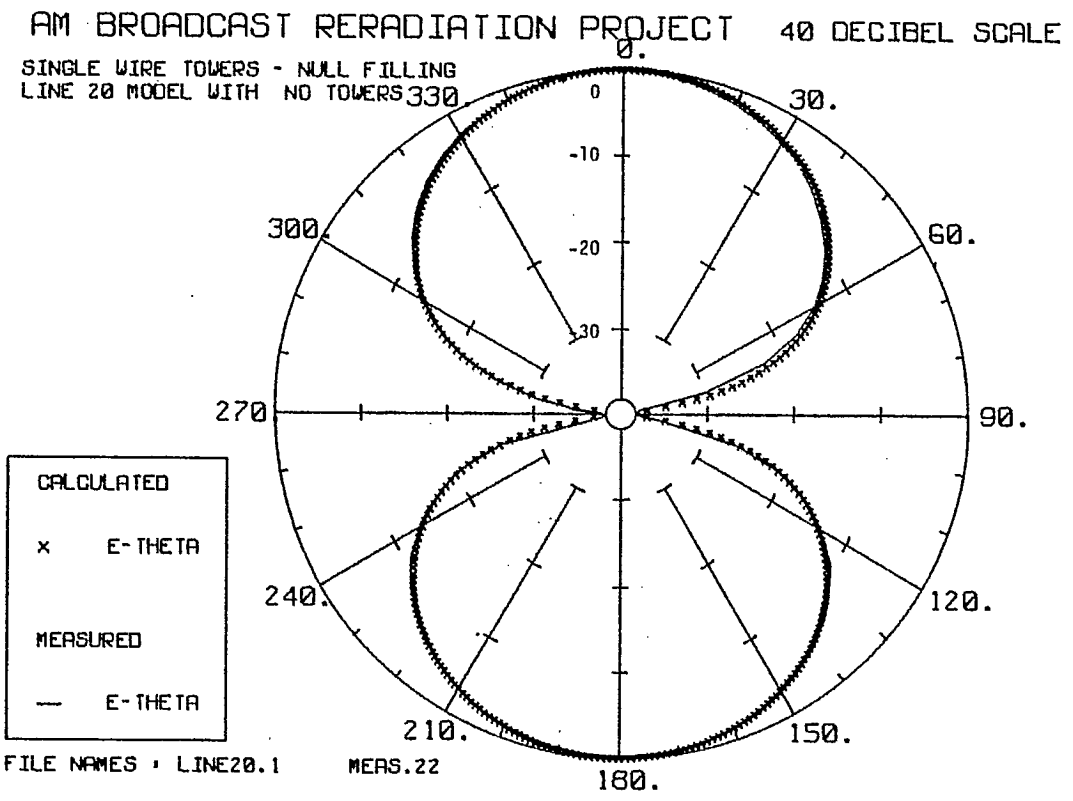

Figure 3.2

Comparison of the computed and measured pattern for the directional array.

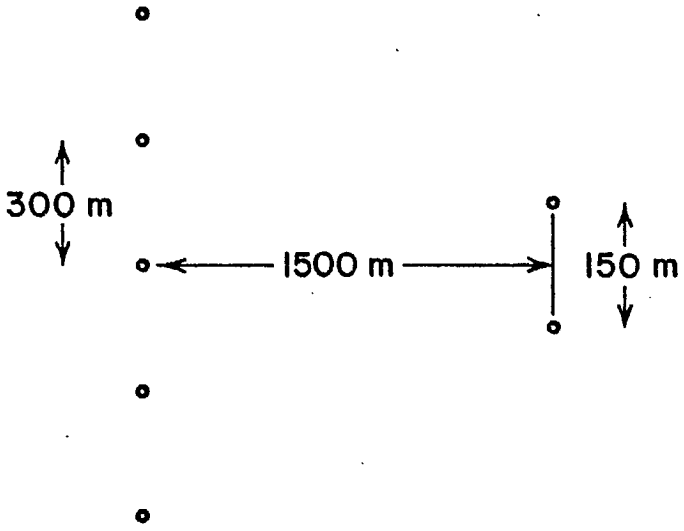

Figure 3.3

Location of the five tower power line relative to the array of Figure 3.1. The power line towers are 50.9 m (166 ft.) tall and of "equivalent radius" 3.51 m. The skywire radius was 0.71 m.

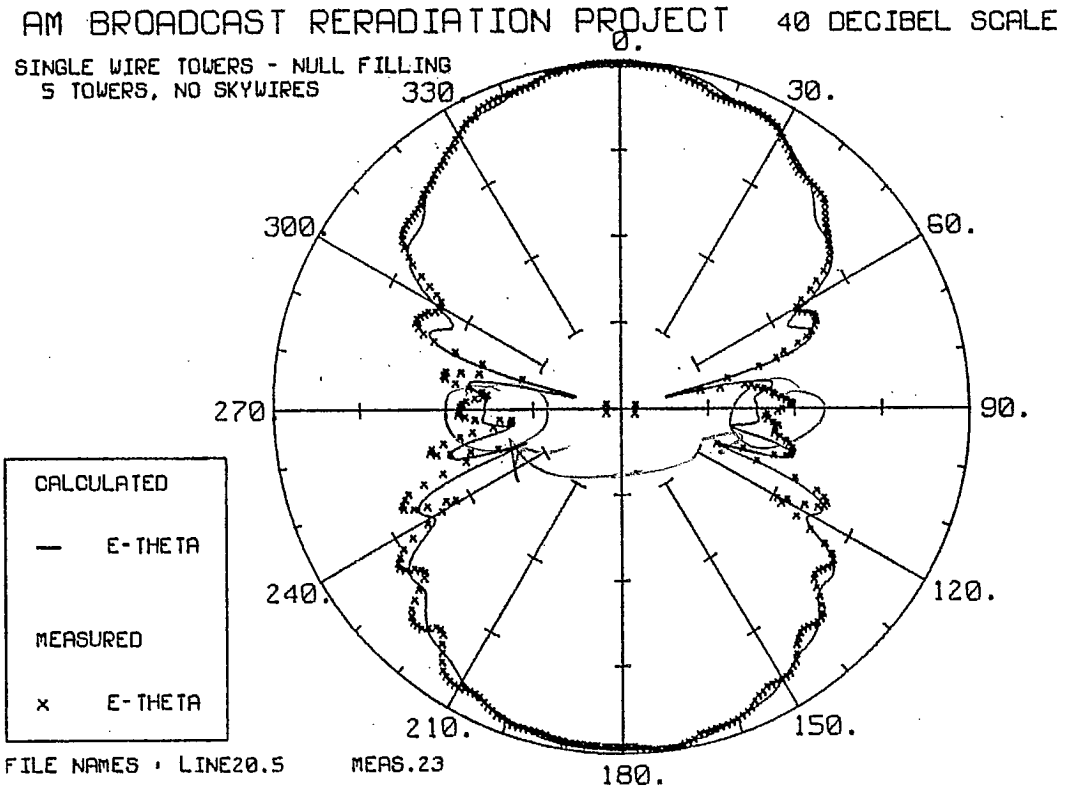

Figure 3.4

Azimuth pattern of the directional array in the presence of the power line towers only (no skywires).

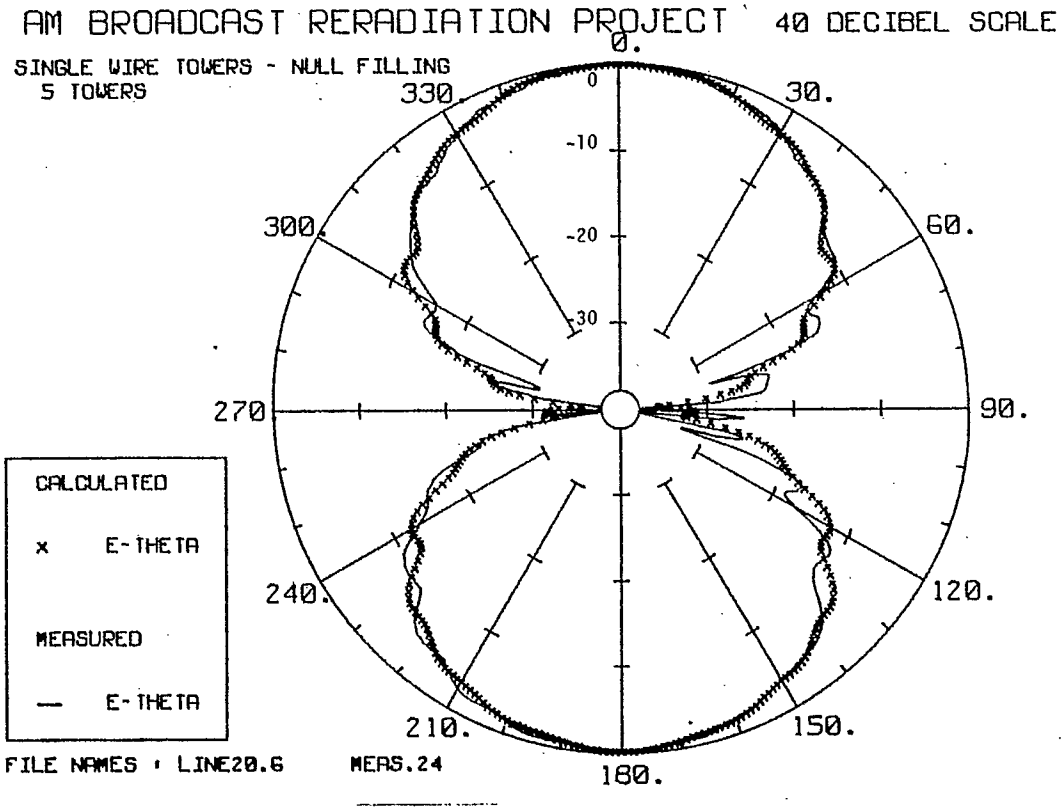

Figure 3.5

Azimuth pattern of the directional array with the power line towers interconnected by skywires at 1,000 kHz.

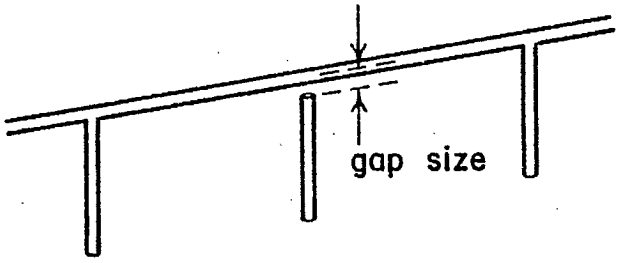

Figure 4.1
Simple computer model of the isolated tower.

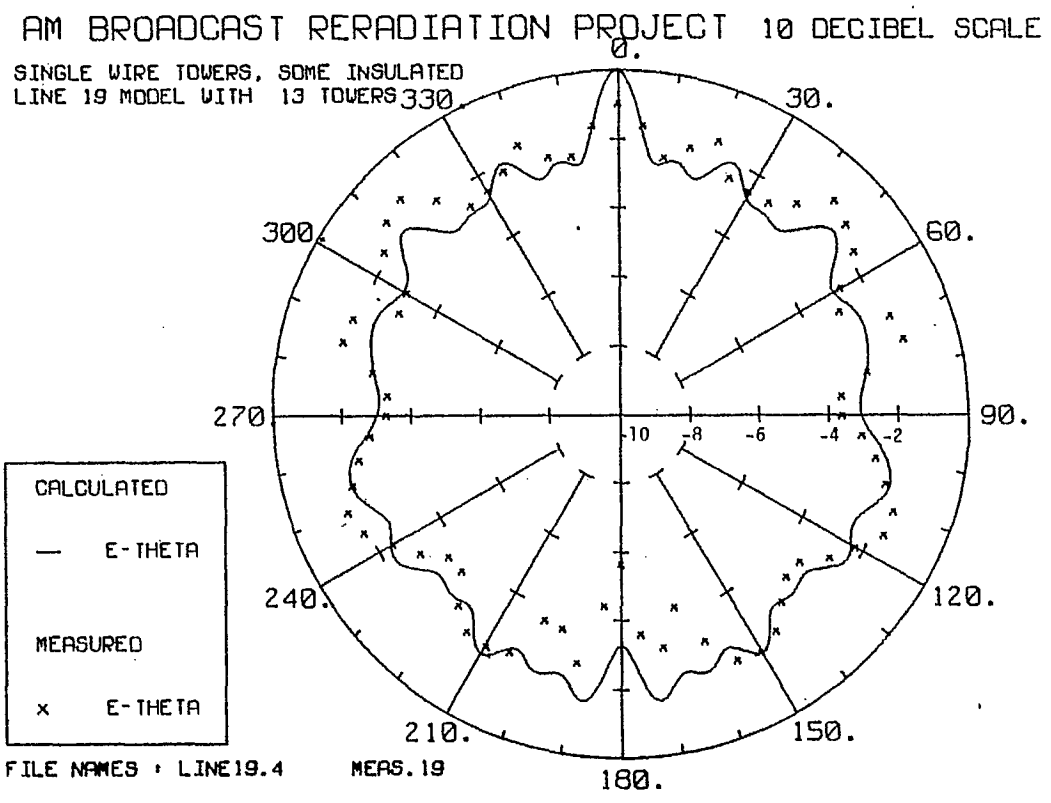

Figure 4.2

Azimuth pattern at 860 kHz for the gap size equal to four times the skywire radius.

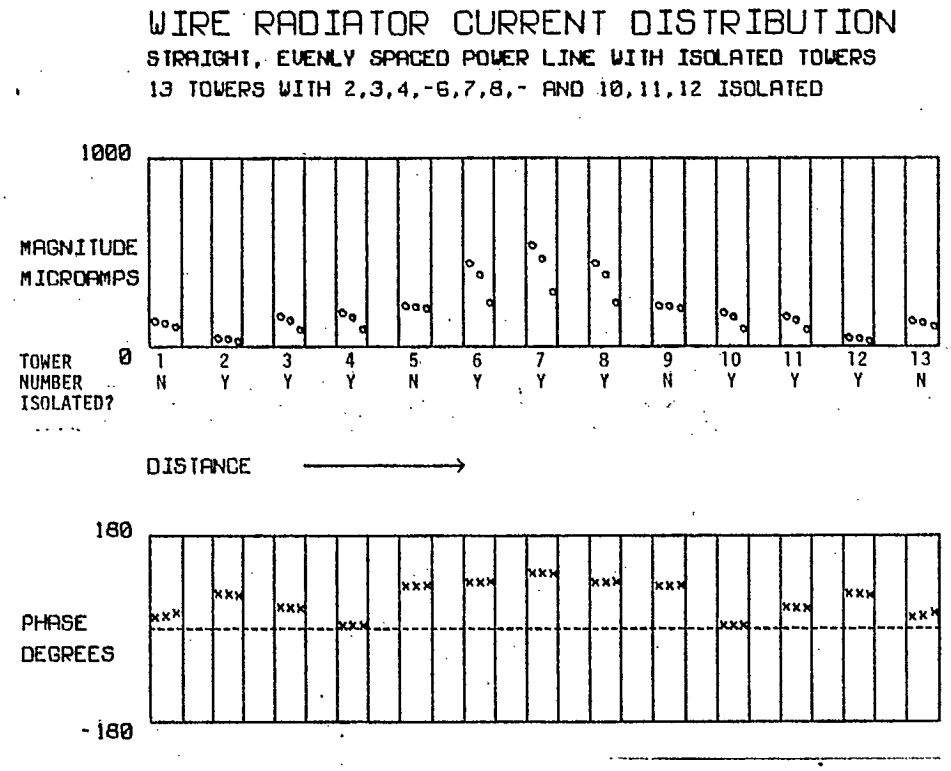

Figure 4.3 (a)

Tower currents on the model of Fig. 3.1 for the gap size equal to four times the skywire radius (at 860 kHz).

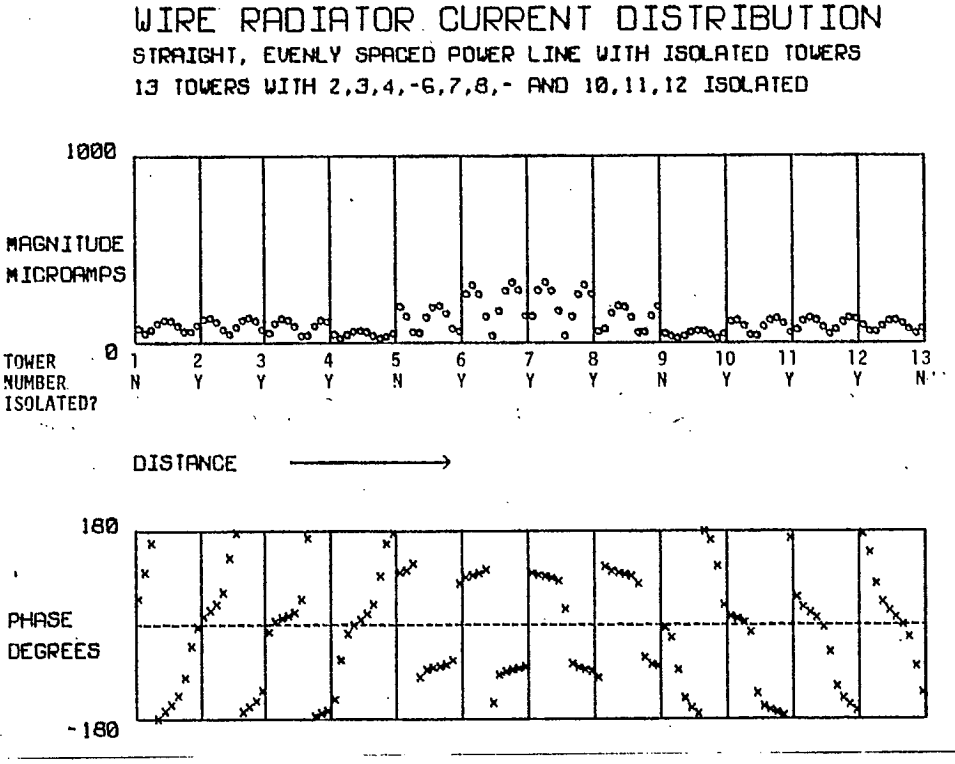

Figure 4.3 (b)

Skywire currents.

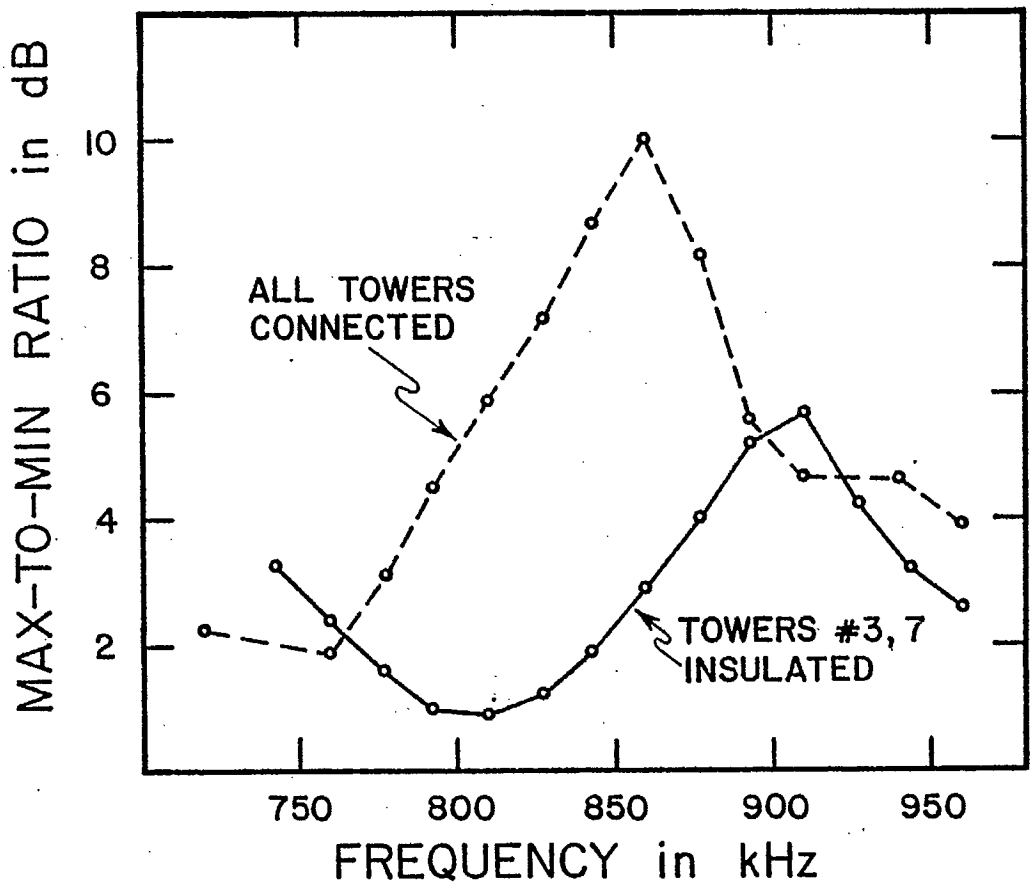

Figure 4.4

Frequency dependence of the max-to-min ratio with some towers isolated.

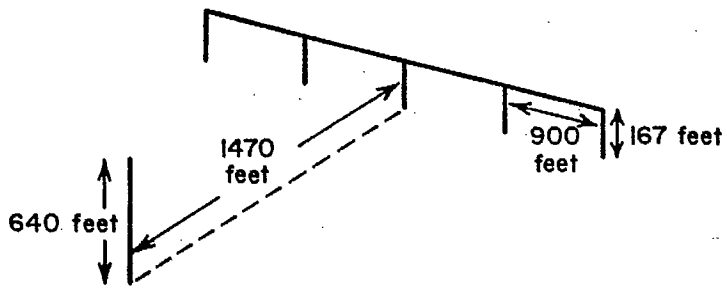

Figure 5.1
Dimensions of the problem.

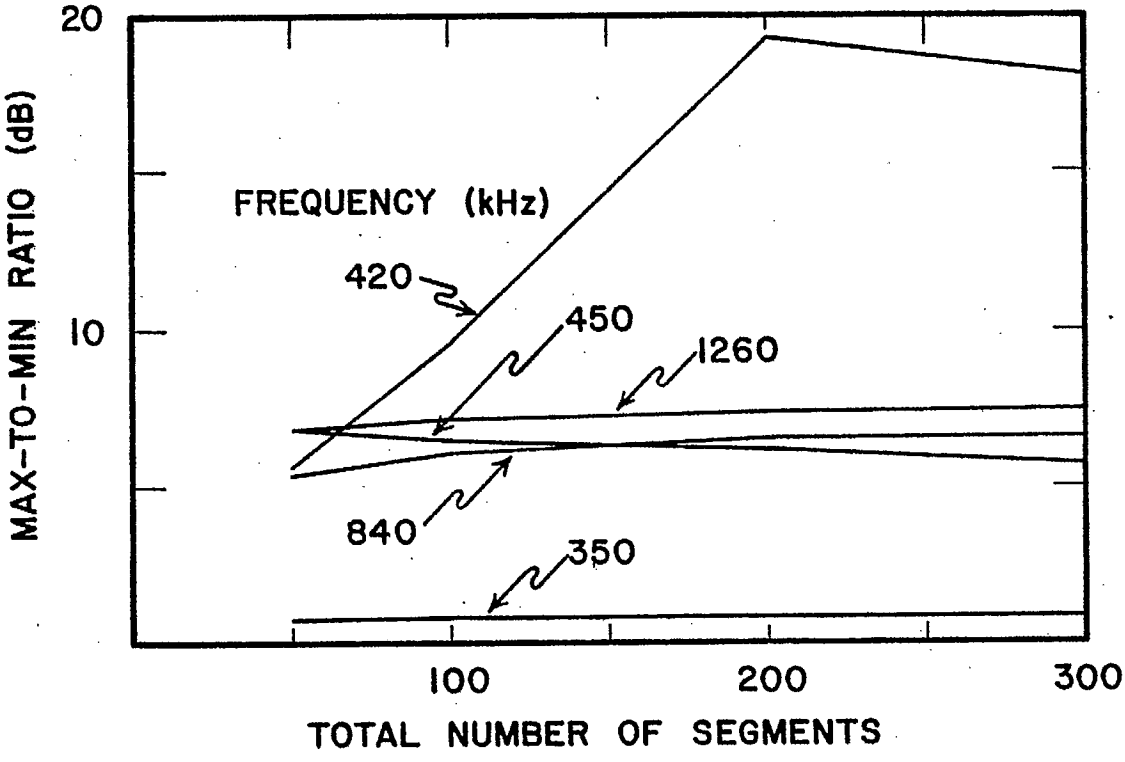

Figure 5.2
The "convergence" of the solution expressed by plotting max-to-min ratio as a function of the total number of segments on the model.

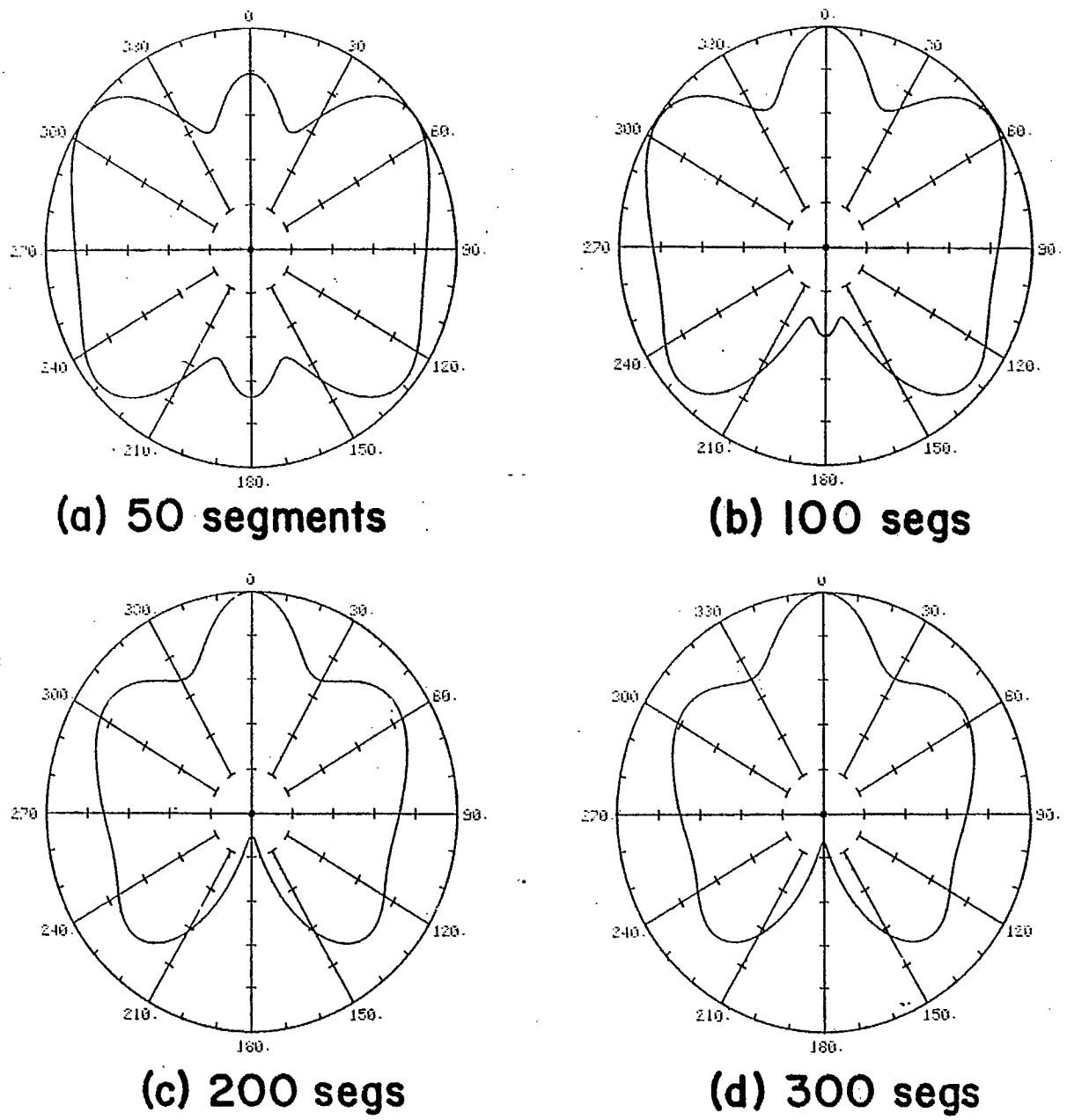

Figure 5.3

This figure illustrates the changes that come about in the azimuth pattern at 420 kHz as the number of segments increases.

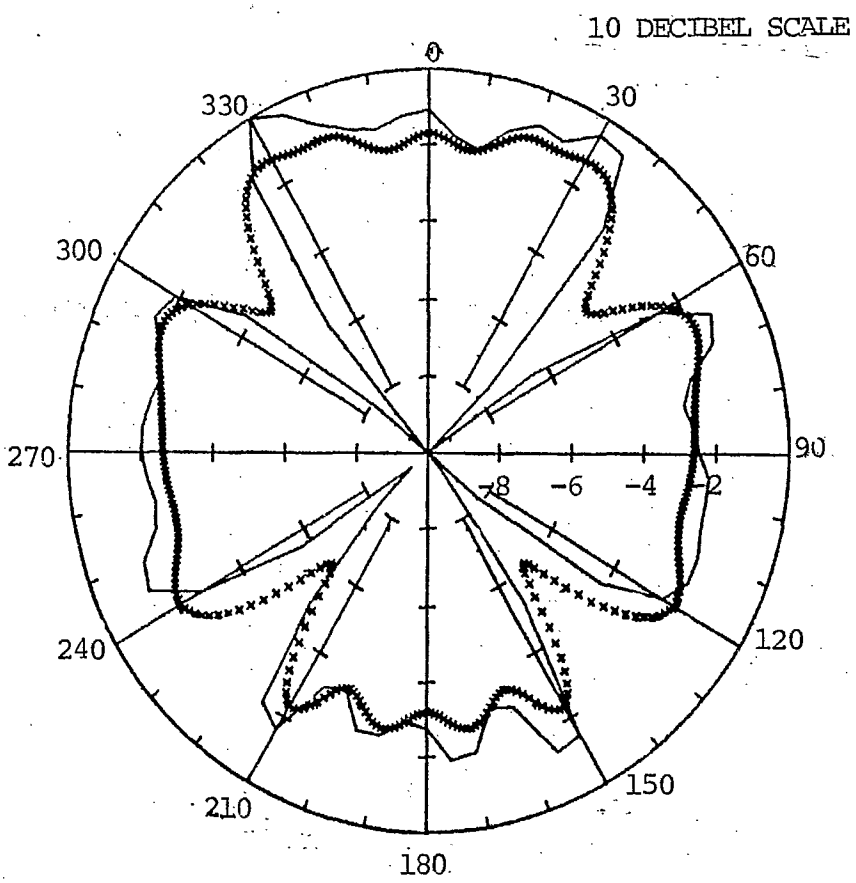

(a)

515 kHz

Figure 5.4
Comparison of computations and measurements.

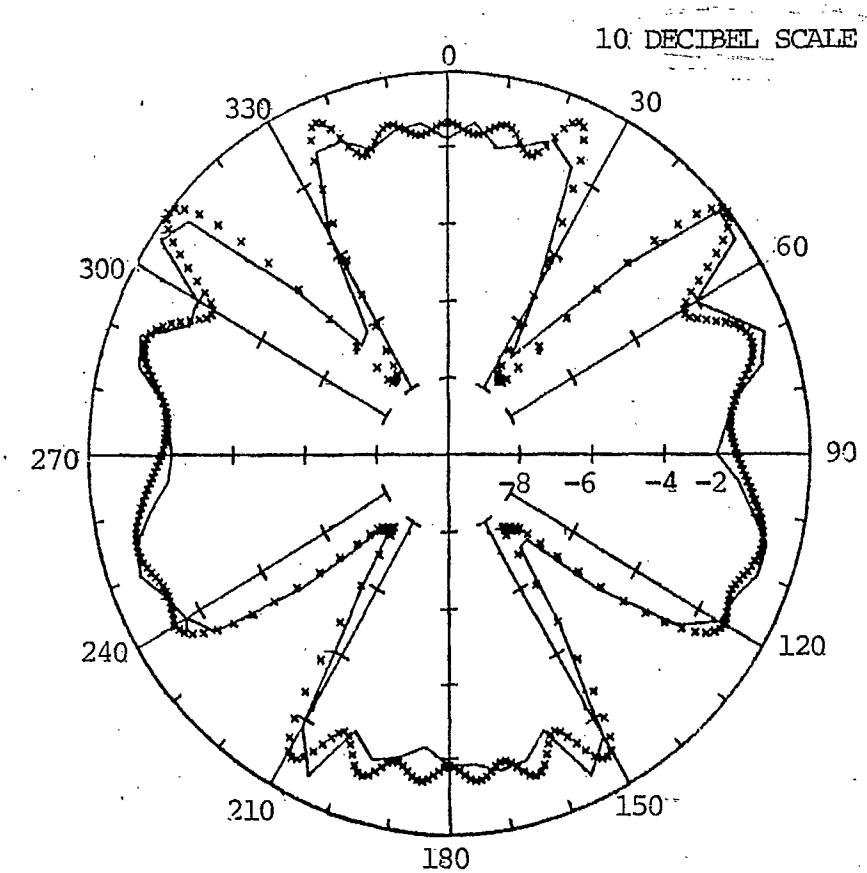

(b)

860 kHz

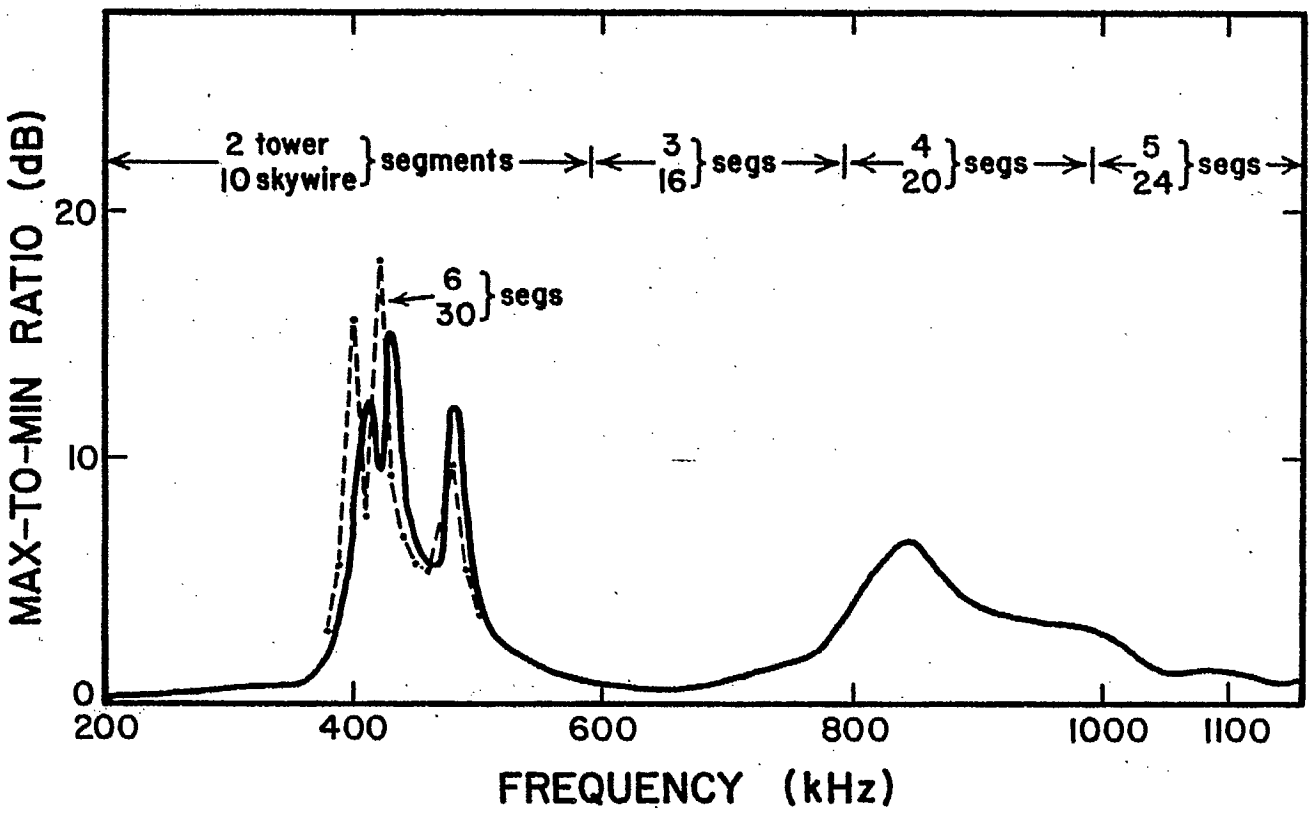

Figure 5.5
The power line's resonances revealed by plotting the max-to-min ratio of the azimuth pattern as a function of frequency.

Figure 5.6
Antenna base current in comparison to antenna integrated current.

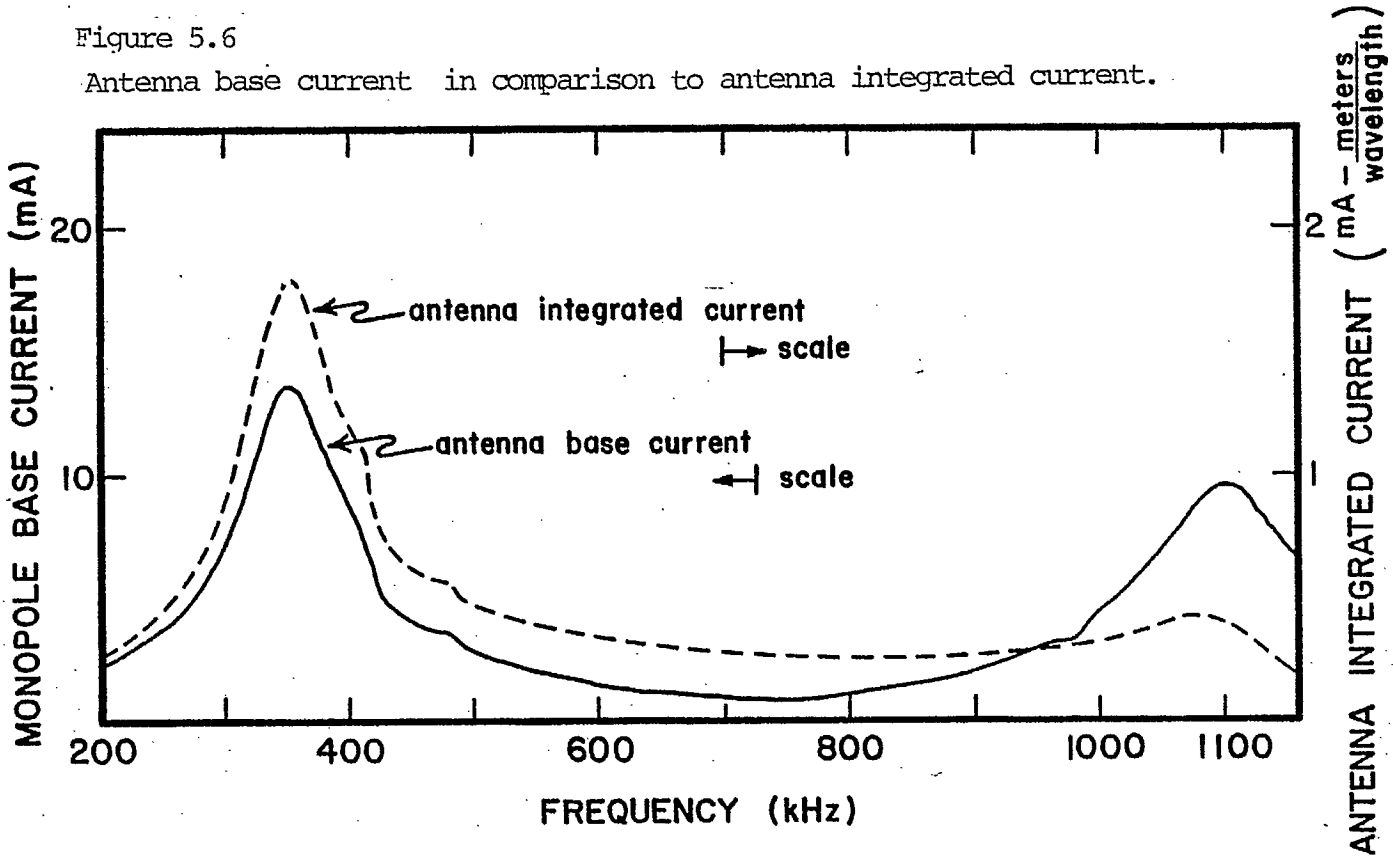

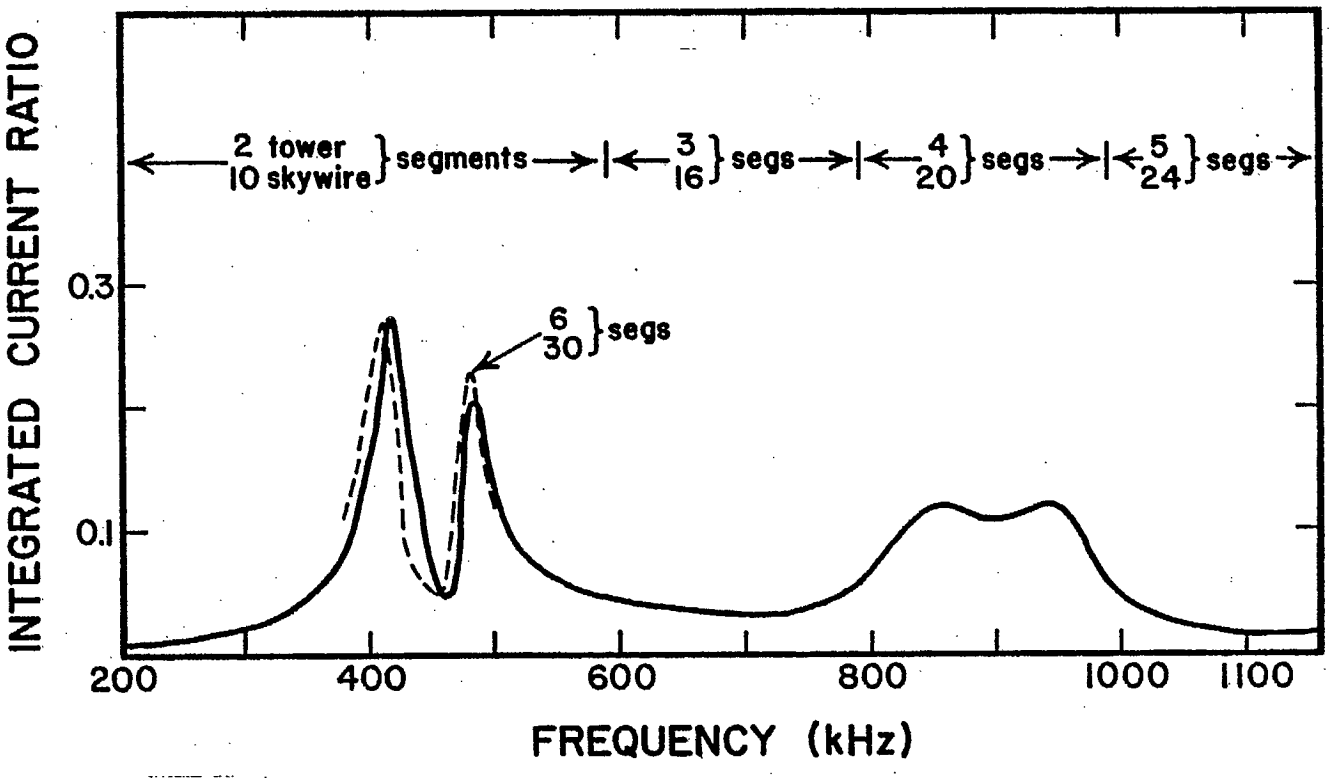

Figure 5.7

The power line's resonances revealed by plotting the ratio of the integrated current on the center tower to the integrated current on the broadcast antenna as a function of frequency.

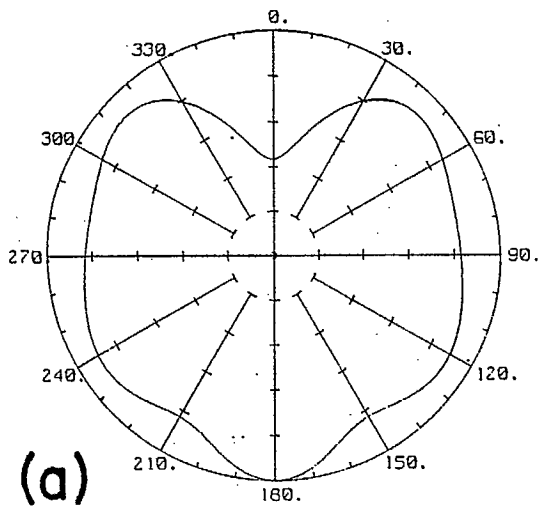

(a)
400 kHz

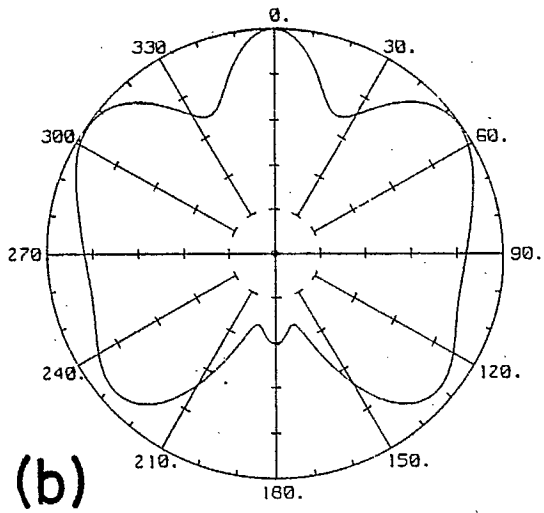

(b)
420 kHz

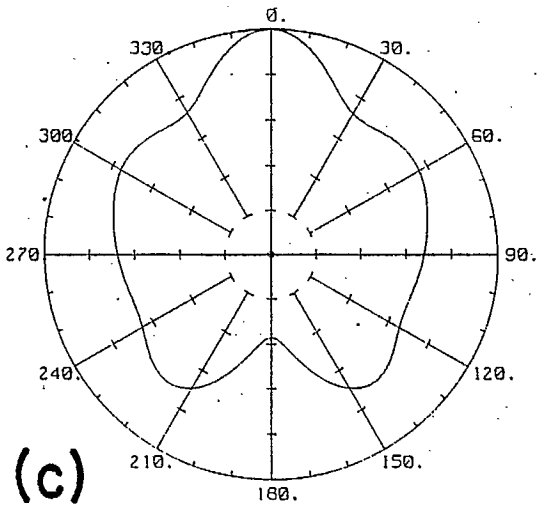

(c)
440 kHz

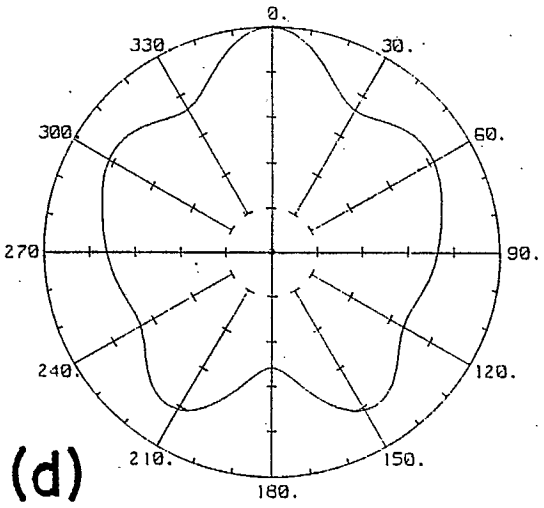

(d)
460 kHz

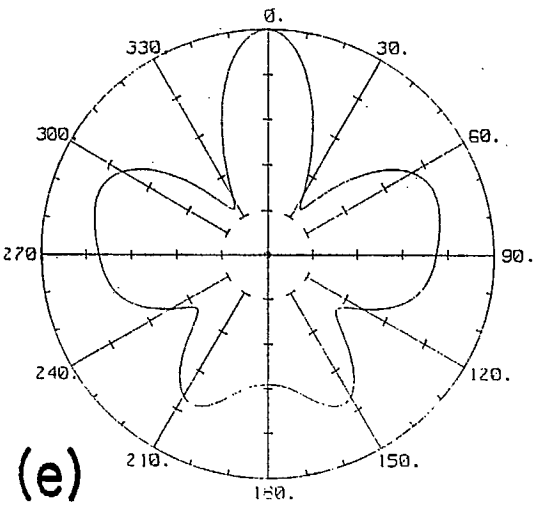

(e)
480 kHz

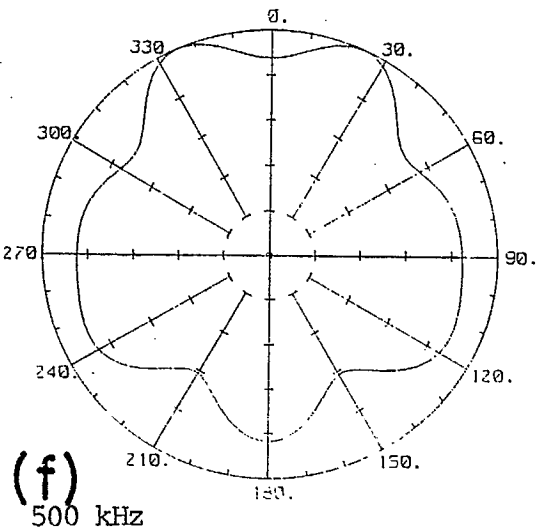

(f)
500 kHz

Figure 5.8
Azimuth patterns in the one wavelength resonance region.

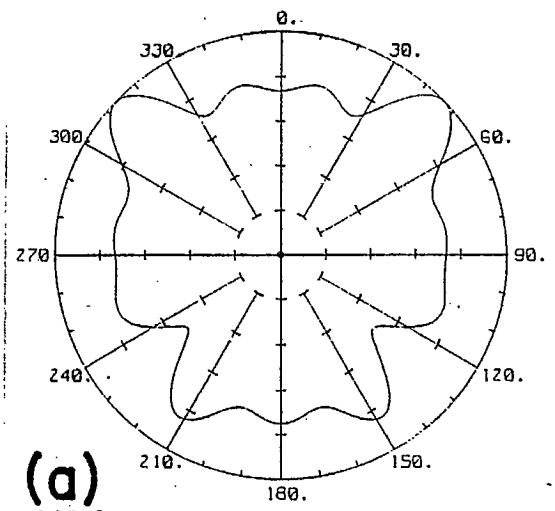

(a)
820 kHz

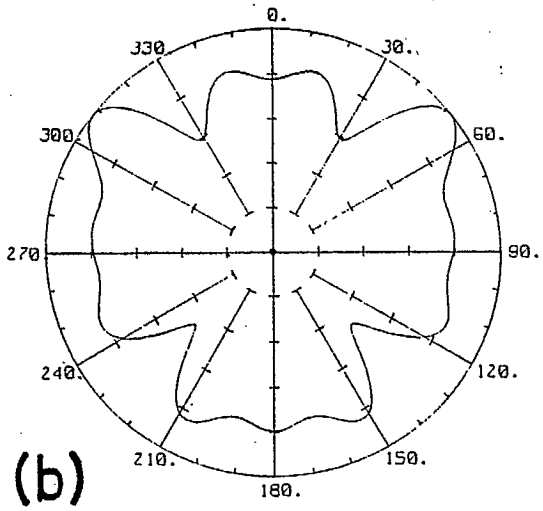

(b)
840 kHz

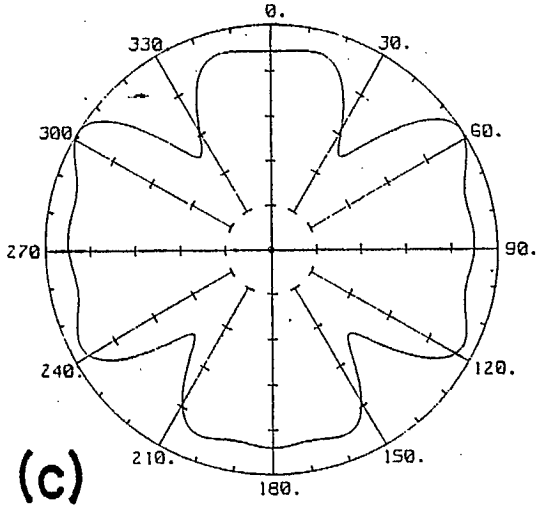

(c)
860 kHz

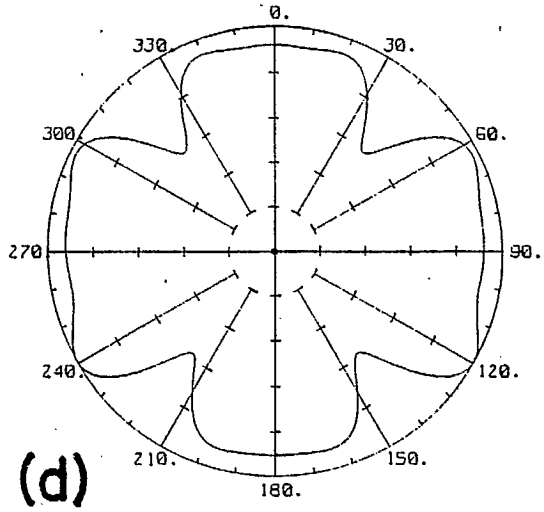

(d)
880 kHz

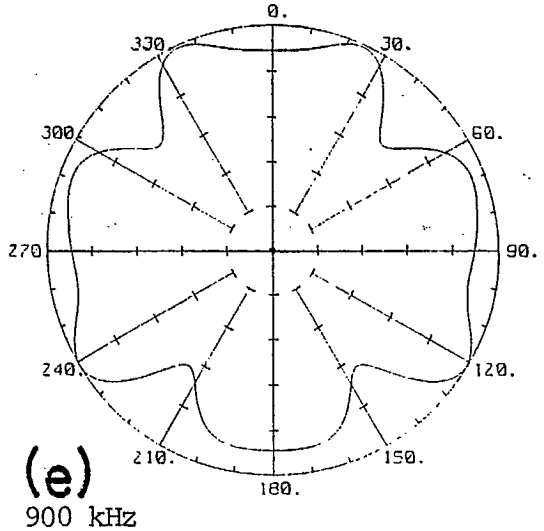

(e)
900 kHz

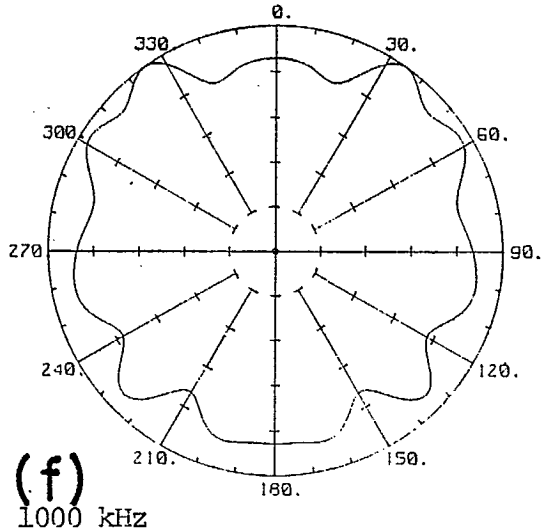

(f)
1000 kHz

Figure 5.9
Azimuth patterns in the two wavelength resonance region.

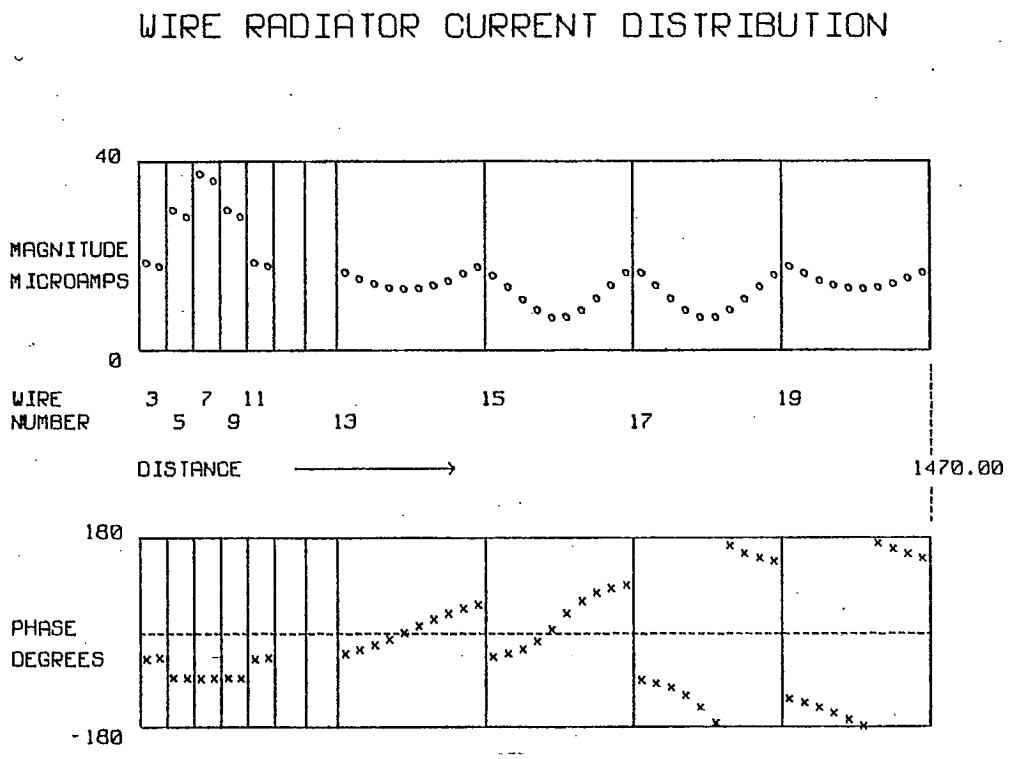

Figure 5.10

RF current distribution at 200 kHz.

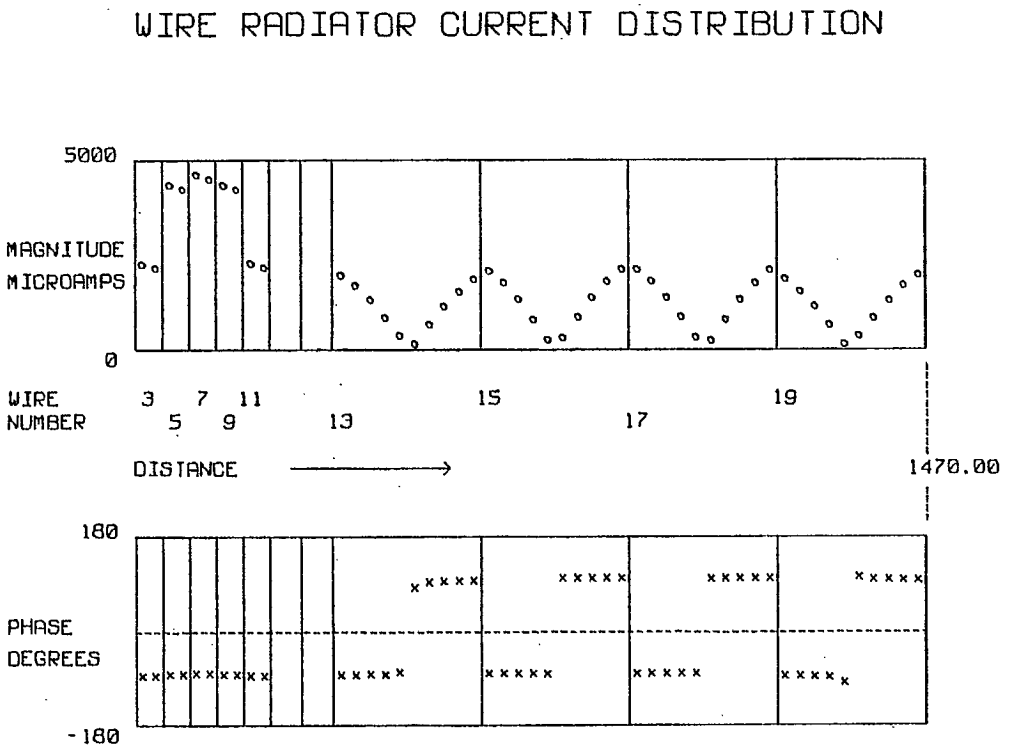

Figure 5.11

RF current distribution for "one wavelength loop" resonance at 420 kHz.

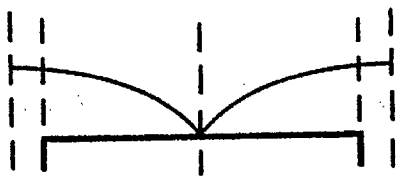

Figure 5.12

Idealization of the RF current distribution for "one wavelength loop resonance".

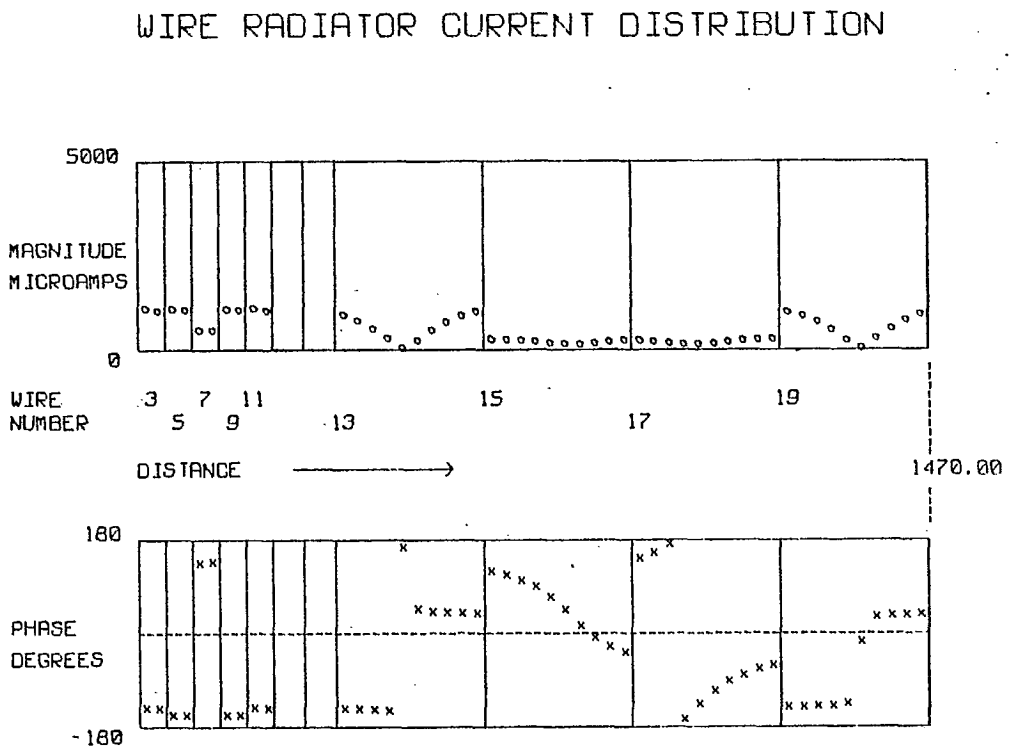

Figure 5.13

RF current distribution at 460 kHz.

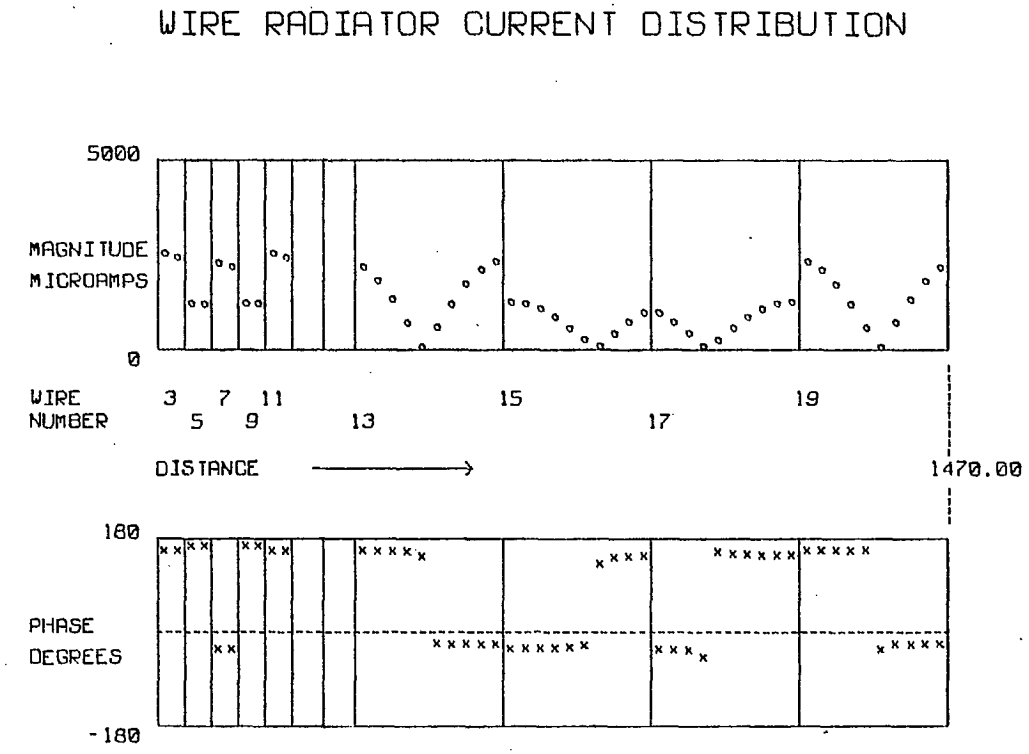

Figure 5.14

RF current distribution for "two wavelength double loop resonance" at 480 kHz.

Figure 5.15

Idealization of the RF current distribution for two wavelength double loop resonance.

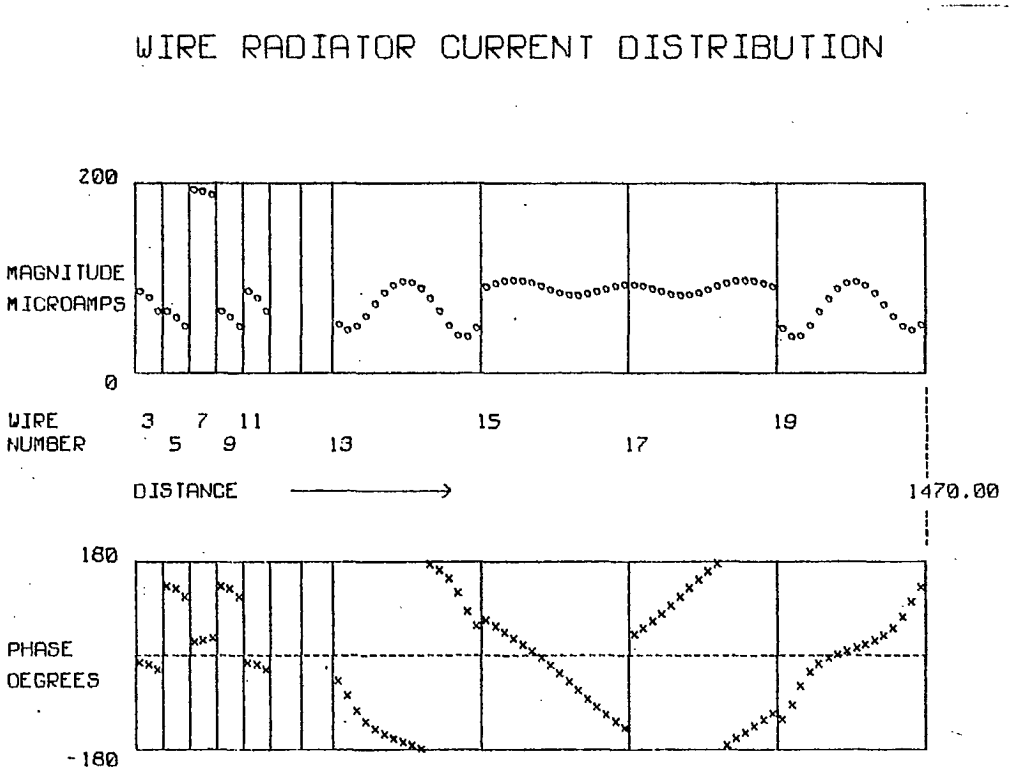

Figure 5.16

RF current distribution at 700 kHz.

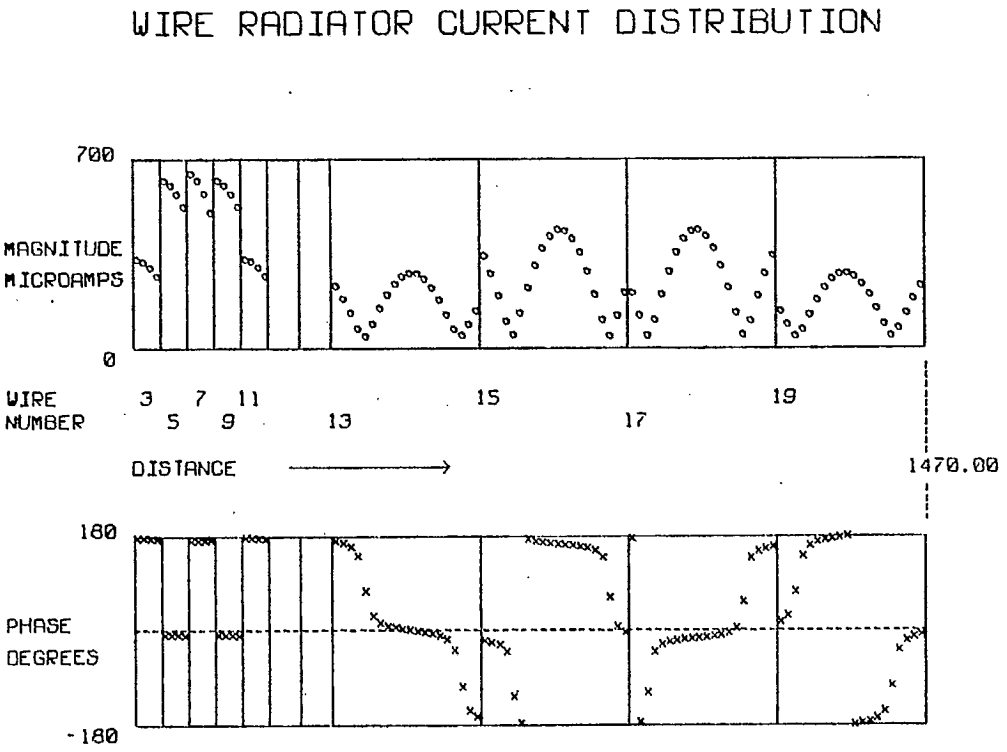

Figure 5.17

RF current distribution for "two wavelength loop resonance" at 840 kHz.

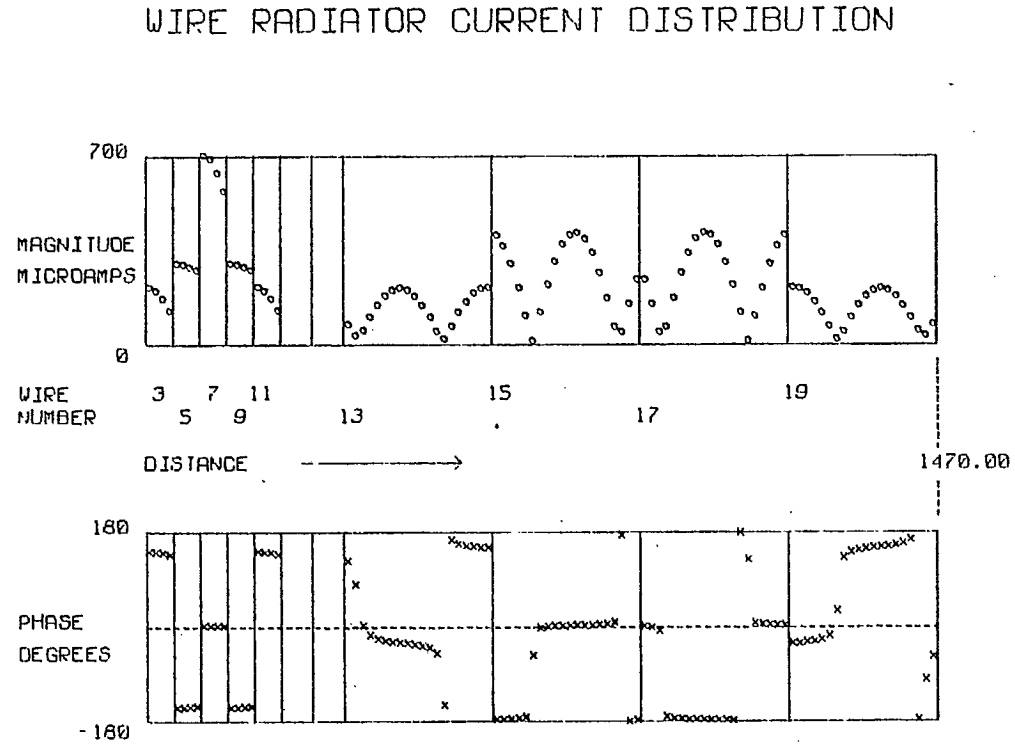

Figure 5.19

RF current distribution at 940 kHz for "four wavelength double loop resonance".

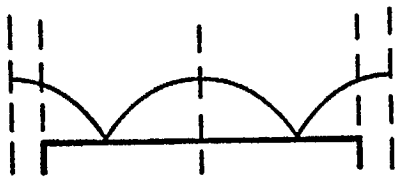

Figure 5.18

Idealization of the RF current distribution for "two wavelength loop resonance".

Figure 5.20
Idealization of the RF current distribution for four wavelength double loop resonance.

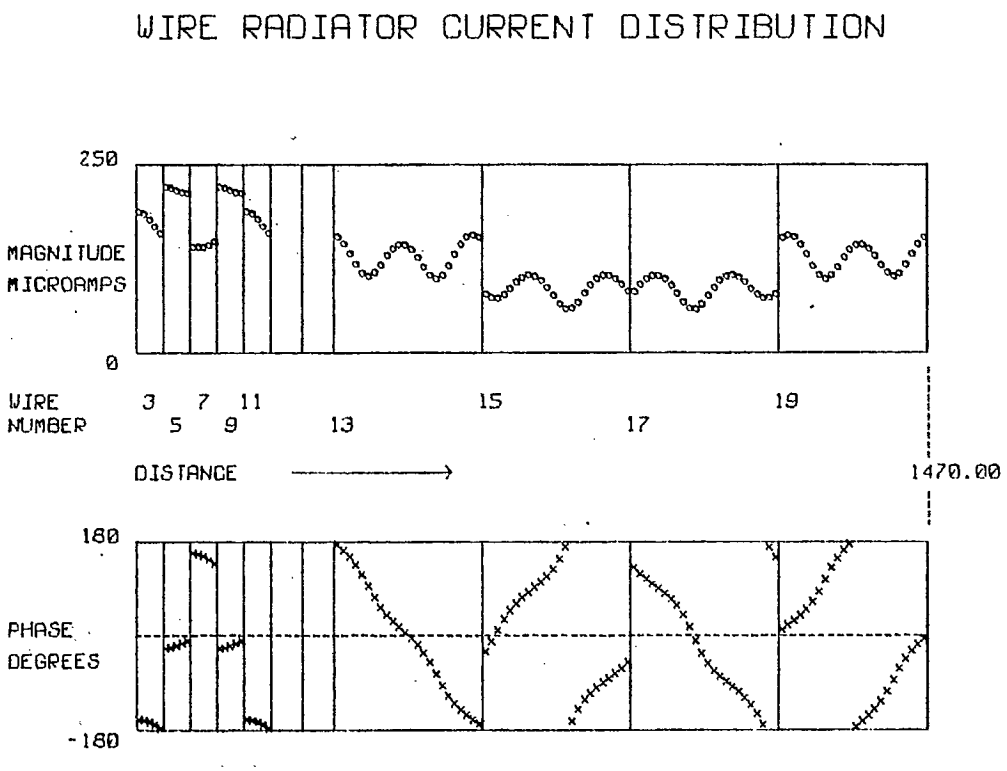

Figure 5.21
RF current distribution at 1100 kHz.

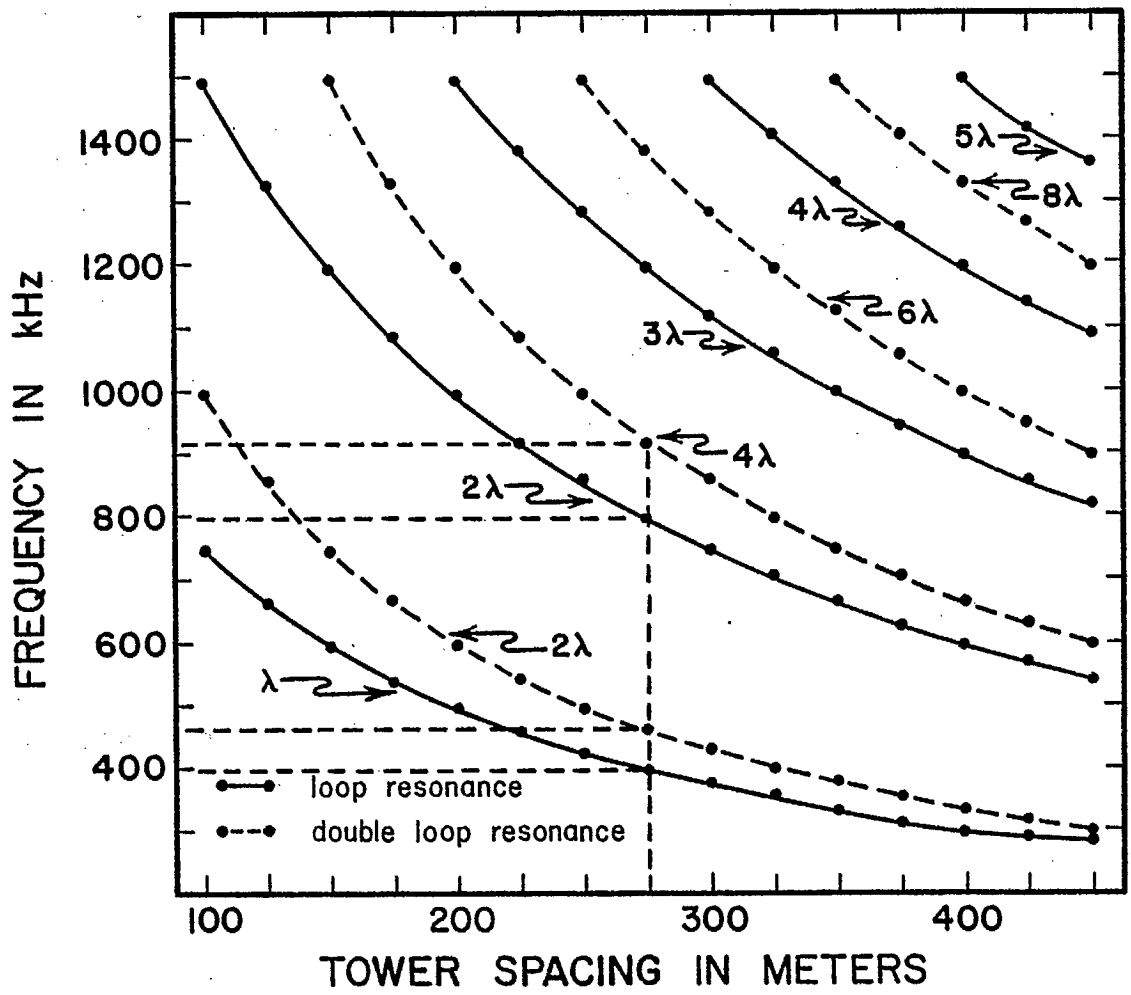

Figure 5.22

Resonant frequency vs. tower spacing for 50.6 m tall towers.

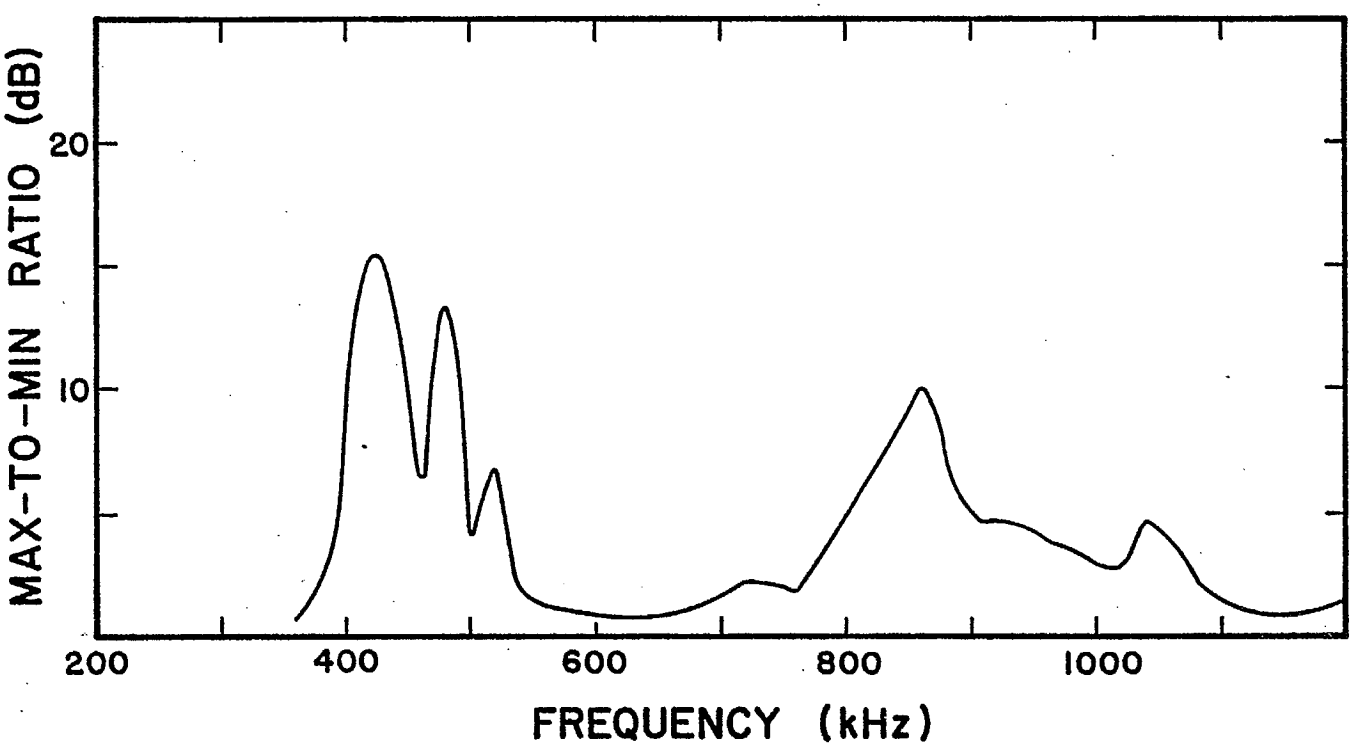

Figure 5.23

Computed curve giving the max-to-min ratio as a function of frequency for nine towers spaced 274.32 m apart.

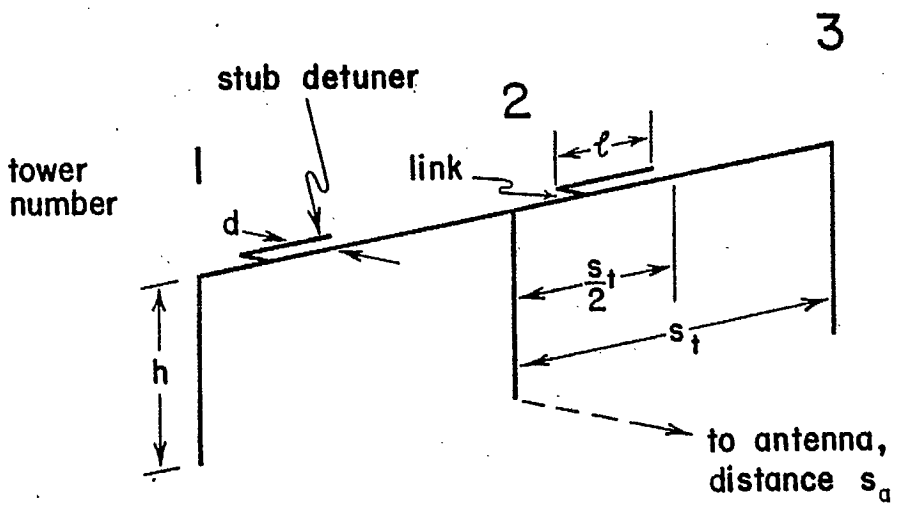

Figure 6.1
The "bent" detuning stub.

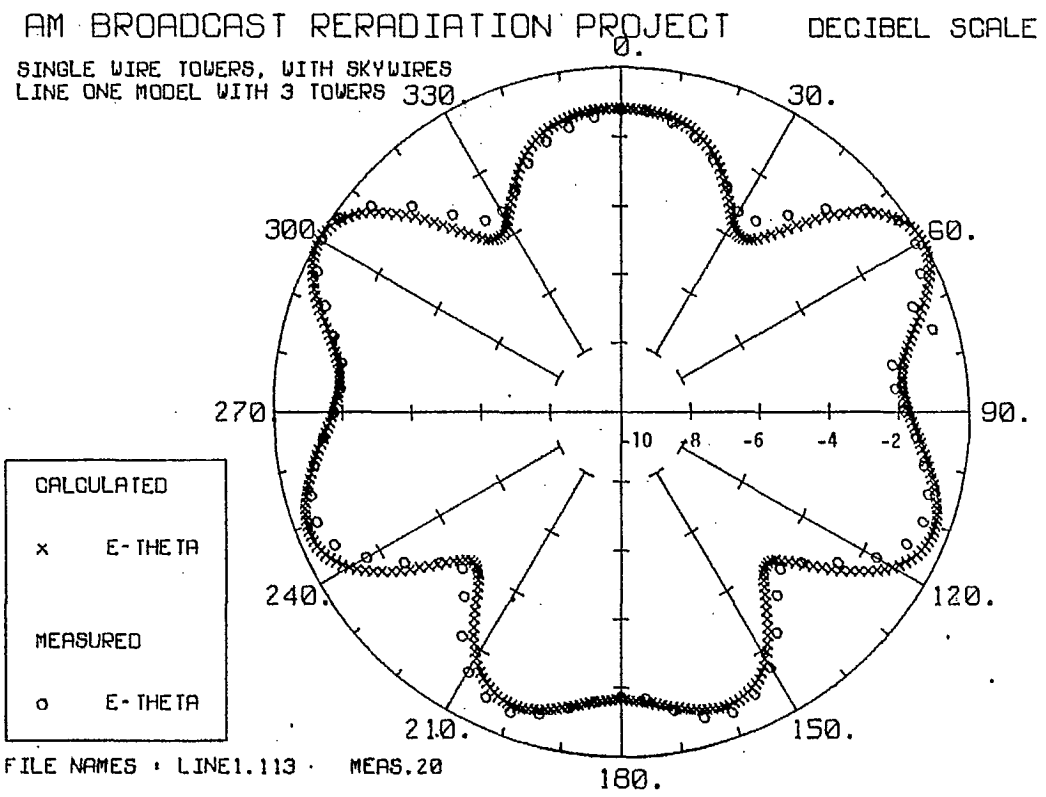

Figure 6.2

Azimuth pattern of the three tower power line with no detuning stubs, at 860 kHz.

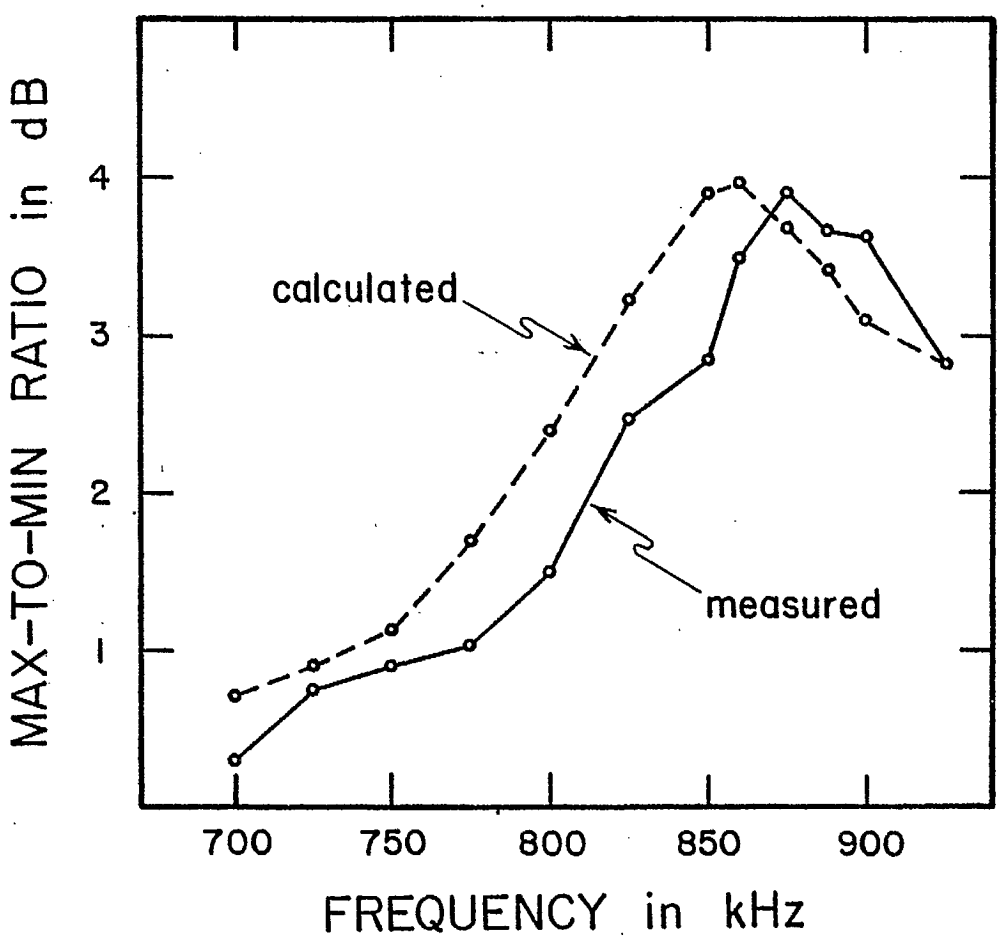

Figure 6.3

The max-to-min ratio as a function of frequency for the power line with no stubs.

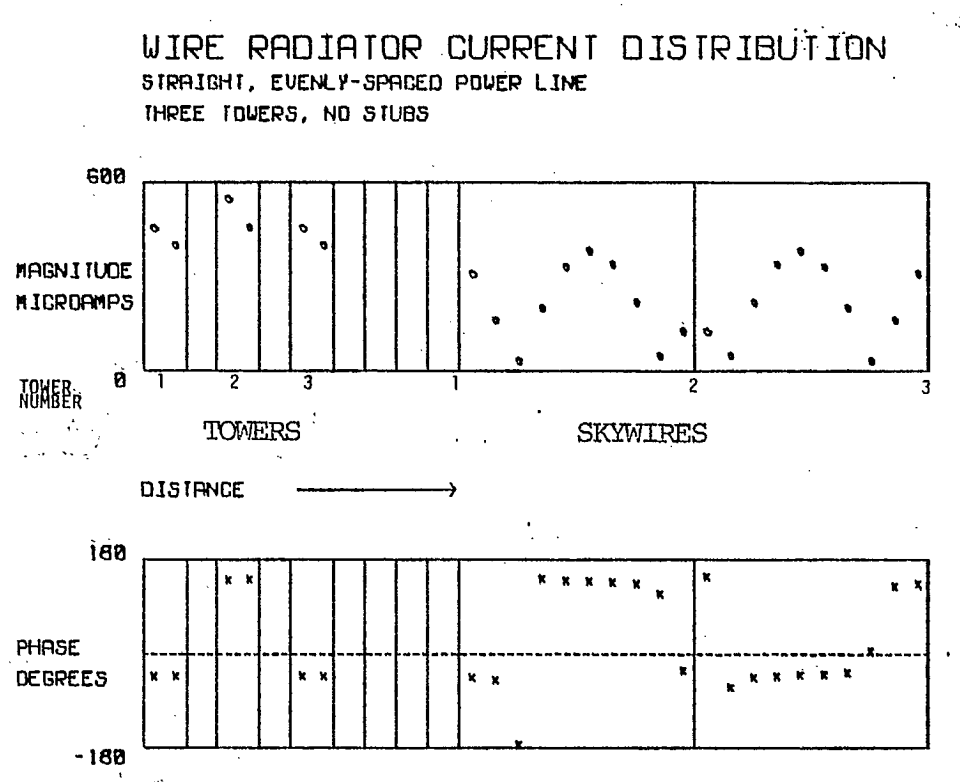

Figure 6.4

RF currents on the towers and skywires of the three tower power line with no detuning stubs.

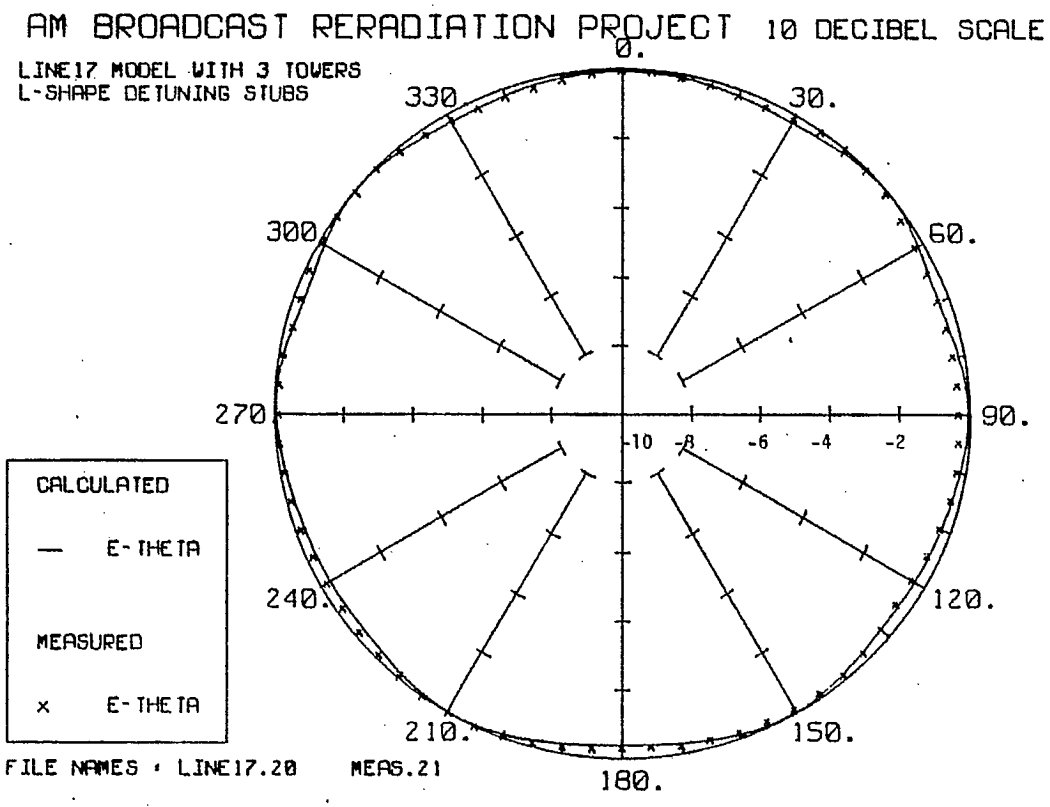

Figure 6.5

Azimuth pattern at 860 kHz using one detuning stub adjusted to that frequency.

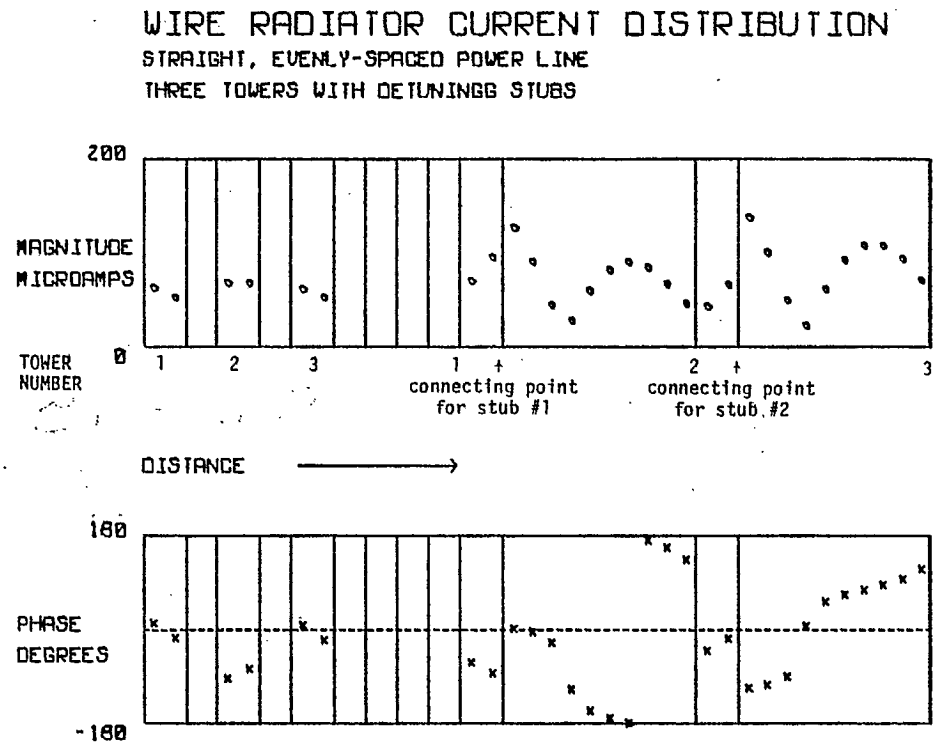

Figure 6.6 (a)

RF currents on the towers and skywires at 860 kHz, with one detuning stub.

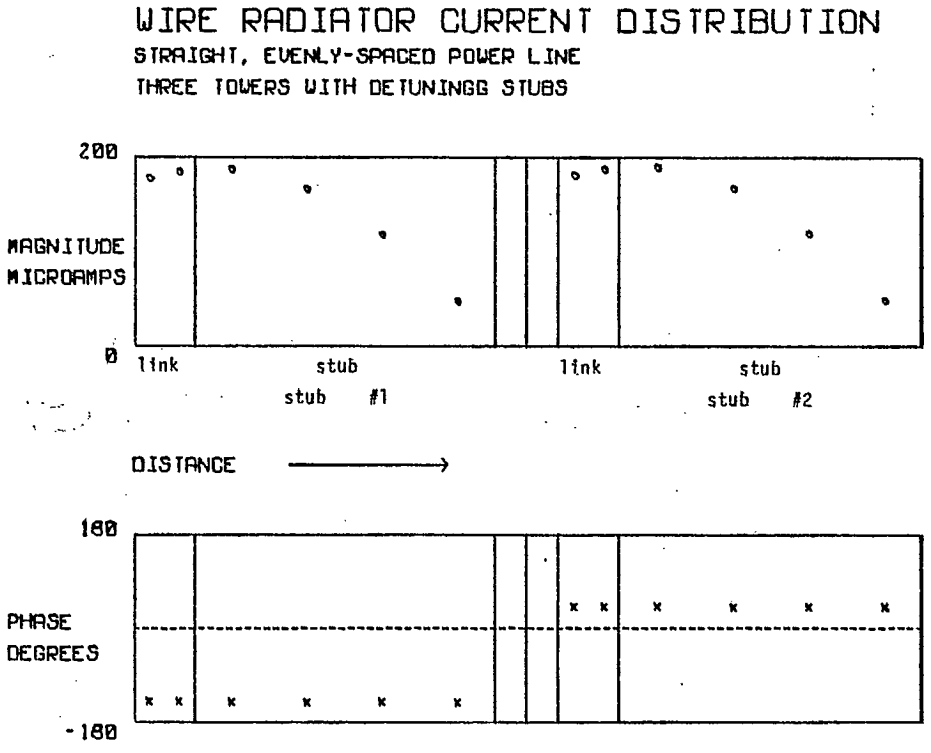

Figure 6.6 (b)

RF currents on the detuning stub.

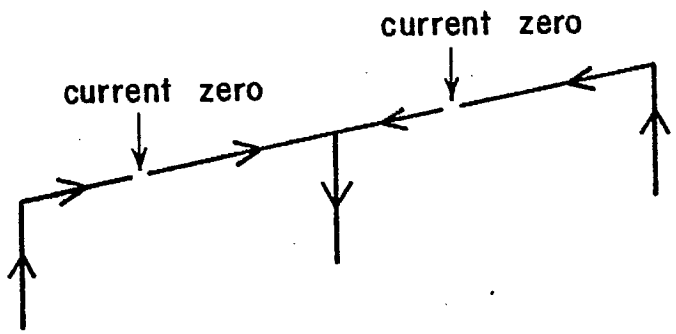

Figure 6.7

Pattern of current flow on the towers and skywires, with one detuning stub.

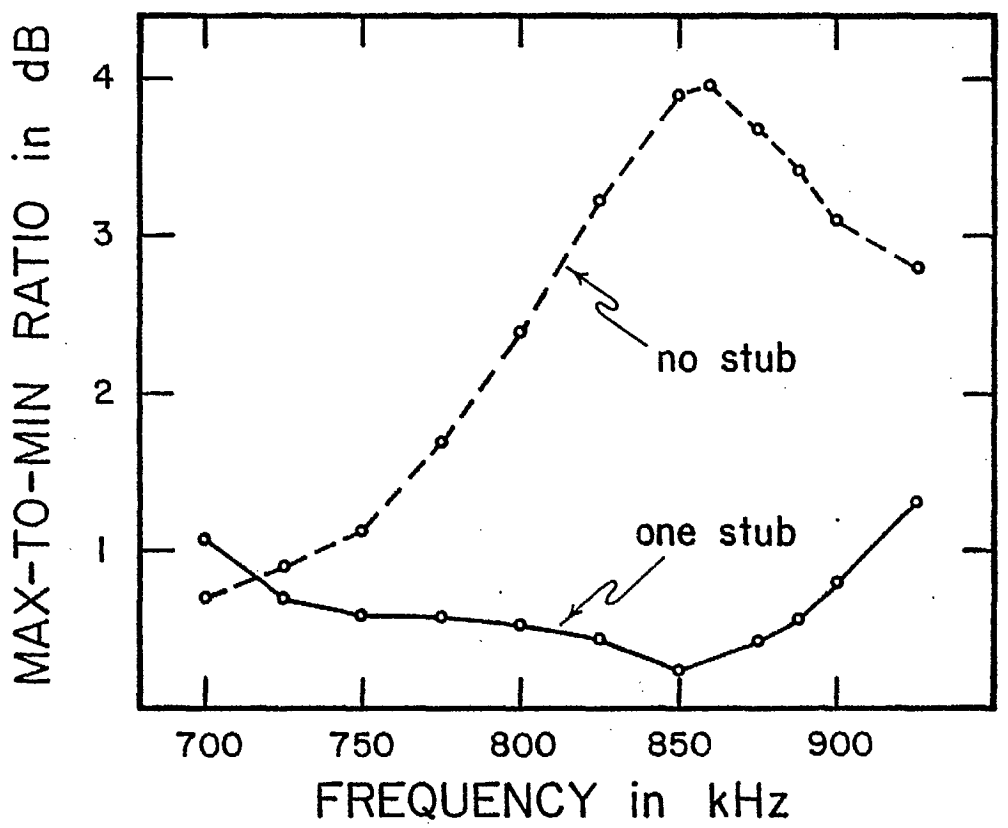

Figure 6.8

Frequency dependence of the max-to-min ratio with one stub.

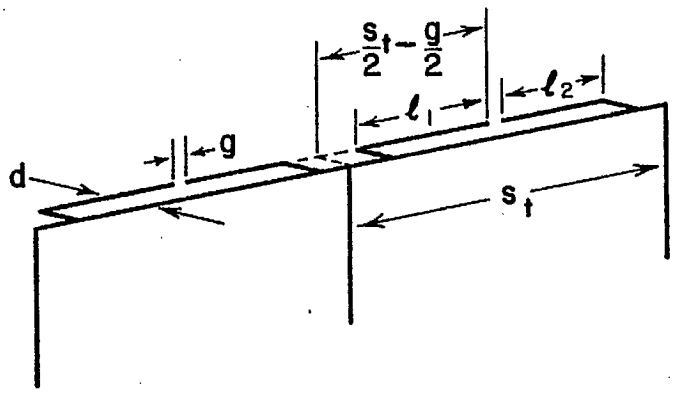

Figure 6.9
Pair of detuning stubs.

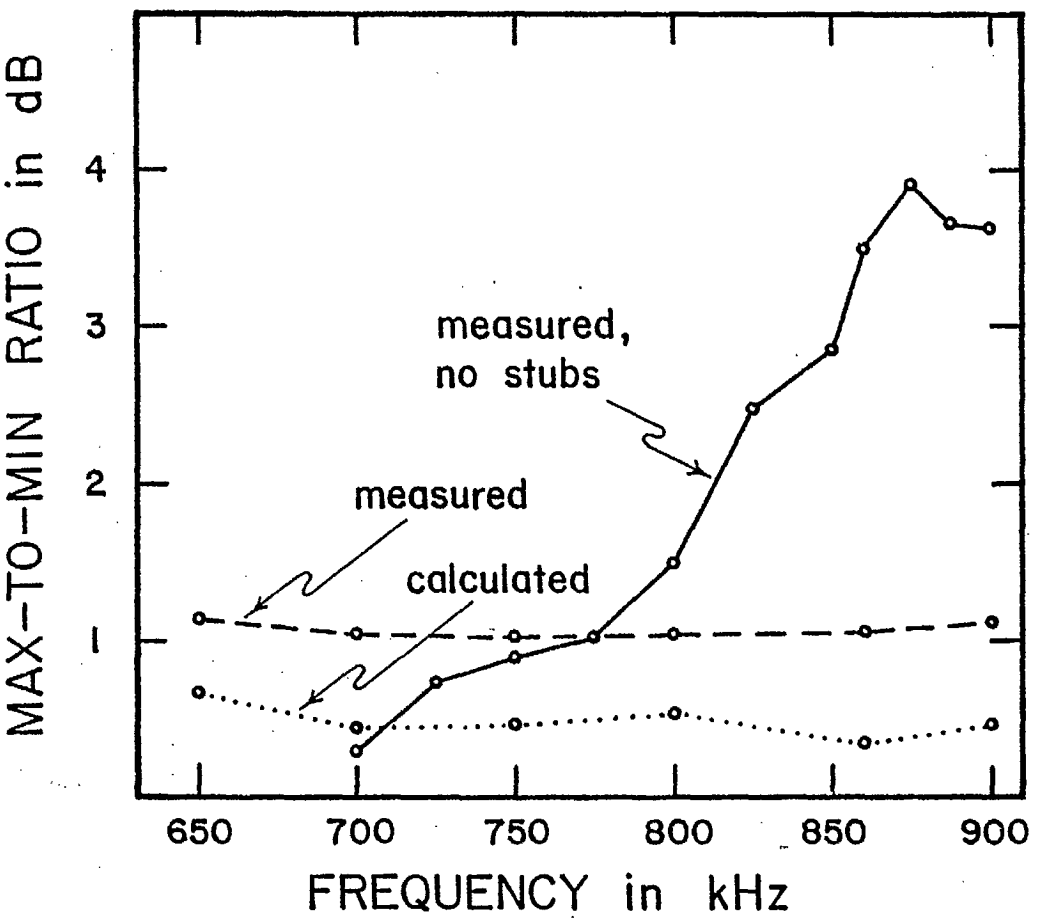

Figure 6.10

Max-to-min ratio vs. frequency for the pair of detuning stubs.

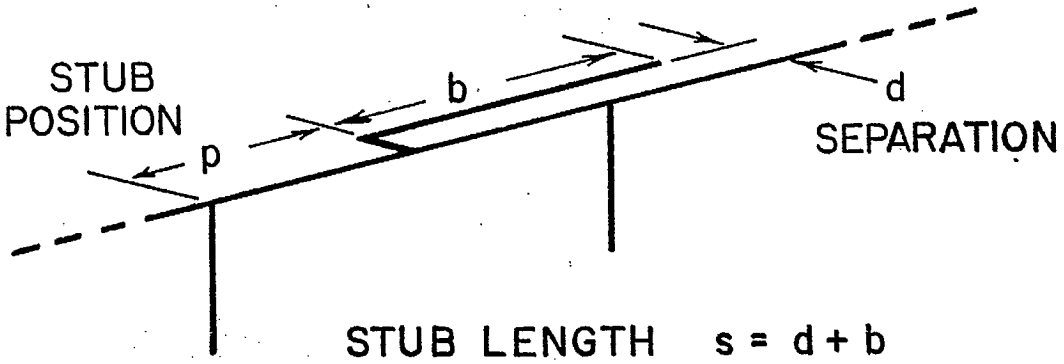

Figure 6.11

Stub configuration for detuning the one wavelength loop resonance mode.

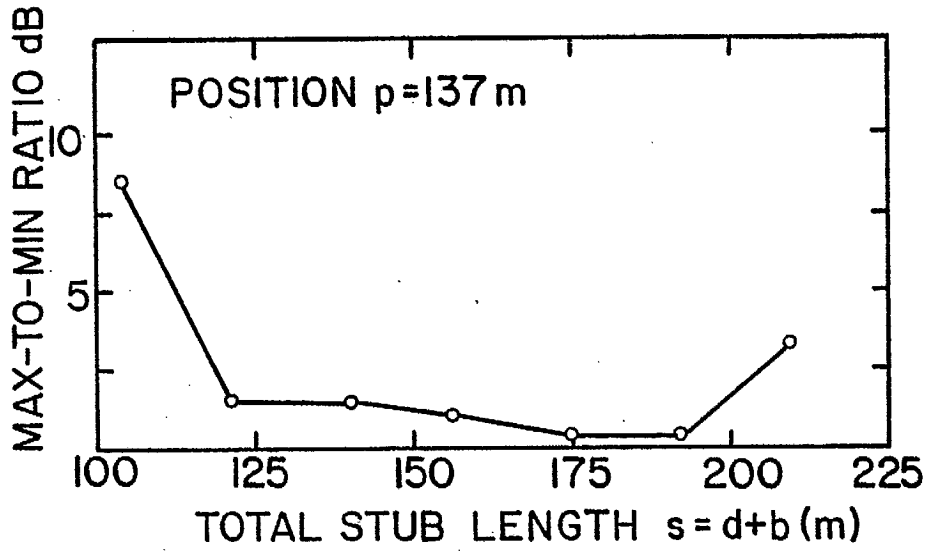

Figure 6.12

Max-to-min ratio vs. total stub length for the one wavelength detuner, at position p = 137 m.

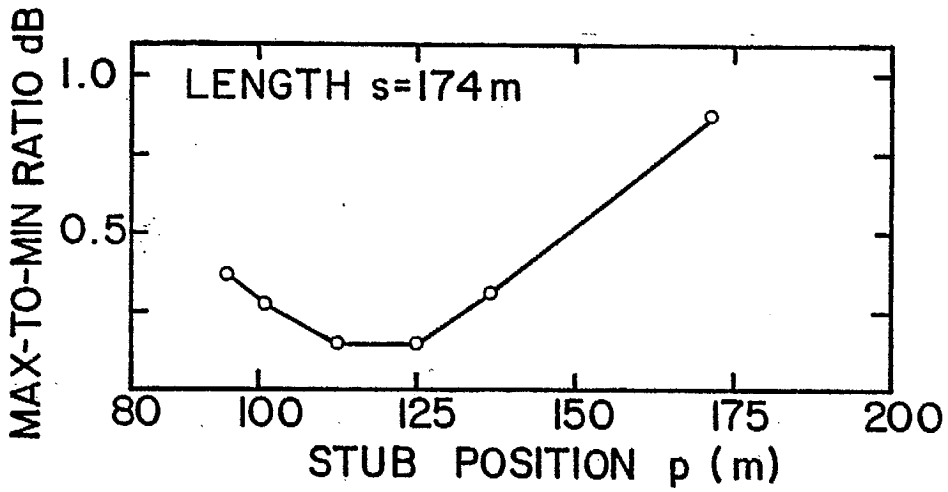

Figure 6.13

Max-to-min ratio vs. stub position with the total length chosen as 174 m.

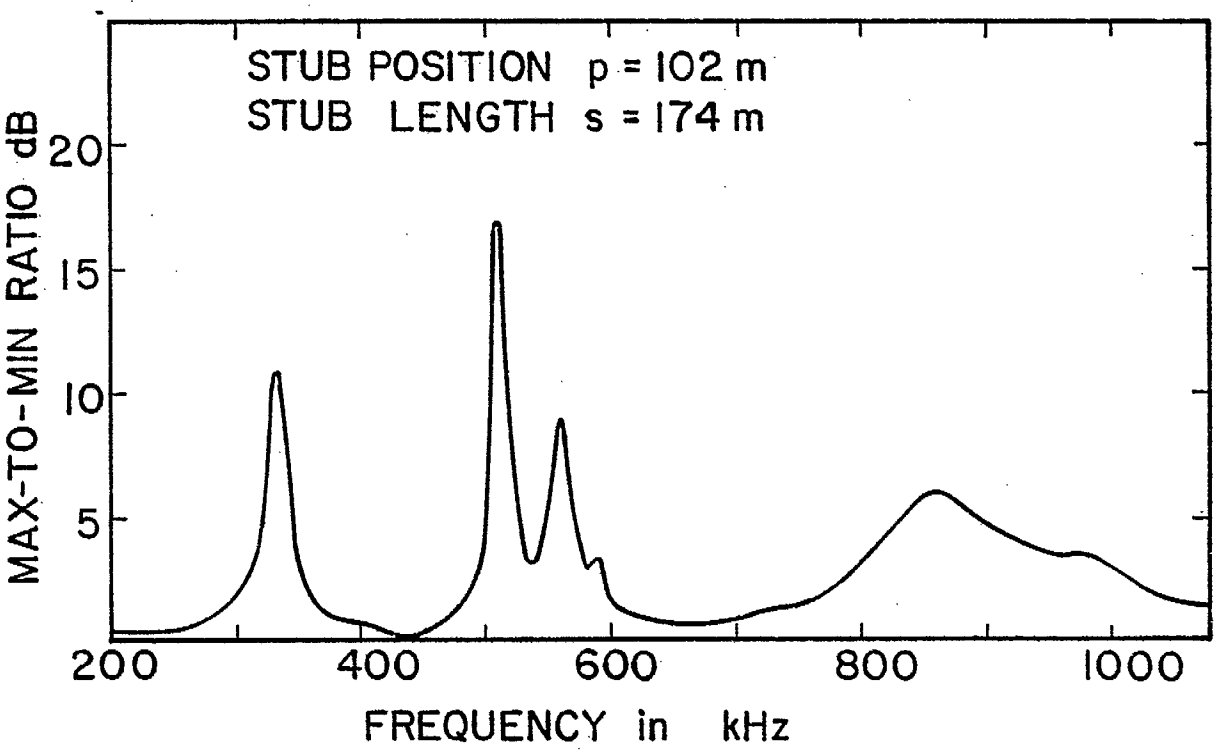

Figure 6.14

Max-to-min ratio as a function of frequency with the detuner for the one wavelength loop resonance mode in place.

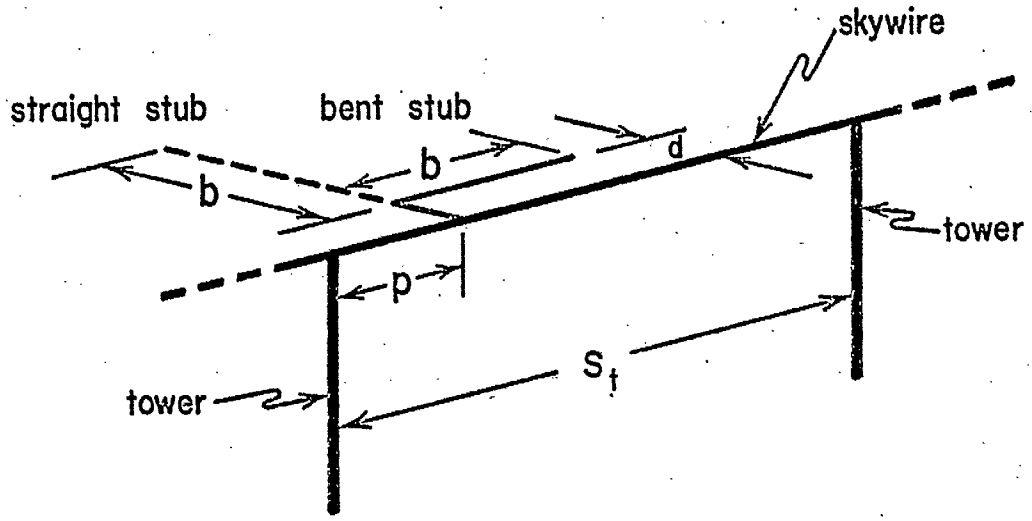

Figure 6.15

Geometry of the "straight" and the "bent" detuning stub.

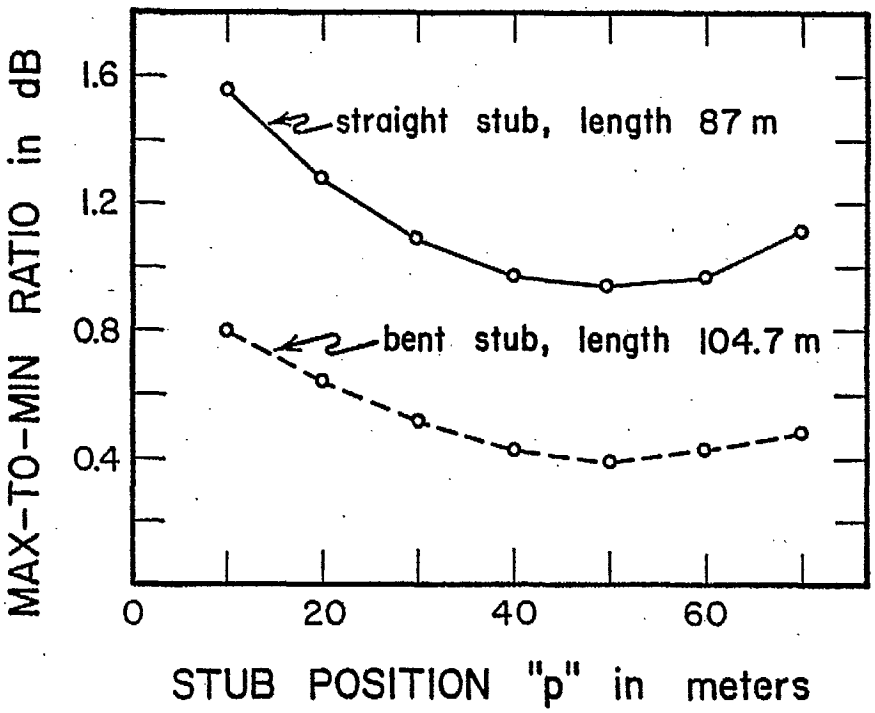

Figure 6.16

Max-to-min ratio as a function of stub position for the "straight" and "bent" stub. Note: straight stub was not optimized, see Figure 2.7.

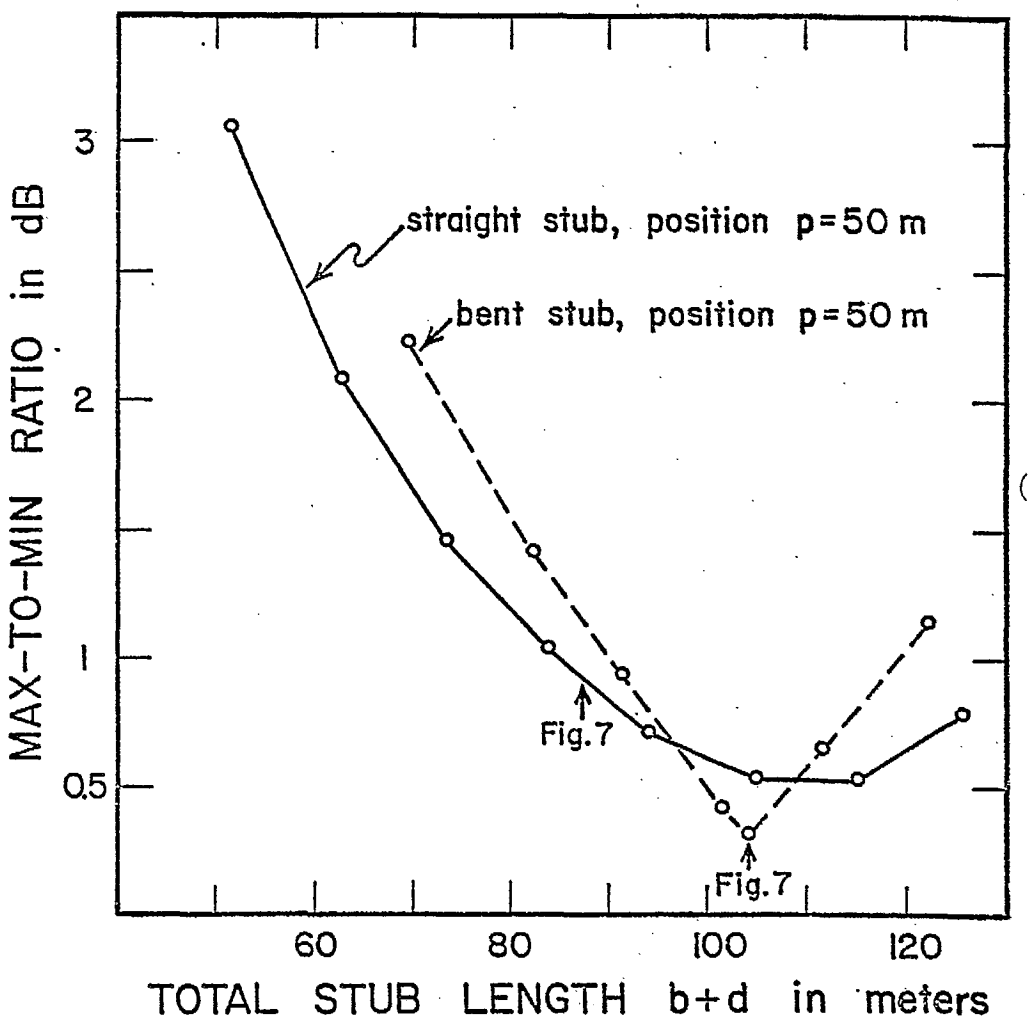

Figure 6.17

Max-to-min ratio as a function of the stub length.

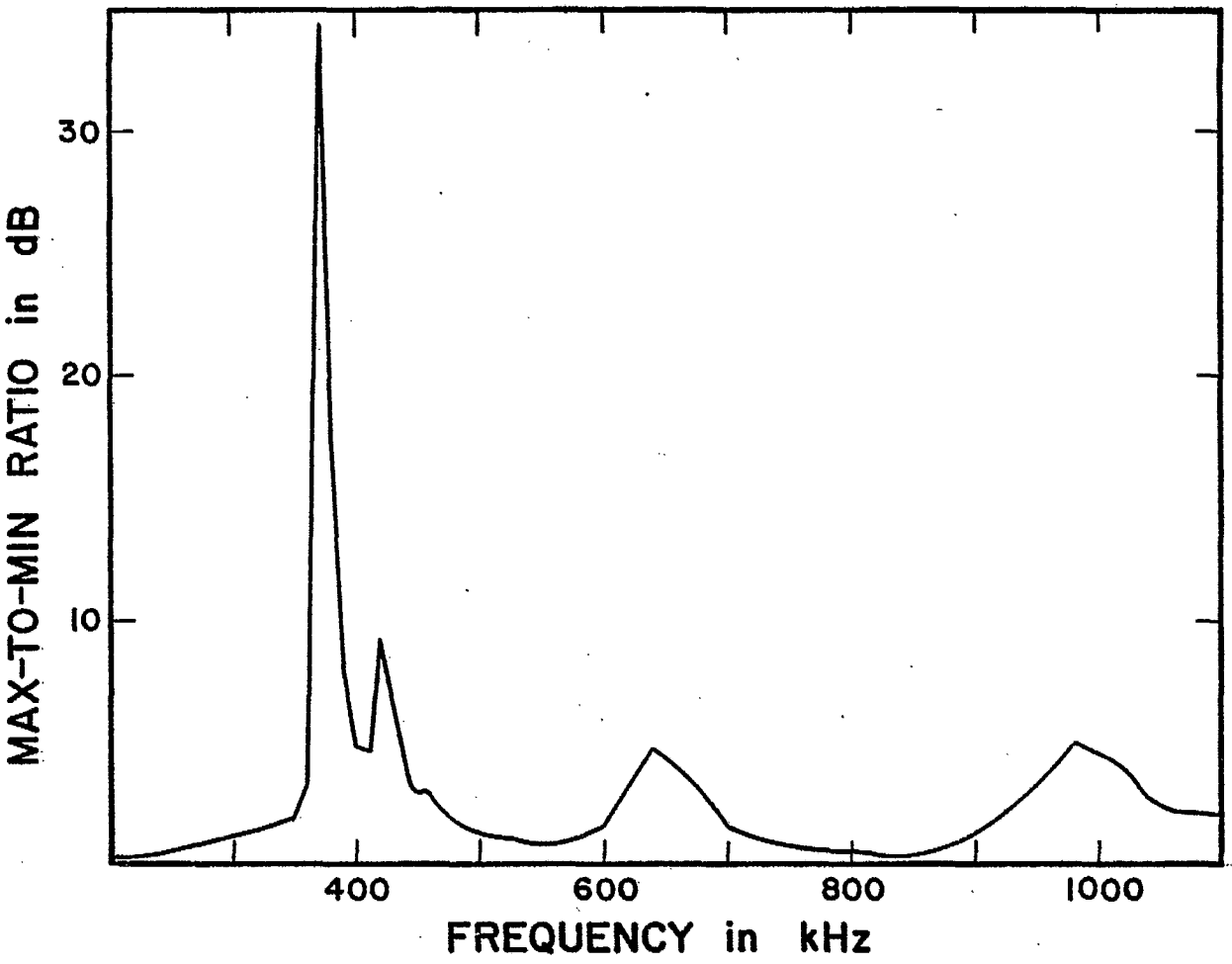

Figure 6.18

Max-to-min ratio as a function of frequency with the detuner for the two wavelength loop resonance modes in place.

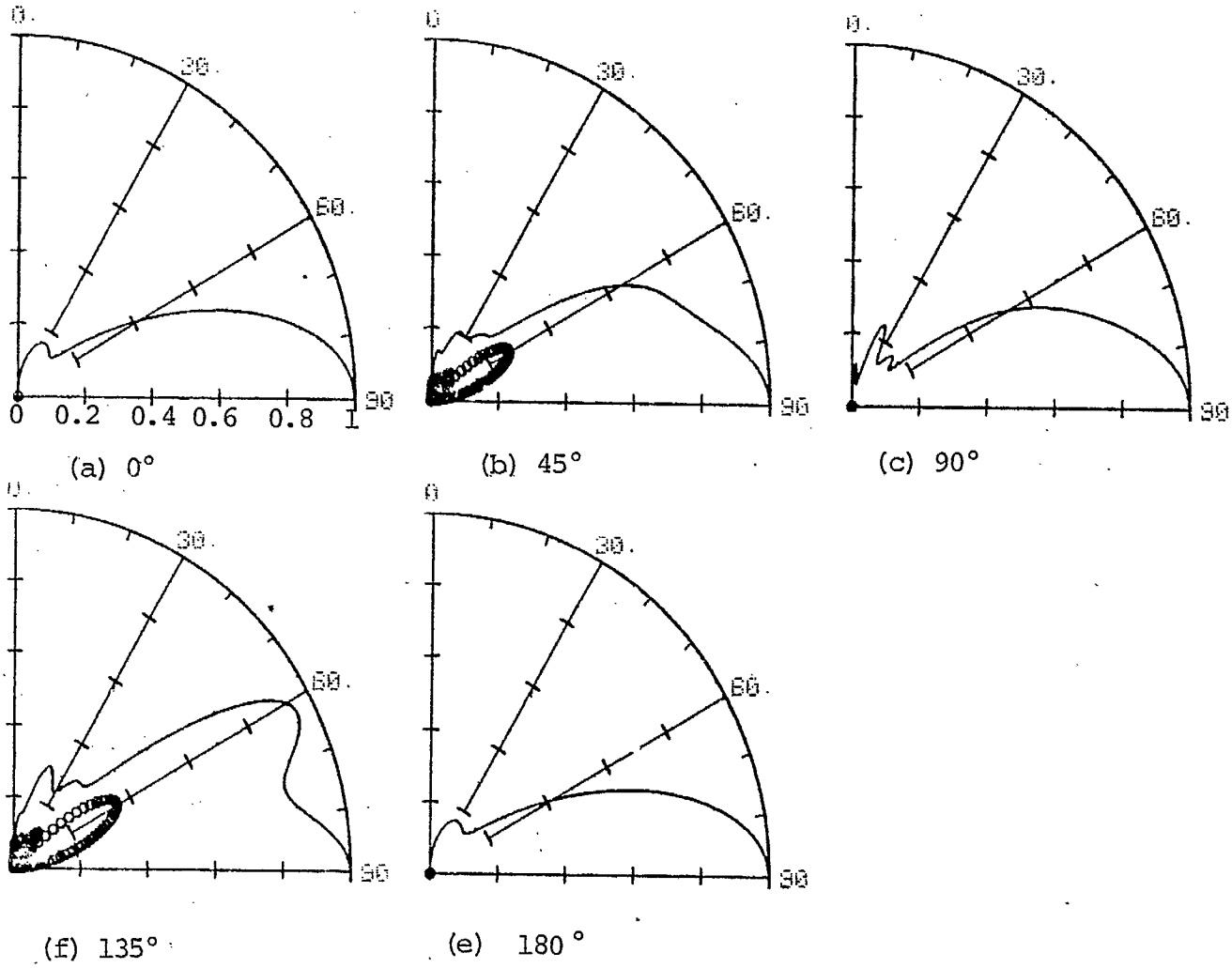

Figure 6.19

Elevation patterns plotted on a linear scale for the five tower power line of Fig. 5.1 at 860 kHz. Each individual pattern is normalized to unity.

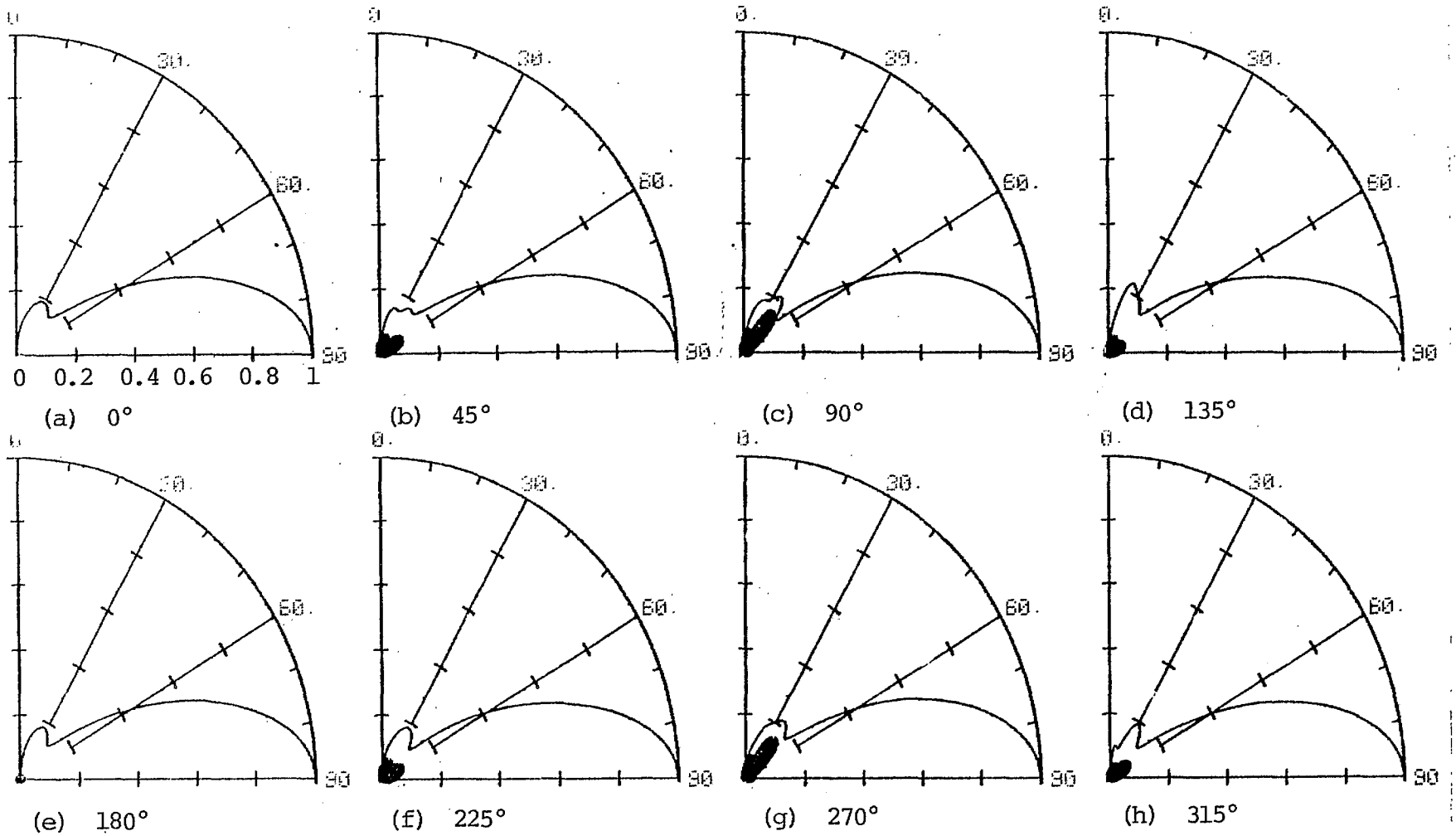

Figure 6.20 Elevation patterns with the "straight" detuning stubs of Figure 6.15.

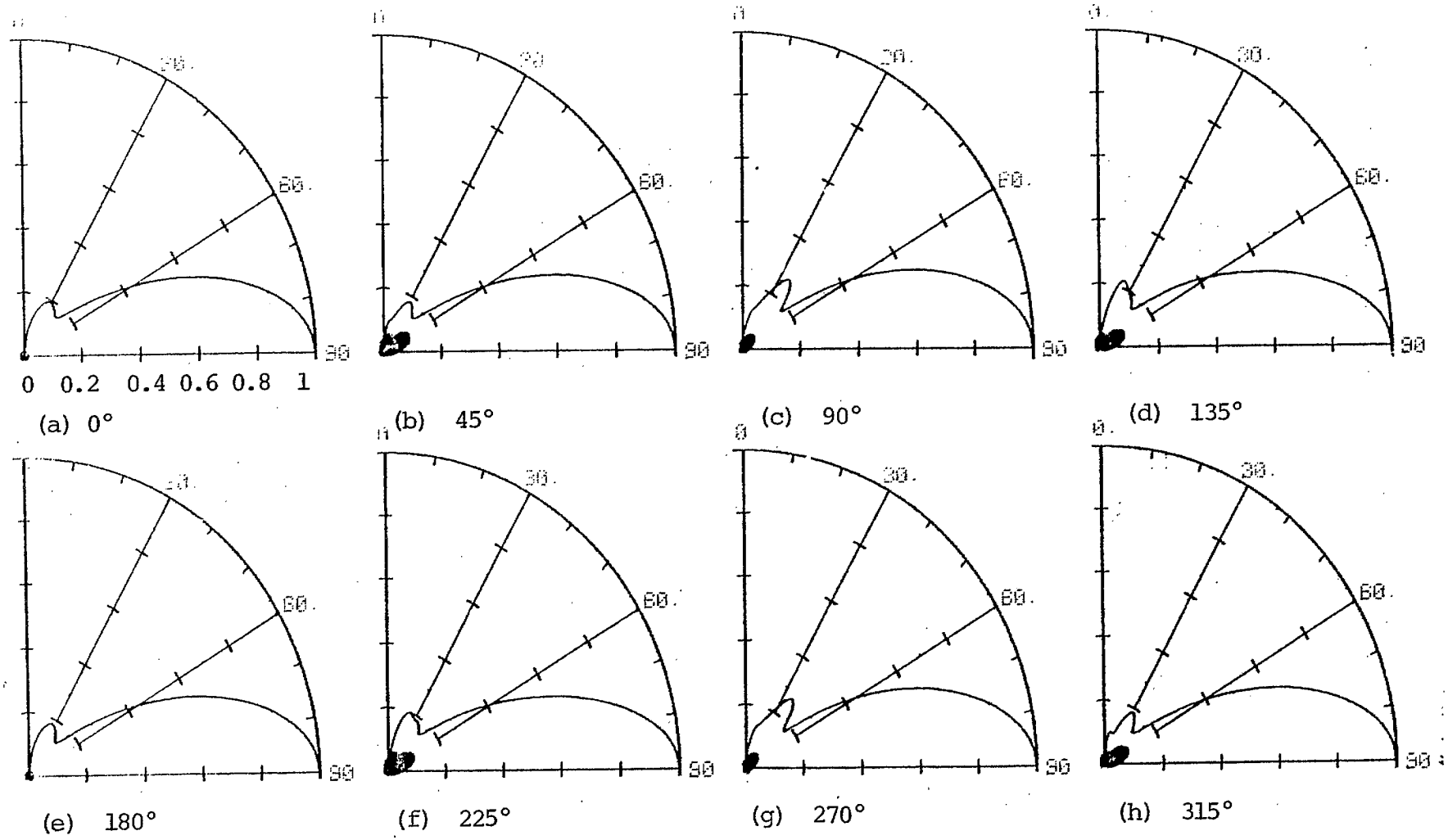

Figure 6.21 Elevation patterns with the "bent" detuning stubs of Figure 6.15.

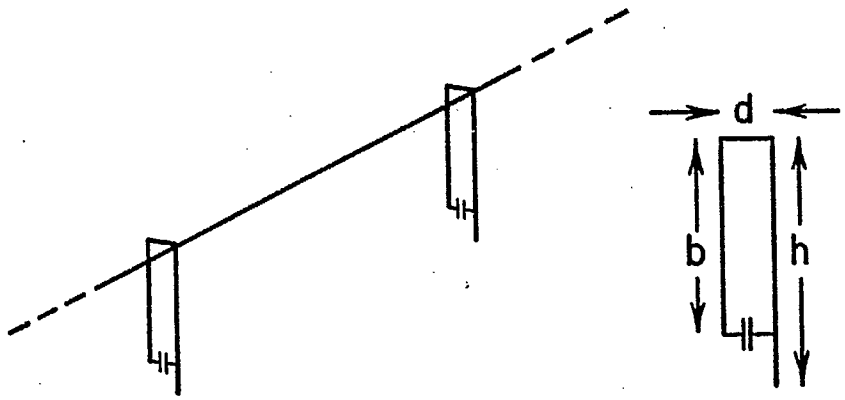

Figure 6.22

(a) Power line with capacitive-loaded detuners on the towers.

(b) Dimensions of the detuner.

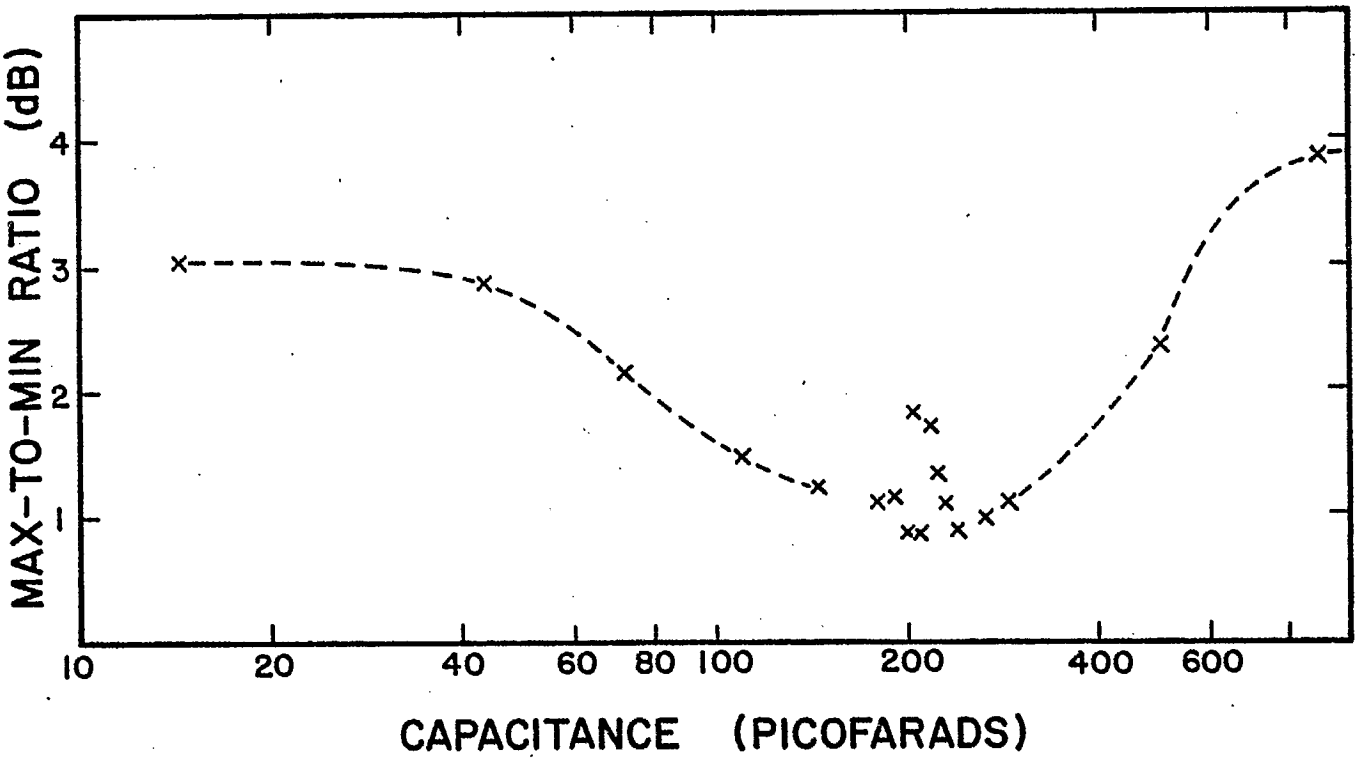

Figure 6.23

The max-to-min ratio of the azimuth pattern as a function of the capacitance for a five tower power line, with each tower "detuned" with a c-loaded short stub, at 860 kHz.

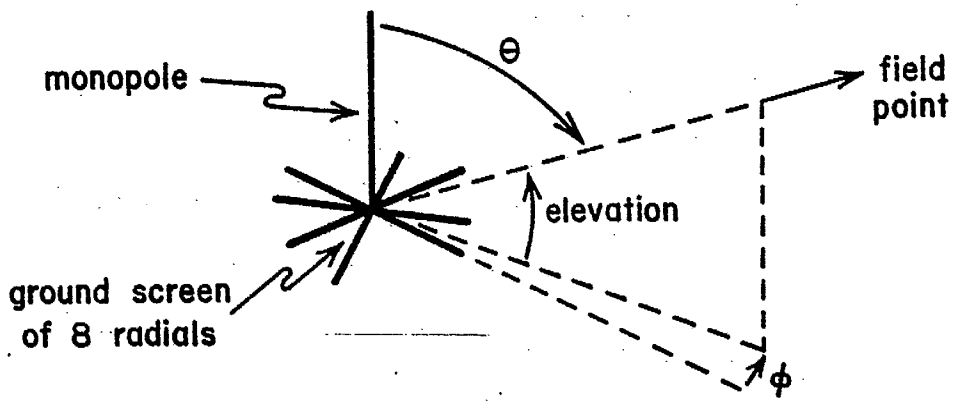

Figure 7.1
Monopole with eight radials.

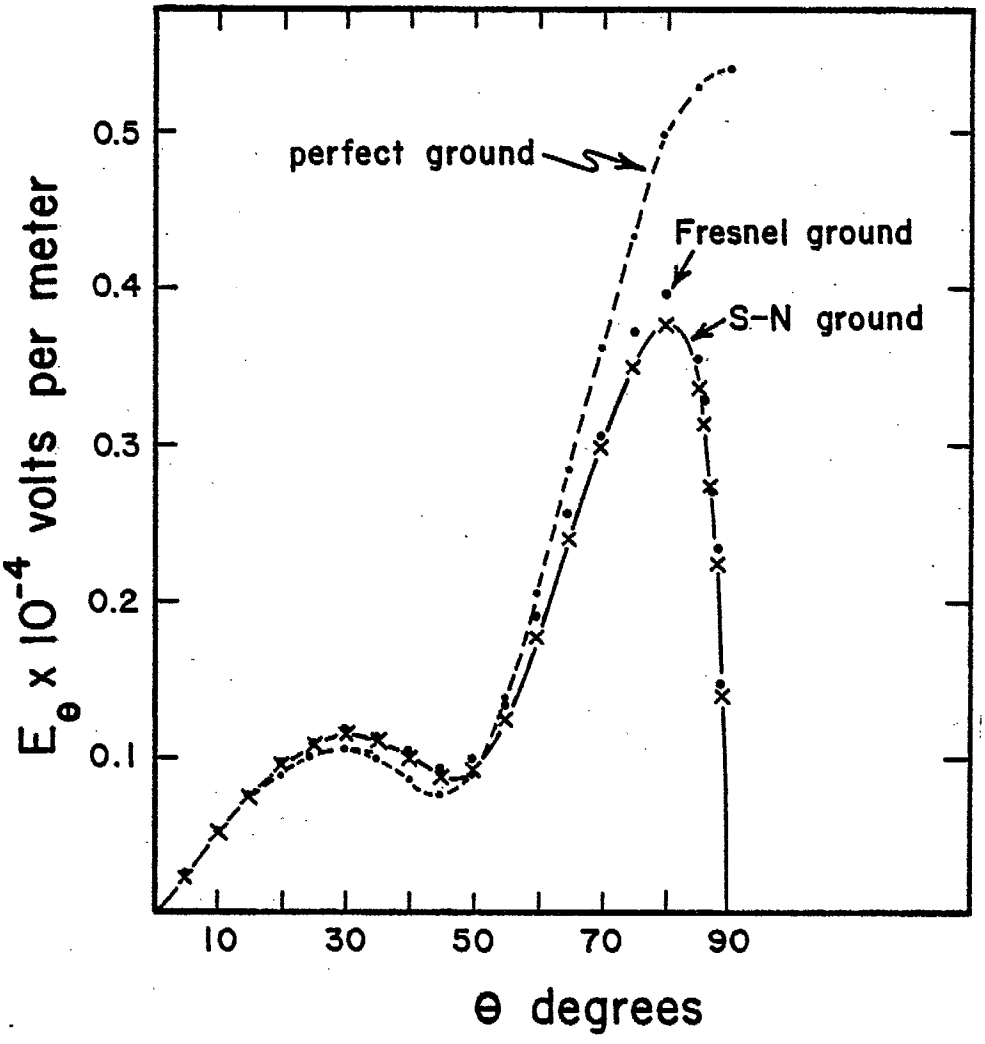

Figure 7.2
Elevation pattern, $\phi = 0°$ at 10,000 m, antenna only.

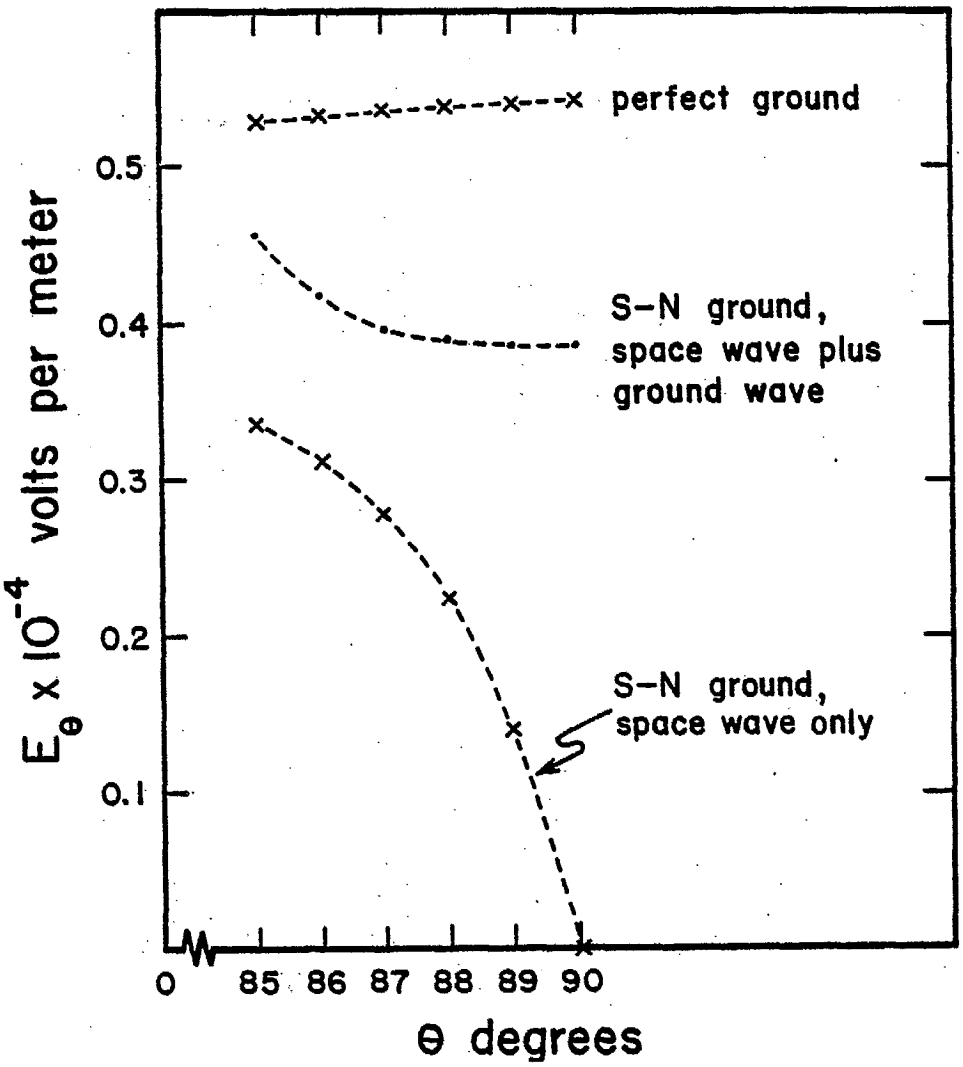

Figure 7.3

Detail of elevation pattern θ = 90 at 10,000 m.

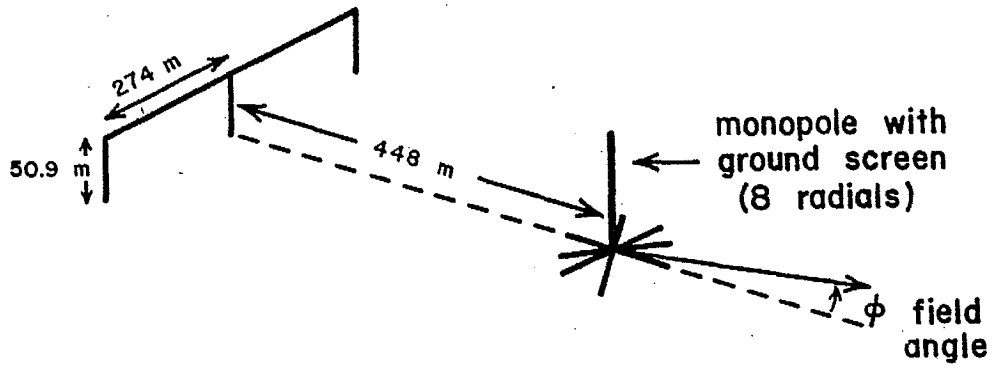

Figure 7.4

Antenna plus "power line".

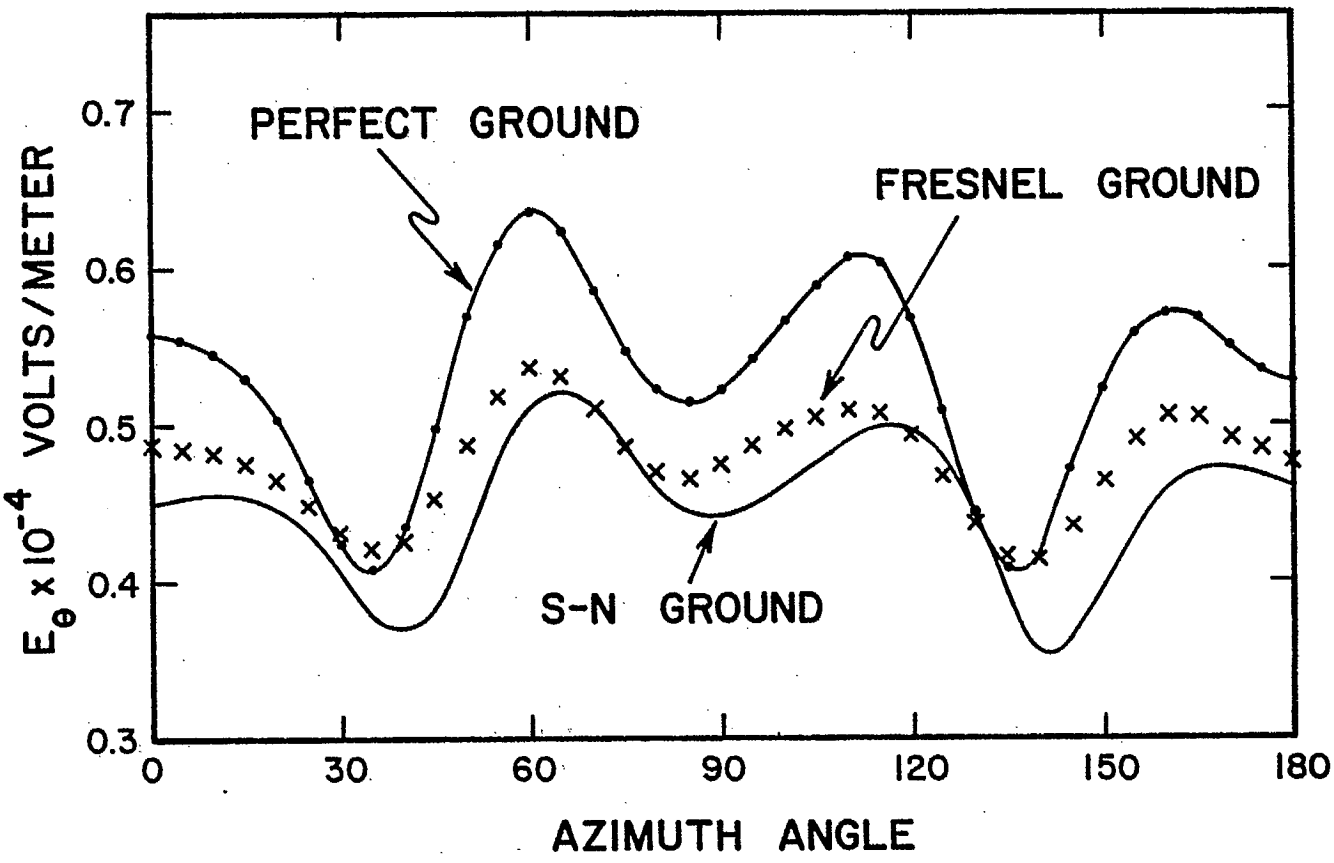

Figure 7.5

Azimuth pattern at 10,000 m with three ground models.

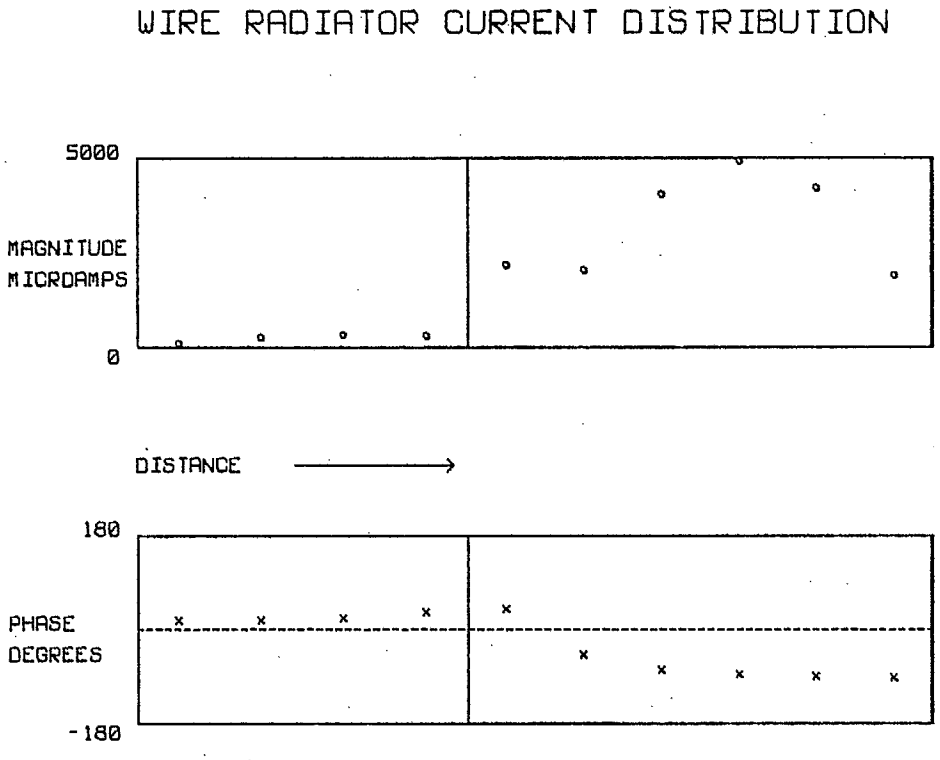

(a)

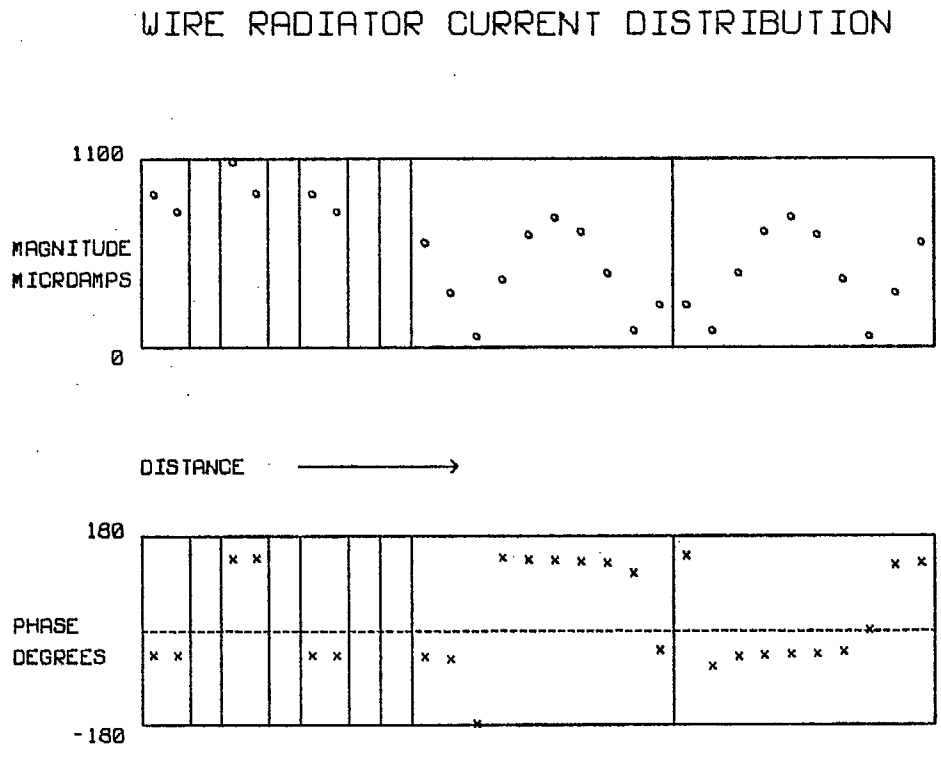

(b)

Figure 7.6

Current distribution with a perfect ground at 860 kHz.

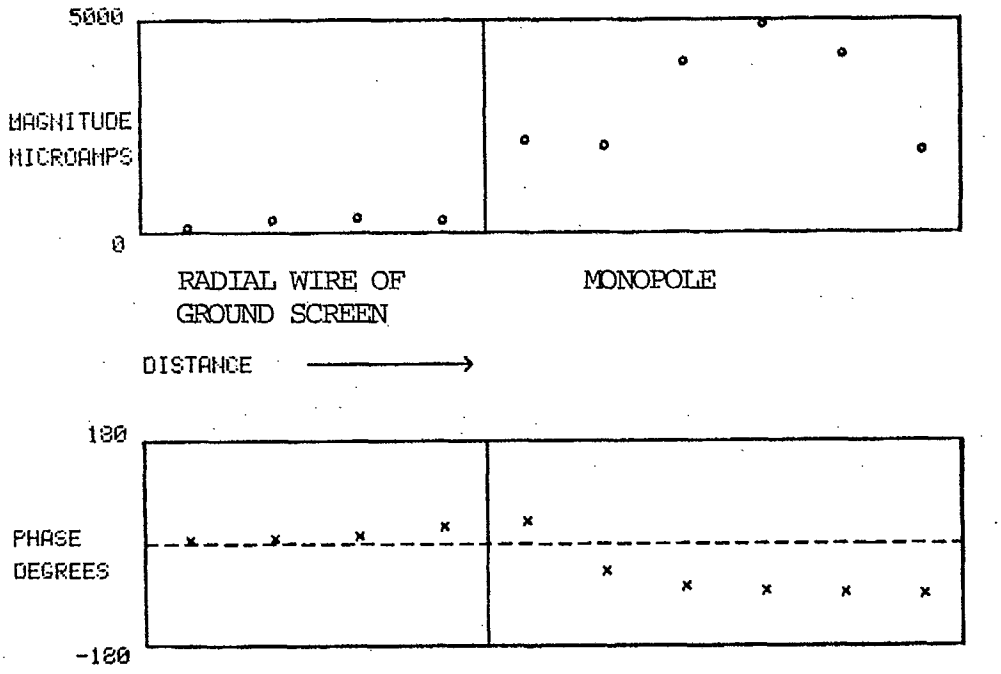

(a)

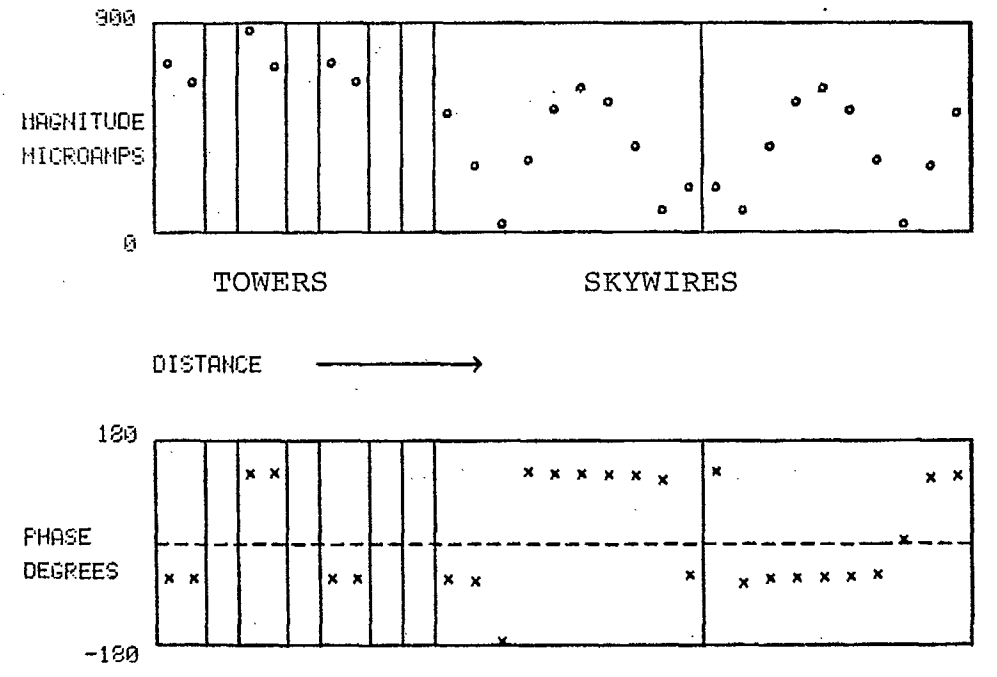

(b)

Figure 7.7
Current distribution with the Sommerfeld-Norton ground at 860 kHz.